Doctor of Philosophy

Modification of Polysaccharides through Sulfonation and Graft Copolymerization as Multiple Functional Binders for Anodes and Alginate Coated Core-shell Si-based Compound as Anode in Lithium-ion Batteries

The Graduate School of the University of Ulsan

Department of Chemical Engineering

Chengxiang He

Modification of Polysaccharides through Sulfonation and Graft Copolymerization as Multiple Functional Binders for Anodes and Alginate Coated Core-shell Si-based Compound as Anode in Lithium-ion Batteries

Supervisor Professor Eun-Suok Oh

A Dissertation

Submitted to

The Graduate School of the University of Ulsan

In partial Fulfillment of Requirements for the Degree of Doctor of Philosophy

By

Chengxiang He

Department of Chemical Engineering and Bioengineering

December 2020

Modification of Polysaccharides through Sulfonation and Graft Copolymerization as Multiple Functional Binders for Anodes and Alginate Coated Core-shell Si-based Compound as Anode in Lithium-ion Batteries

Thesis for the degree of Doctor of Philosophy

by

Chengxiang He

Has been approved

_____

Committee Chair Prof. Won Mook Choi

_____

Committee Member Prof. Junbom Kim

_____

Committee Member Prof. Sung-Gu Kang

_____

Committee Member Prof. Jung Kyoo Lee

_____

Committee Member Prof. Eun-Suok Oh

Department of Chemical Engineering and Bioengineering

University of Ulsan

December 2020

ABSTRACT

The investigation on active Lithium-ion battery materials (such as Silicon-based anode, NCM cathode and so on) with ever-increasing energy density draw much more attention, whereas the limits of conventional auxiliary materials, such as binders and conducting additives are being researched. Binders adhere active substances to active substances, active substances to current collectors as well, yielding an interconnected electrode structure that ensures mechanical integrity during the lithiation/delithiation process. Even though the battery binder only accounts for a fraction of battery weight and cost, it is a bottleneck technology in the development of high energy density active materials that experience significant volume variation and side-reactions.

In the other hand, most electrodes are using poly(vinilydene fluoride) (PVDF) as binder, but this fluorinated polymer is expensive and requires the use of a volatile and toxic organic solvent such as N-methyl-pyrrolidone (NMP) in the processing. The toxic NMP solvent not only damage the environment, but also harm the health of operators when manufacture the lithium-ion batteries. Hence, the development of novel eco-friendly, low cost and water-soluble binders which recently have gained increasing attention as a promising performance booster for lithium ion batteries with high energy density. Such water soluble polymer binders are either natural, or modified, or synthesized, and they were observed with profoundly enhanced chemical/physical interactions with the electrode materials, stronger mechanical adhesion and evidently improved volume variation durability, leading to dramatic improvements in the electrochemical performances of Si-based anodes, spinel/layered oxide cathodes and S cathodes.

In our first research, the water-soluble polysaccharides binders were modified to improve the ionic conductivity. Various polysaccharides have been much attention to potential binder candidates for lithium-ion batteries due to their strong adhesion through number of hydroxyl and carboxyl functional groups as well as water soluble characteristic. On the contrary, the endeavor to improve lithium ion transport through polysaccharide binders has been hardly done. For this purpose, the sulfonation of traditional sodium alginate (Alg) and carboxymethyl cellulose (CMC) binders are performed to introduce sulfo (SO_3H) functional groups to the backbone of the polysaccharides. The sulfonation increases the ionic conductivity of the polysaccharide at least 2 mS/cm higher than, compared to unsulfonated polysaccharides in the solution state. Such an increase in the ionic conductivity of binder results in the enhancement of cyclic performance of $Li_4Ti_5O_{12}$ (LTO) electrodes. For instance, the sulfonated CMC-containing LTO electrode shows 153.2 mAh g^{-1} at the 100th cycle, whereas the unsulfonated CMC-containing LTO electrode has 117.6 mAh g^{-1}. The difference becomes more significant as the charge/discharge current rates increase. Besides, various characterization

demonstrates that the sulfonated polysaccharides own superior electrochemical properties when used to LIB binder.

In our second research, water-soluble conductive binder system would be designed to enhance the electrochemical performance for pure Si anode. Alginate is a kind of natural polysaccharides binder which possess much amount of hydroxyl and carboxyl groups, leading to a good adhesion strength for active materials, especially for Si-based anode. Herein, the adhesive property of alginate was boosted by graft copolymerization with acrylic acid (AA) and butyl acrylate (BA) forming Alg-ABAA binder. AA monomer provides abundant hydroxyl groups which can improved the adhesion strength between Si anode and copper foil, in addition, monomer BA could endow the new binder flexibility. After then, the conductive two dimensional (2D) layered material MXene was connected to the binder Alg-ABAA, the water-soluble conductive binder Alg-AABA-Mx was well synthesized. When employed the binders Alg-AABA and Alg-AABA-Mx to the pure nano Si particles (SiNPs) anode, the capacity of electrodes was dramatically increased. In the case of Alg-ABAA-Mx/SiNPs electrode, even the capacity is lower than Alg-ABAA/SiNPs electrode, it shows an excellent performance in high rate cycling.

In the last research, a type of a core-shell Si-based compound was well synthesized. It is well known that Silicon was supposed to the next generation anode material for lithium-ion batteries due to (1) its specific capacity of 4,200 $mAhg^{-1}$ and volume capacity of 9,786 mAh cm^{-3}, the highest known for a LIB anode; (2) relatively low working potential (0.5 V vs. Li/Li^{+}); and (3) the natural abundance of element Si and its environmental benignity. However, the practical implementation of Si anodes is still blocked due to three major problems. First, poor cycle-life of silicon materials results from pulverization during the huge volumetric fluctuations (>300%) which accompany lithium ion intercalation and deintercalation. Second, drastic irreversible capacity loss and low coulombic efficiency is caused by mechanical fracture of Si anodes during the alloying/dealloying process. Finally, the solid electrolyte interphase (SEI) breaks as the nanostructure shrinks during delithiation. This results in the exposure of the fresh silicon surface to the electrolyte and the reformation of the SEI, resulting in the SEI growing thicker with each charge/discharge cycle. Our purpose is to prolong the cycle life of electrode when using the Si-based material as anode. The polysaccharide alginate was coated on the surface of SiNPs through chemical bond by amidation reaction, therefore the formed core-shell Si-polymer material was used to the lithium-ion batteries as anode. During the charge and discharge process, the core-shell Si-based anode could alleviate the pulverization and keep a long cycle life, maintain a stable and relatively high capacity. Even the inner resistance of the Si-Alg electrode is increased compare to the pure SiNPs electrode, the sacrifice got the stable and long cycle in return.

ACKNOWLEDGEMENT

The PhD career is a long but precious period in my entire life. I experienced suffering and happiness, struggling and enjoying at the same time. I would miss the time when I was a PhD candidate. And now it is my pleasure to acknowledge the roles of several individuals who were instrumental for completion of my PhD research. I wouldn't finish my research without their help.

First of all, I would like to express my gratitude to Prof. Eun-Suok Oh who is my advisor, he brought me to the fantastic world of lithium-ion battery and taught me a lot include the research section and how to be a qualified researcher importantly. At the same time, he gave me so many chances to attend the domestic and international conferences, so I had the good fortune to contact the excellent researchers and know the most state-of-the-art information about batteries. In addition, he also took care of my health and life very often. He is an extremely responsible and nice professor and scientist I've ever seen in my life.

Actually, I changed my research area from master (organic synthesis) to PhD (lithium-ion battery), so I faced many problems and questions on the first two years during my PhD period. Fortunately, Bolormaa Gendensuren who is one of my lab members gave me a lot of help on my research selflessly. I would like to give my appreciate and gratitude to her, she always pointed out my mistake and offered correct method and good advices. Of course, I would thank another lab member who called Yanchunxiao Qi, we work together recently, she is a nice partner and friend to me. We discussed a lot about research and life. In addition, I would like to thank Dr. Minh Hien Thi Nguyen who helped me solve so many problems on research and Mi Tian who give me new research ideas and plentiful joys. At last, I express my gratitude to all of my lab members, they support me a lot when I was down. Certainly, our lab is like a warm family, they gave me a lot of sweet memories in my mind and would never forget.

I am so grateful to the committee members who attend my dissertation defense, include Prof. Won Mook Choi, Prof. Junbom Kim, Prof. Sung-Goon Kang, and Prof. Jung Kyoo Lee. Thank you all very, very much for sparing your valuable time to my defense. Thank you for your affirmation and giving me a lot of valuable advices. I would improve my research according to your advices in the future.

Next, I want to say it's worth spending five years in Chemical Engineering department, University if Ulsan. It has so many advanced instruments and excellent professors, it's a perfect place to do scientific research.

I also want to acknowledge the BK 21 plus project which give me financial support for my PhD study. The financial support let me focus on the research without any worries on life in Korea.

Finally, I would like to say “Thank you, I love you” to my all family, my parents, little brother, nephew and others. They encourage me to overcome the problems in my life and give me love all the time. I feel warm and build up my confidence again and again when I talk with them through communication tools.

Table of Contents

Overview of dissertation

The main content of this dissertation is about modifying and designing novel water-soluble polymeric binders with multiple functions, then employed them as binders for $Li_4Ti_5O_{12}$ and Si anodes in lithium-ion batteries. The other part is about designing a core-shell structured Si-based compound as anode for lithium-ion batteries, to endure the volume expansion of Si during lithiation/delithiation process. The brief overview of this dissertation as follows:

Chapter 1 introduced some background knowledge about lithium-ion batteries, including the history of battery, classification of battery and battery commercial market at present. Battery is playing an indispensable role in our modern life, so the battery is an important subject which should be studied with more attention.

Chapter 2 described the main parts and materials of lithium-ion battery briefly. Every material is important in a battery, it's like the barrel theory, the comparative worst material in the lithium-ion battery determines the performance of the battery. Hence the appropriate and superb performance material is the main topic of our research. In our case, we focus on the binders in lithium-ion batteries, some paragraphs introduced the binders in detail from all aspects in this chapter.

Chapter 3 showed the detailed synthesis procedure and method about sulfonated polysaccharide binders, displayed and explained all of the results about sulfonated binders Alg-S and CMC-S used for LTO anode as binder in lithium-ion battery. As expected, the sulfonated binders improved the ionic conductivity compare to the original polysaccharides, the coin-cells with them as binders exhibited better electrochemical performance.

Chapter 4 described how to synthesis of conductive polymeric Alg-ABAA-Mx binder, and the instruments when did the research, displayed and explained all of the results about MXene bonded conductive binder Alg-ABAA-Mx applied for Si anode as binder in lithium-ion battery. Finally, the coin-cell with Alg-ABAA-Mx as binder showed better electrochemical performance, especially in high rate current.

Chapter 5 showed how we made the core-shell structured anode Si-Alg, displayed and explained all of the results about core-shell structured anode Si-Alg applied in lithium-ion battery. The Si-Alg anode alleviated the huge volume expansion of Si during charge/discharge process and prolong the coin-cell's cycle life. It's an effective way to enhance the application of Si as anode in lithium-ion batteries.

List of tables

List of figures

1 Background of Battery

Imagine yourself not being able to move around while using your mobile phone because its battery is busted and will only work while it is plugged in to a power source. I bet you would think that is too inconvenient, am I right? When our phone's battery ran out, we tend to think of all possible ways to recharge it so we could use our phone again. It is on these instances that we actually realize how important portable batteries have become in our lives now. These batteries are used in almost all portable electronic devices. Batteries have made our life so convenient that sometimes we tend to overlook their importance. Changing channels on television, talking on the phone while walking around, using your laptop while on the move or taking pictures would never be so easy if batteries were not invented. These scenarios prove that batteries are present in almost all aspects of our daily lives.

Batteries are devices used to store and generate electrical energy. Apart from being used in daily household products, batteries are used in automobiles, computer data stations or even forklift equipment. These batteries are specially built to power devices that require high power output. They are called lithium acid batteries with a signature letter of A. They should not be used for smaller appliances as they might damage it with its large amount of power. However, they can be used to power a home in case of a power blackout.

The batteries that we use in regular household appliances are known as lithium or lithium ion batteries. They provide instant power when required but do not last forever as their energy gets drained out. Some of their applications can be in portable radios, TV remotes or toys. An interesting thing about these batteries is that they can even be used to power electric cars! They come in various sizes to support different devices. Some examples of their size are double A or triple A. Nickel cadmium batteries, or also known as Ni Cad batteries, are rechargeable batteries. These rechargeable batteries do not only make our lives easier but also more economical. Because of them, we do not need to buy and change our hand phone's battery every time it dies. Applications of this battery can be in mobile phones, cordless phones, Mp3 players and cameras. Even though, these batteries tend to be more expensive as compared to regular batteries, in the long run, they are proven to be more economical as you do not have waste money on batteries again and again.

Batteries have been so successful due to the fact that they are portable. Manufacturers of batteries always try to out-do their competitors by coming out with various types of batteries that can last longer. Due to their success, more gadgets were invented that could be used on the move. Proper care and usage of batteries is important to avoid any mishaps. You should not try to recharge batteries that

are not meant to be recharged as this can cause the battery to leak and damage your appliances. Ensure that batteries are being used in a dry environment to be able to take full advantages of them.

1.1 History of battery

A series of remarkable events which are related to battery inventions is depicted in a chronological manner, as shown in **Figure 1-1**. The development of battery has gone through a very long historical process until now. Alessandro Volta reported that he has developed a reliable source of electrical current in 1800. He has invented the wet-cell battery. Volta theorized that electrical current was caused by the contact of dissimilar metals amid moisture. He went on to build a stack of alternating copper and zinc discs. Each pair of discs was separated from the next by cardboard that had been soaked in salty water. This voltaic pile produced continuous electrical current. After around 59 years, Gaston Planté invented the lead-acid cell in 1859, the first rechargeable battery. His early model consisted of a spiral roll of two sheets of pure lead, separated by a linen cloth and immersed in a glass jar of sulfuric acid solution. Lithium batteries were proposed by British chemist M. Stanley Whittingham, now at Binghamton University, while working for Exxon in the 1970s. Whittingham used titanium (IV) sulfide and lithium metal as the electrodes. However, this rechargeable lithium battery could never be made practical. In 1980s, John B. Goodenough demonstrated a rechargeable lithium cell with voltage in the 4 V range using lithium cobalt dioxide ($LiCoO_2$) as the positive electrode and lithium metal as the negative electrode. This innovation provided the positive electrode material that enabled early commercial lithium batteries. Since then, much attention was paid to improve the Li-based systems, and the Li-ion battery was first commercialized by Sony in 1991.

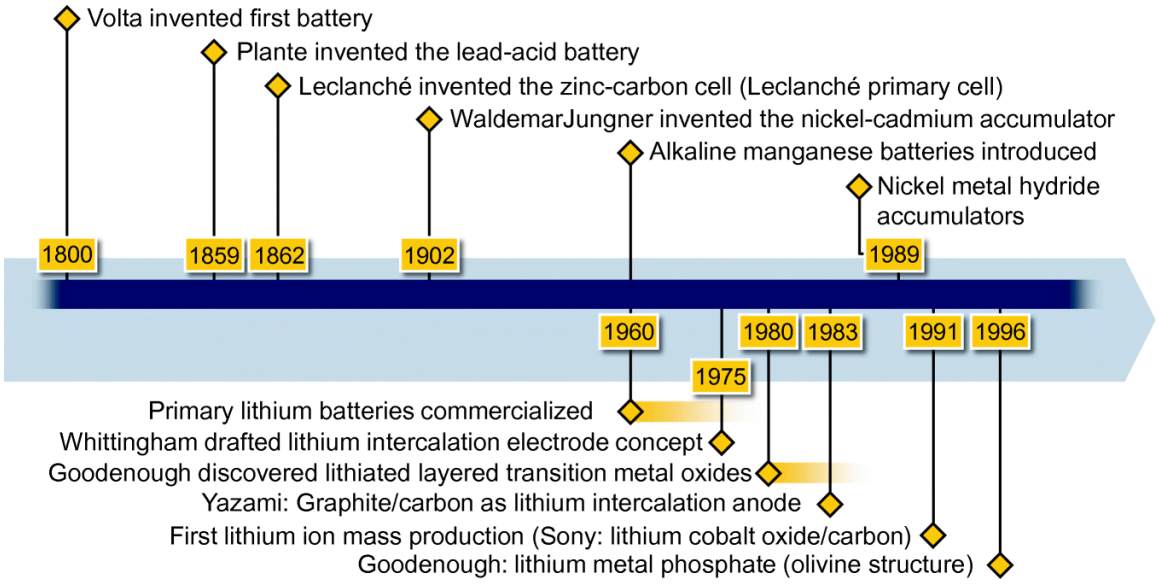

Figure 1-1 Brief history of the invention of batteries.

1.2 Classification of battery

Batteries generally can be classified into different categories and types, ranging from chemical composition, size, form factor and use cases, but under all of these are two major battery types, primary batteries and secondary batteries.

A primary cell or battery is one that cannot easily be recharged after one use, and are discarded following discharge. Most primary cells utilize electrolytes that are contained within absorbent material or a separator (i.e. no free or liquid electrolyte), and are thus termed dry cells.

A secondary cell or battery is one that can be electrically recharged after use to their original pre-discharge condition, by passing current through the circuit in the opposite direction to the current during discharge.

The following table summarizes the *pros* and *cons* of primary and secondary batteries.

Table 1-1 A comparison of pros and cons between primary batteries and secondary batteries.

Primary	Secondary
Lower initial cost.	Higher initial cost.
Higher life-cycle cost ($/kWh).	Lower life-cycle cost ($/kWh) if charging in convenient and inexpensive.
Disposable.	Regular maintenance required.
Disposable.	Periodic recharging required.
Replacement readily available.	Replacements while available, are not produced in the same sheer numbers as primary batteries. May need to be pre-ordered.
Typically lighter and smaller; thus traditionally more suited for portable applications.	Traditionally less suited for portable applications, although recent advances in Lithium battery technology have led to the development of smaller/lighter secondary batteries.
Longer service per charge and good charge retention.	Relative to primary battery systems, traditional secondary batteries (particularly aqueous secondary batteries) exhibit inferior charge retention.
Not ideally suited for heavy load/high discharge	Superior high discharge rate performance at

rate performance.	heavy loads.
Not ideally suited for load-leveling, emergency backup, hybrid battery, and high cost military applications.	Ideally suited for load-leveling, emergency backup, hybrid battery and high cost military applications.
Traditionally limited to specific applications.	The overall inherent versatility of secondary battery systems allows its use and continuing research for a large spectrum of applications.

Li-ion battery is a typical secondary battery, and its structure and principle of operation was illustrated in **Fig. 1-2**.

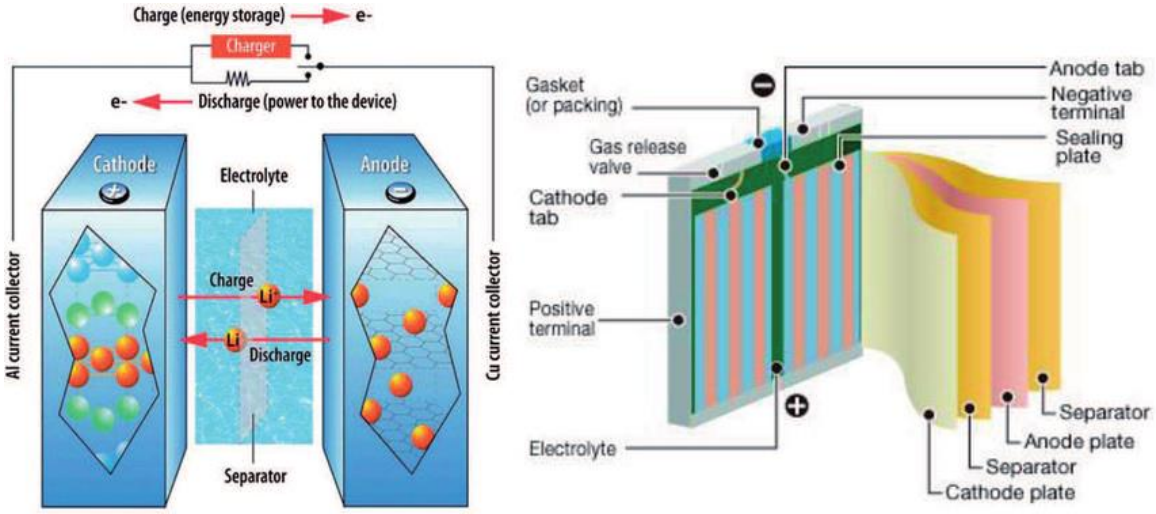

Figure 1-2 Structure and principle of operation of a Li-ion battery.

1.3 Global battery market

The global battery market is expected to reach USD 132.55 billion by 2024, according to a new report by Grand View Research, Inc. Majorly consisting of primary and secondary batteries, the growth will be attributed to growing demand for secondary batteries that are rechargeable on account of rising demand for smart gadgets and electronics such as tablets, smartphone and other portable devices including the digital camera and laptop.

Technological advancements in terms of cost reduction and enhanced efficiency are expected to open new avenues for the global market over the forecast period. Rising use in aircraft emergency systems in case of non-availability of APU's for braking, ground operations and restarting the APU is expected to fuel high capacity battery demand. Low cost and high density of lead acid battery will encourage

use in an emergency power supply and grid storage applications thus supplementing the market growth.

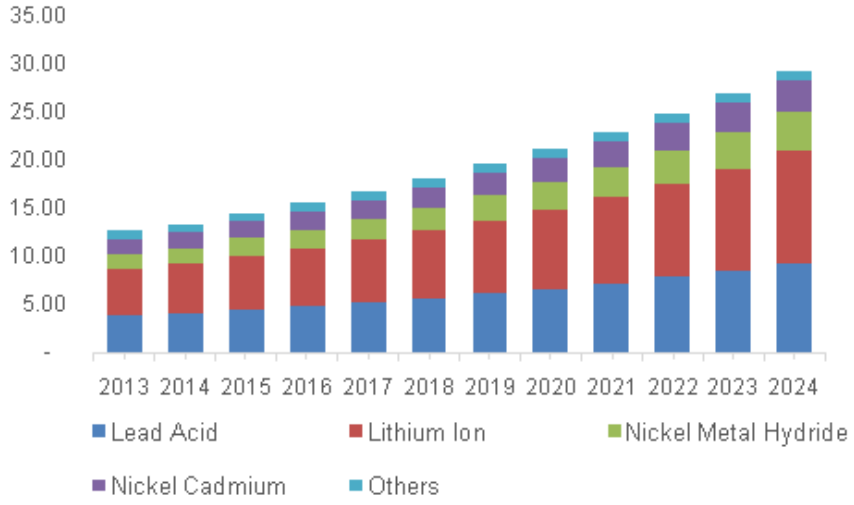

Figure 1-3 The change of different type batteries market share over time.

The substantial benefits that lithium-ion technology offer over lead-acid technology means that using lithium-ion batteries is becoming an ever more popular choice. Lithium-ion batteries has become an increasingly popular choice with substantial advantage of lithium-ion technology over lead-acid technology. The global lithium-ion battery market trend was analyzed in **Fig. 1-4**. From 2016 to 2024, gross annual growth rate of lithium-ion battery market is expected to reach 10.6%.

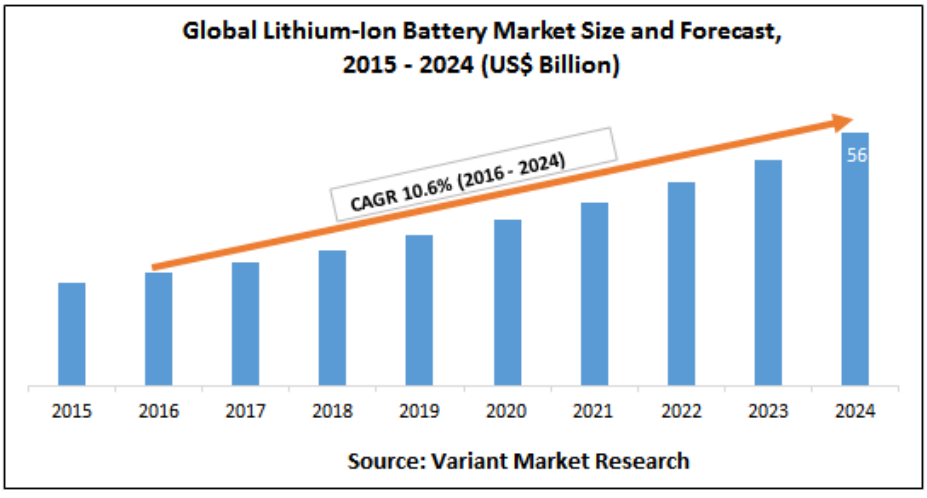

Figure 1-4 Global lithium-ion battery market size and forecast, 2015-2024 (USD Billion).

2 Main Lithium-ion Battery Materials in Practice

In this chapter, the main lithium-ion battery materials including electrode composite, electrolyte and polymeric separator will be introduced briefly. Due to my research is mainly on designing and modifying water-soluble polymer binder, it will have some paragraphs emphasize on binders related to my research.

2.1 Lithium-ion batteries components and materials

As shown in Fig. 2-1, the full cell of lithium-ion battery mainly contains: A-current collector, B-anode, C-electrolyte, D-cathode, E-current collector.

The structure of most common lithium-ion batteries is like a sandwich which include cathode-electrolyte-anode[1]. In our research, we just focus on the LIB with liquid organic lithium-ion solution (containing solvents and Li salts) as the electrolyte. The coin cell was assembled by rolling and crimping within a vacuum glove box. Then the organic electrolyte can wet cathode and anode materials, porous polymeric separator and all parts inside of the coin cell, it's beneficial to active materials happen electrochemical reactions and transport the ions and electrons during charge/discharge process. Outside of the sandwich is current collector, usually Cu foil at the anode side and Al at the cathode side. The electrode composites involve the active material powder of spherical or ellipsoid particles with diameters ranging from nanometers to micrometers. The active materials are mixed with conducting additives and binder form a slurry, and then coat it on current collector through coating machine to product the electrode.

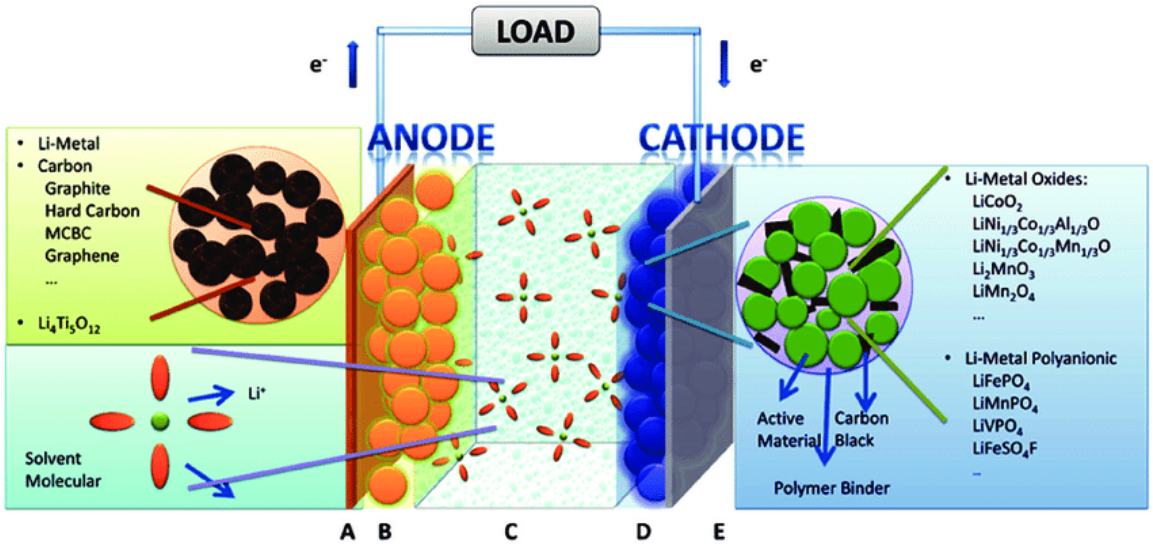

Figure 2-1 The hierarchical structure of lithium-ion batteries.

As a matter of fact, the working principle of lithium-ion battery is the transportation and storage of Li^+ and electrons inside and outside of battery. During the charge process (as shown in Tab. 2-1), Li^+ migrate from the negative electrode (anode, e.g. lithium-metal-oxide, where the metal can be manganese, cobalt, iron, etc.) towards the positive electrode (cathode, e.g. graphite) by the oxidizing anode producing an equivalent number of electrons. In this period, the electrons transport to the positive electrode through the external circuit[2].

As a matter of course, the discharge process is reverse compare to the charge process, where LiC_6 releases Li^+ which transport through the electrolyte and rejoin the metal-oxide to produce $LiMO_2$.

During the lithiation/delithiation process, the oxidation occurs at the anode, and reduction occurs at the cathode. The overall electrochemical equation is displayed in Tab. 2-1[3].

Table 2-1 Electrochemical reaction during charge/discharge process.

Electrode	Charge	Discharge
Cathode	$LiMO_2 \rightarrow Li_{1-x}MO_2 + xLi^+ + xe^-$	$Li_{1-x}MO_2 + xLi^+ + xe^- \rightarrow LiMO_2$
Anode	$C + y\,Li^+ + ye^- \rightarrow Li_yC$	$Li_yC \rightarrow C + yLi^+ + ye^-$
Overall	$LiMO_2 + \frac{x}{y}C \rightarrow \frac{x}{y}Li_yC + Li_{1-x}MO_2$	$\frac{x}{y}Li_yC + Li_{1-x}MO_2 \rightarrow LiMO_2 + \frac{x}{y}C$

2.1.1 Cathode active materials

Various cathodes materials are used in commercial lithium-ion batteries to meet various applications at present, as shown in Tab. 2-2. Most of the cathode materials have layered structure, which is beneficial to release and storage the Li^+ during charge/discharge process. Besides, there are also some other structures like spinel and olivine[4–8]. Nowadays, all the attention is paid on several cathode materials displayed in Tab. 2-2. The Li-cobalt cathode is commonly used in mobile phones, tablets, laptops and cameras. On the other hand, the derivative Ni additive cathode is applied on more powerful devices like medical and industrial devices, and transportation tools, etc.

The layered oxides such as $LiCoO_2$ suffers from the instability that limits their potential window and capacity. Moreover, the toxicity and the high production cost of the Co-based materials are undesirable. On the other hand, Li-rich layered oxides ($Li_{1+x}M_{1-x}O_2$)[9], where M is a mixture of transition metals (Ni, Mn, and Co), is promising as they can work at high discharge voltages of >4.5 V and deliver high specific capacities. However, they suffer from large voltage decay during cycling and high irreversible capacity loss at the first cycles, which limit their use. Moreover, olivine materials

such as $LiFePO_4$ are competitive candidates surpassing the stability of layered oxides at elevated temperatures due to their high thermal and structural stability[10]. However, their low electronic and ionic conductivity stand as an obstacle to expand their use for high energy Li-ion batteries.

The well-designed cathode materials must have the following several criterions[11]: (1) energy density; (2) rate capability; (3) cyclic performance; (4) safety and eco-friendly; (5) cost. The cathode structure and the ratio of every elements would affect the electrochemical performance, so we should design the better cathode materials step by step.

Table 2-2 Characteristics of commercial lithium-ion battery cathode materials.

Material	Structure	Potential vs. Li/Li+, average V	Specific capacity, mAh/g	Specific energy, Wh/kg
$LiCoO_2$	layered	3.9	140	546
$LiNi_{0.8}Co_{0.15}Al_{0.05}O_2$	layered	3.8	180-200	680-760
NCA				
$LiNi_{1/3}Co_{1/3}Mn_{1/3}O_2$	layered	3.8	160-170	610-650
NMC				
$LiMn_2O_4$	spinel	4.1	100-120	410-492
Variants (LMO)				
$LiFePO_4$ (LFP)	olivine	3.45	150-170	518-587

2.1.2 Anode active materials

The anode plays a critical role in lithium-ion batteries working process which can directly influence the battery's electrochemical performance. The battery's behavior would be determined by anode active material's physical and chemical properties to a great extent, so it should be considered and controlled when designing a new anode active material. Some excellent characteristics of the raw materials make them effectively apply in lithium-ion batteries as anode. However, they have some natural defects which limit their applications in a wider field. Hence, choosing the anode material properly and modifying or designing them correctly is very important for improving the battery's electrochemical performance. The most widely used anode active materials were presented in Fig. 2-2[12].

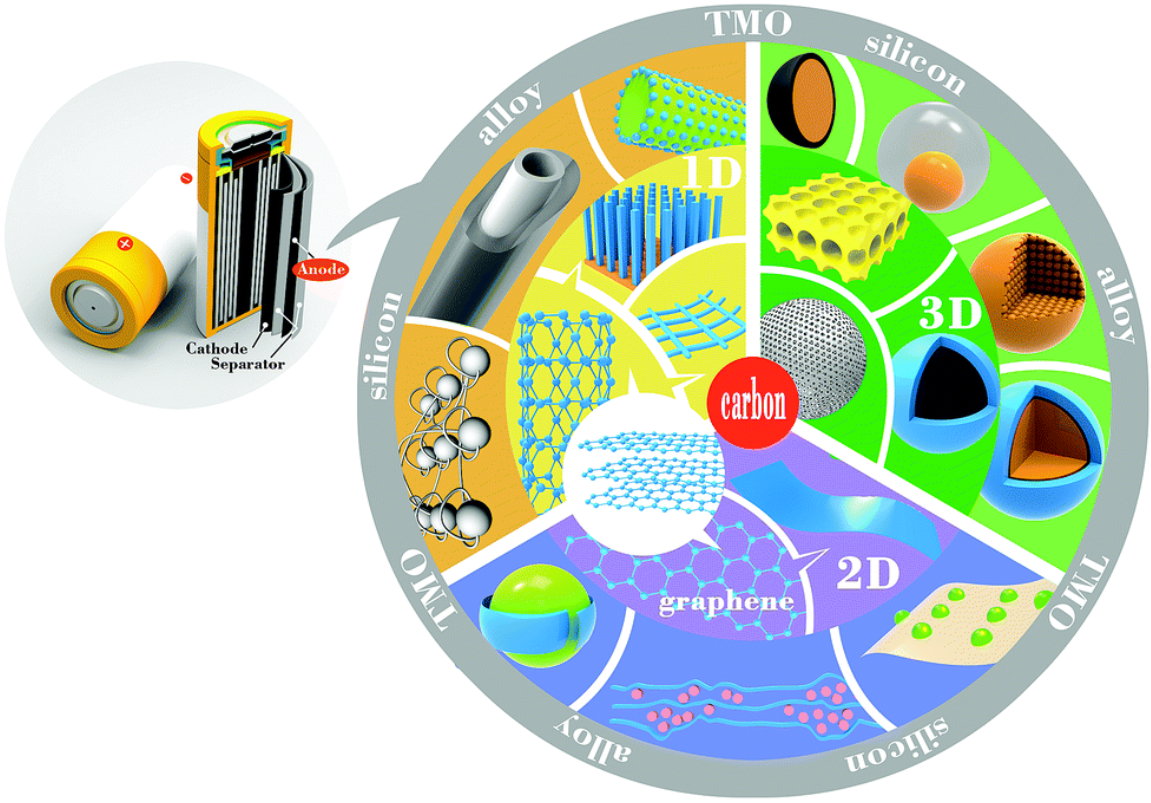

Figure 2-2 Schematic diagram of the recent anode materials for lithium-ion batteries.

From the statement of last paragraph, we know the anode plays an important role in the whole battery performance. The battery behavior not only depends on the intrinsic properties of the anode material including the physical and/or chemical properties and energy storage capacity, but also lies on the crystallinity or amorphous structure of the anode material as well as the shape, size and component state. Although some inherent properties of the material make it stand out for lithium storage, crude material without architectural arrangement may present issues during charge/discharge process (Tab. 2-3)[13–16]. Hence, the appropriate structural design is more important than the selected material. In my research, a kind of core-shell structure Si-based anode material was designed for prolong the battery's cycle life with comparatively high stable capacity.

Table 2-3 The advantages and disadvantages of different anode materials.

Material	Advantages	Disadvantages
Carbon	(1) High electronic conductivity (2) Nice hierarchical structure (3) Abundant and low-cost resources	(1) Low specific capacity (2) Low rate capacity (3) Safety issues
Alloys	(1) High specific capacity (400–2300 mAh g^{-1})	(1) Low electronic conductivity

	(2) Good security	(2) Large volume change (100%)
Transition metal oxides	(1) High specific capacity (600–1000 mAh g^{-1}) (2) Nice stability	(1) Low coulombic efficiency (2) Large potential hysteresis
Silicon	(1) Highest specific capacity (4200 mAh g^{-1}) (2) Rich, low-cost, clean resources	(1) Large volume change (300%)

2.1.3 Auxiliary materials: Conductive additives and binders

Except anode or cathode active material and current collector, the electrode also including another two auxiliary materials: conductive additive and binder. Even they occupy a small ratio in the electrode composite, they play a key role in lithium-ion batteries, they are essential for keeping battery working properly in a high efficiency.

Binder and conductive additives are located in the spaces between the active material particles to bind the particles and to make electrical contact between the active materials particles. Nowadays, most commonly used conductive additives contain carbon black, super P, VGCF and CNT with small particle size and large specific surface area[17–20]. The conductive additives can improve the electron transportation efficiency and reduce the inner resistance of the batteries. PVDF is one of the most widely used conventional binders in lithium-ion batteries due to its binding capability, good electrochemical stability, and the ability to transport ions to the active material surface. However, PVDF need the toxic NMP solvent, it's harmful to our health and environment[21–24]. At present, much more attention was paid on eco-friendly water-soluble natural binders and its derivatives. It will be introduced in detail in the following independent section.

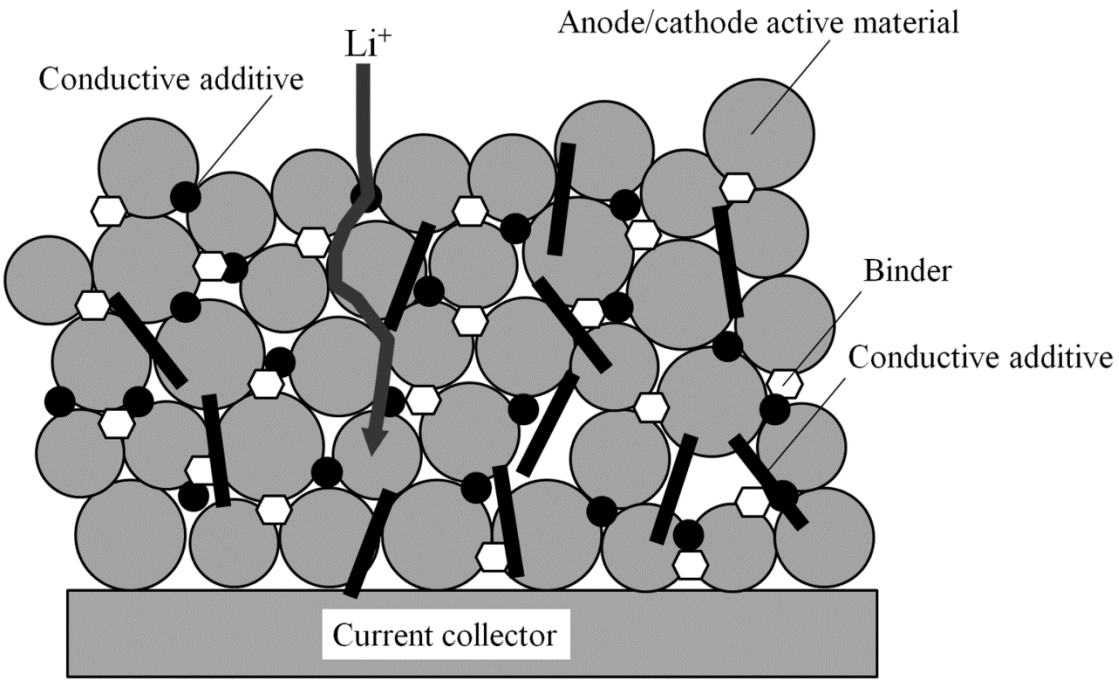

Figure 2-3 Schematic description of the active material layer formed on the current collectors in a lithium-ion battery.

2.1.4 Electrolyte

As the "blood" of battery, electrolyte is an indispensable solvent providing the path for Li^+ movement, Li^+ migrate backward and forward between negative and positive electrode during lithiation/delithiation process. Generally, the electrolyte system consists of a lithium salt (1 M), dissolved in a mixture of different linear carbonates, e.g., dimethyl carbonate (DMC), ethyl methyl carbonate (EMC) or dimethyl carbonate (DEC), and a cyclic carbonate such as propylene carbonate (PC) or ethylene carbonate (EC), all of the chemical structures as shown in Fig. 2-4[25–27]. The most commercially applied lithium salt is lithium hexafluorophosphate ($LiPF_6$) while alternatives such as lithium tetraborate ($LIBF_4$), lithium bis-(oxalato)borate (LiBOB) or ionic liquids (ILs) are possible[25,28–32]. Electrolyte additives are used up to 5%, either by weight or by volume[33]. Due to the application of additives, the electrolyte properties can be influenced: improvement of the flammability, enabling overcharge protection[33–35] or the SEI formation[36–41]. The SEI is formed during the first charge/discharge (formation cycles) of the LIB cell and is essential for safety and performance due to its protection of the electrolyte from further reductive decomposition at the anode surface[42–44].

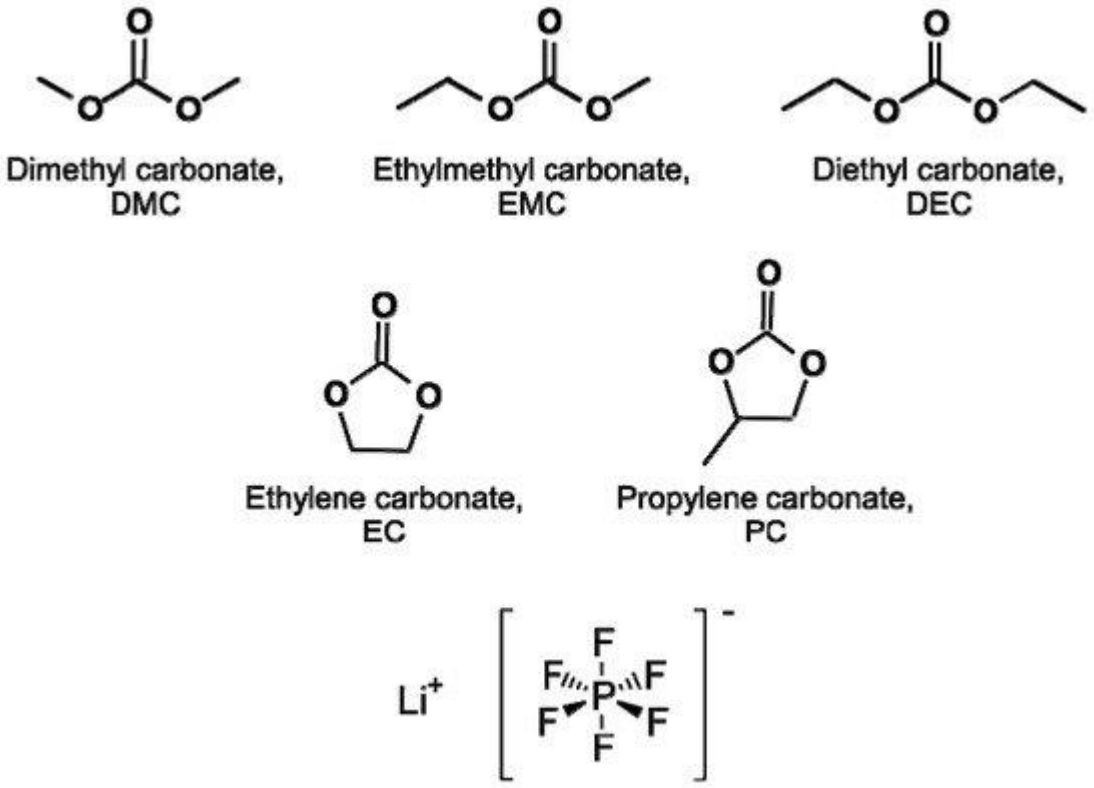

Figure 2-4 Structures of six of the most important linear and cyclic organic carbonates and the conducting salt lithium hexafluorophosphate for the electrolyte system in lithium-ion batteries.

2.1.5 Porous separator

One of the most crucial important battery components to ensure the battery working in safety is the porous polymeric separator, a thin membrane that physically separates the anode and cathode to avoid battery short circuit, the SEM image of separator applied in lithium-ion batteries as shown in Fig. 2-5. The primary function of the separator is to prevent the direct physical contact between the anode and cathode, in the meantime, it facilitate the Li^+ to move back and forth inside of the battery.

Nowadays, various porous separators can be selected for lithium-ion batteries, but the most commonly used separators are PP (Polyproylene), PE (Polyethylene) and PP/PE/PP[45–47]. The challenge with designing safe battery separators is the balance between mechanic robustness and porosity/transport properties[48]. The separator design should consider following limits: (1) it can endure the serious condition, stable at > 4 V; (2) it doesn't react with other chemicals inside of the battery; (3) low cost[49].

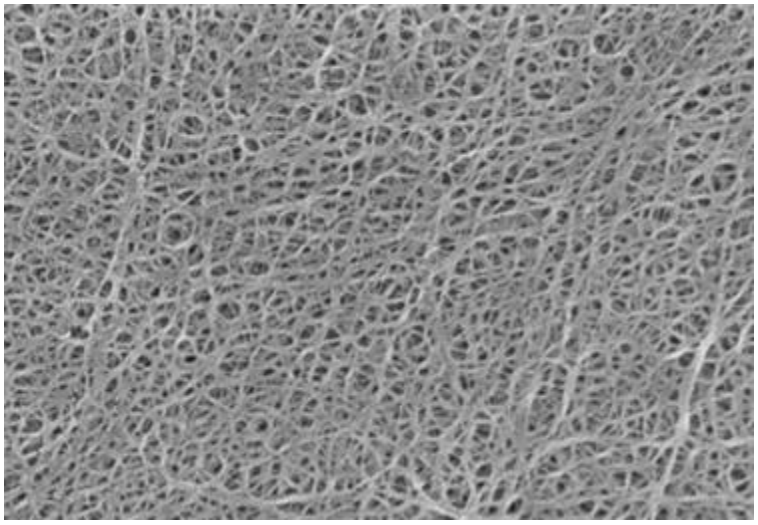

Figure 2-5 SEM image of porous polymeric separator membrane for lithium-ion batteries.

2.2 Detailed introduction of binders for lithium-ion batteries

In LIBs, a polymeric binder plays an important role to adhere the active materials and ensure the adhesion of the active materials on metallic current collectors like Cu or Al, to form an integrated electrode. However, polymeric binder is a kind of insulate material, to ensure the electrochemical performance of electrodes, uniform binding by a polymeric binder is required to be maintained after the liquid electrolyte is absorbed into the binder matrix. Of course, the binder should be insoluble in a liquid electrolyte and should have good chemical stability against lithium salts and SEI components such as Li_2CO_3, LiF, and LiOH[50–52]. More importantly, it was demonstrated that the mechanical strength of a binder in a dry state can be changed by the binder-electrolyte interaction. This means that the swell ability of the binder in the electrode with the electrolyte affects the mechanical strength (binding ability and adhesion property) of the binder.

There are many kinds of structured polymeric binders were explored by researchers, most of them were applied to the Si-based anode and can obtained better battery performance, as shown in Tab. 2-4[53–56].

Table 2-4 Various structured polymer as binder system.

	Linear-type		Branched-type	Crosslinking	Self-healing
	Homopolymer	Copolymer			
Polymer chemistry		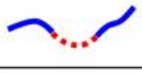		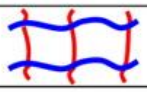	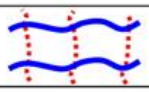
	Identical unit	Two or more different monomer units	Formed by the replacement of a substituent	3D crosslinked structure based on chemical covalent bond	3D crosslinked structure based on hydrogen bond
Binders	PVDF, CMC, PVA, PAA, PAA-Na	SBR, alginate, P(AA-co-VA)	β-cyclodextrin (β-CDp)	PAA-CMC, PVA-PAA, c-PAA	
Function	No/weak interaction between a binder and Si	Weak interaction between a binder and Si	Strong interaction between a binder and Si	Covalent bond between a binder and Si	Recovering binder-Si or binder-binder interaction

On the other hand, various polymeric binders are applied in lithium-ion batteries commercially, it also can be classified into two types: organic-based binder and water-based binder according to the different solvents.

2.2.1 Organic-based binders

One of the typically organic-based binders is PVDF, which is the most commonly used binder for both anode and cathode of LIBs due to the excellent electrochemical and thermal stability and good adhesion between the current collectors and electrode films. Whereas, application prospect of PVDF was limited due to some drawbacks like low flexibility, readily swollen at elevated temperatures, more seriously and also should dissolved in the organic solvent such as N-methyl-2-pyrrolidone (NMP), N,N-dimethylacetamide (DMAc), N,N-dimethylformamide (DMF). As we know, the most common organic solvent of NMP was expensive, volatile, combustible, toxic, low flexibility, and poor recyclability[22,57–60].

2.2.2 Water-based binders

In the last few years, lots of efforts have been paid attention to seek for alternative water-based polymers to build up the electrochemical performance. For example, Alginate[61,62], CMC[63,64], SBR[65,66],

LA_{133}[21,67], polyacrylic acid (PAA)[68,69], polyvinyl alcohol (PVA)[70,71], polyethylene glycol[72,73] (PEG has been successfully used in LIBs because it was cheaper, was environmentally friendly, and also has the better solubility), and polyamide imide (PAI)[74,75] have possibly used water instead of NMP. At the same time, some natural polysaccharides like chitosan[76–78], starch[55,79,80], and agarose[81], were widely applied to lithium-ion batteries as anodic binders for different type anodes, and many kinds of gums[82–84] also showed remarkable performance such as an increase in the cycling stability of silicon anodes at rigorous temperature and high mechanical properties because of their numerous hydroxyl and carboxylic groups.

There are so many advantages by using water-based binders for lithium-ion batteries[85,86], like (1) no more usage of organic (toxic) solvents in the mixing and coating processes; (2) reduced manufacturing cost of aqueous vs. solvent processing. Elimination of expensive solvent recovery steps, reduction of capital cost for coating equipment and elimination of expensive inactive components; (3) simplification of machinery. Machinery size reduction (water extraction is faster than NMP one, therefore the drying section for coating line is reduced); (4) fast drying speed and low drying temperature require less electric power and yield to higher production rate; (5) no dry room required for cell assembly, only humidity control is required during electrolyte filling, etc.

2.2.3 Our research objects

The effective binders applied in lithium-ion batteries should better possess following characteristics: (1) good cohesion and adhesion ability; (2) electrochemical stability in the required serious potential; (3) undergo minimal electrolyte-swollen; (4) good ionic and electronic conductivity. Some raw binder materials have natural advantages to enhance the battery's performance, but they also have some defects that limit their wider applications. When design some new binders, the selected raw polymeric binders are important, and in the meantime we should remedy the defects on raw binders or endow them some new properties through modifying or graft polymerization and other methods, then we can get a novel binder which have more advantages and less disadvantages.

In our research, we focus on designing or modifying water-soluble binders for anodes. Alginate and CMC are both natural water-soluble polysaccharide binders which have abundant carboxyl groups and hydroxyl groups on the backbone of them, so they have excellent adhesion strength for anodes in lithium-ion batteries, especially for Si-based anode.

Hence, we choose Alginate and CMC as our research objects, and we introduce the $-SO_3H$ to the backbone of them to improve the ionic conductivity, we obtained the better electrochemical performance when employing the new modified binder Alg-S and CMC-S to the $Li_4Ti_5O_{12}$ in the first

research. In the second research, we grafted AA (Acrylic acid) and BA (Butyl acrylate) monomers to the backbone of Alg through copolymerization, forming a novel binder Alg-ABAA, after that, the conducting material MXene was also chemically connected with Alg-ABAA, and obtained high adhesive and conductive binder Alg-AABA-Mx. It also got better electrochemical performance when use them as binders for SiNPs anode.

3 Electrochemical Performance of Polysaccharides Modified by the Introduction of SO_3H as Binder for High-powered $Li_4Ti_5O_{12}$ Anodes in Lithium-ion Batteries

3.1 Introduction

LIBs are widely utilized in portable electronics, power tools, and hybrid/full electric vehicles due to their high energy and power densities[87,88]. LIBs consist of four main components: anode and cathode materials, organic electrolyte, and polymer separator. Although polymeric binder occupies a small portion in the LIB electrode, it is a crucial component to maintain electrode integrity, to improve the cell performance, and especially to prolong the cycle life[89,90].

PVDF is the most common binder for LIB because of its superior chemical, electrochemical, and thermal stabilities, and moderate adhesion between active materials and current collectors[21,22]. However, it suffers from problems such as the use of toxic organic solvents (e.g. N-methyl-2-pyrrolidone), low flexibility, high cost and poor recyclability[91,92]. In the last few years, much attention has been paid to alternative water-soluble or water-dispersed binders, for example, sodium-alginate (Alg)[61,62], carboxymethyl cellulose (CMC)[63,64], styrene-butadiene rubber (SBR)[65,66], polyacrylic acid (PAA)[68,69], and other water-based polymers[93–95], which showed many advantages like environmentally friendly, good electrochemical performance, high adhesion to the current collector and an excellent electrochemical stability under the experimental conditions employed[96]. In addition to typical water-soluble polysaccharide binders such as CMC and Alg, some natural polysaccharides like chitosan[97–99], starch[79,100,101], and agarose[81], were widely applied to lithium-ion batteries as anodic binders for different type anodes, and many kinds of gums[82–84] also showed remarkable performance such as an increase in the cycling stability of silicon anodes at rigorous temperature and high mechanical properties because of their numerous hydroxyl and carboxylic groups.

In the meantime, many researchers developed different strategies to modify those binders to enhance their performance and endow them with other novel properties, such as strong adhesion, and good ionic and electronic conductivities[102,103]. Qin et al[104]. synthesized novel ionic binders containing fluorinated sulfonic acid side chains to facilitate the transportation of Li^+ ions during high rate charging/discharging. It was also reported that lithium ion-exchanged Nafion as a binder for high capacity silicon electrodes improved the cycling performance and protonic conductivity due to the sulfonic acid groups ($-SO_3H^+$) in the Nafion[105]. Our study here is to introduce the sulfonic acid groups to the backbone of the Alg and CMC binders in order to boost their ionic conductivity and to

investigate the effect of functional groups on the electrochemical performance in high-powered $Li_4Ti_5O_{12}$ electrode, resulting from better ionic conductivity.

3.2 Experimental

3.2.1 Synthesis of sulfonated alginate and carboxylmethyl cellulose

Sodium-alginate (CAS no.9005-38-3) and sodium-carboxymethyl cellulose (CAS no.9004-32-4) were obtained from Alfa Aesar. N-Hydroxysuccinimide (NHS, Alfa Aesar) and 1-(3-Dimethylaminopropyl)-3-ethylcarbodiimide hydrochloride (EDC, Sigma-Aldrich) were used to activate the carboxy groups in Alg and CMC. 3-Amino-1-propanesulfonic acid (Sigma-Aldrich) was used to introduce sulfonic acid functional groups in this amidation reaction.

1 g of purified Alg was added in 100 mL of phosphate buffer solution (PBS, pH 6.0) with stirring until Alg was totally dissolved. 4.8 g EDC and 1.09 g NHS dissolved in PBS buffer were added to the Alg-PBS solution to activate the carboxylic acid groups in the Alg. The resulting mixture was stirred at room temperature for 15 min and 3-amino-1-propanesulfonic acid (1.04 g) was subsequently added to the Alg-PBS solution. After then, triethylamine (TEA) was added dropwise into the above solution to adjust pH to 7.4. This mixture solution was vigorously stirred for 9 h at room temperature. The crude product collected by suction filtration was repeatedly washed with ethanol and water for three times. The final product, denoted as Alg-S, was dried in a vacuum oven at 50 °C before use. The CMC-S was produced with the same method as Alg-S.

3.2.2 Preparation of electrodes and coin cells

In this research, the lithium titanium oxide ($Li_4Ti_5O_{12}$, LTO) adopted in this study was purchased from Posco ESM Co., (davg=10 μm). Alg-S/LTO electrodes were prepared by mixing the LTO particle, super P, and as-prepared Alg-S binder by a weight ratio of 80:10:10 respectively in an adequate amount of distilled water. In case of CMC-S binder, SBR was also used to keep the integrity of anode due to extremely brittle CMC characteristics, and the weight ratio of LTO particles, super P, SBR, and CMC-S is 80:10:5:5. After mixing in a planetary ball mill at 500 rpm for 30 min, a homogeneous slurry was obtained and coated onto 20-μm-thick Al-foil by an automatic film-coating apparatus. The electrodes thereafter were dried at 60 °C for 30 min in a convection oven and in a vacuum oven for a whole night to completely remove remaining solvent before coin cell assembly. The mass loading of the electrodes were 3 ± 0.5 mg/cm^2. As references, the electrodes using pure Alg and CMC were prepared according to the same procedure. 1 M $LiPF_6$ in 1:1:1 ethylene carbonate : dimethyl carbonate : ethyl methyl carbonate by volume (Panaxetec Co., Korea) was used as electrolyte in

CR2032 coin-half cells. These were assembled in an argon-filled glove box with lithium foil as a counter electrode.

3.2.3 Characterization of materials and electrochemical properties

In this research, the structure analysis of the modified Alg and CMC binders were recorded by nuclear magnetic resonance (NMR) spectroscopy (Bruker Avance™ III HD 300MHz, Switzerland) and Fourier transform infrared (FT-IR) spectroscopy (Thermo Scientific™ Nicolet™ iS™). A video-connected device (Theta Lite 100, KSV Instrument Ltd.) and a texture analyzer (TA-PLUS, Lloyd Instruments Ltd.) were used to measure the contact angles of thin binder films and 180° peel strength of the LTO electrodes. Electrochemical impedance spectroscopy (EIS) with a frequency range of 100 kHz to 0.01 Hz and cyclic voltammograms (CV) of the coin-half cells at a scan rate of 0.5 mV/s within a voltage range of 1–2.6 V were performed by BioLogic Science Instruments (EC-LAB). The coin cells were galvanostatically charged/discharged from 5 mV to 2.0 V in a battery test system (WBCS3000, Wonatech, Korea) at 0.1 C for the first 2 cycles and at 1 C for the subsequent 100 cycles. The rate capability was also tested at a variety of current rates between 0.1 C and 10 C using a battery cycler (PNE solution Co., Korea).

3.3 Results and discussion

3.3.1 NMR

NMR characterization tool was first used to identify the chemical structures of our products and the result is shown in Fig. 3-1. From the comparison in the NMR spectra between pure original polysaccharides (Fig. 3-1(a,c)) and sulfonated polysaccharides (Fig. 3-1(b,d)), it is clear that some groups of resonance peaks appeared after amidation, indicating the formation of new compounds. In the case of Alg-S (Fig. 3-1(b)), the new main peaks on 3.08, 2.49, 1.85 ppm chemical shift are assigned to the methylene peaks in 3-amino-1-propanesulfonic acid, which was used for introducing sulfonic acid groups. Very similarly, the peaks on 3.05, 2.39, 1.83 ppm chemical shift in the CMC-S sample (Fig. 3-1(d)) are the methylene peaks in CMC-S. These indicate successful synthesis of the sulfonated polysaccharides, Alg-S and CMC-S.

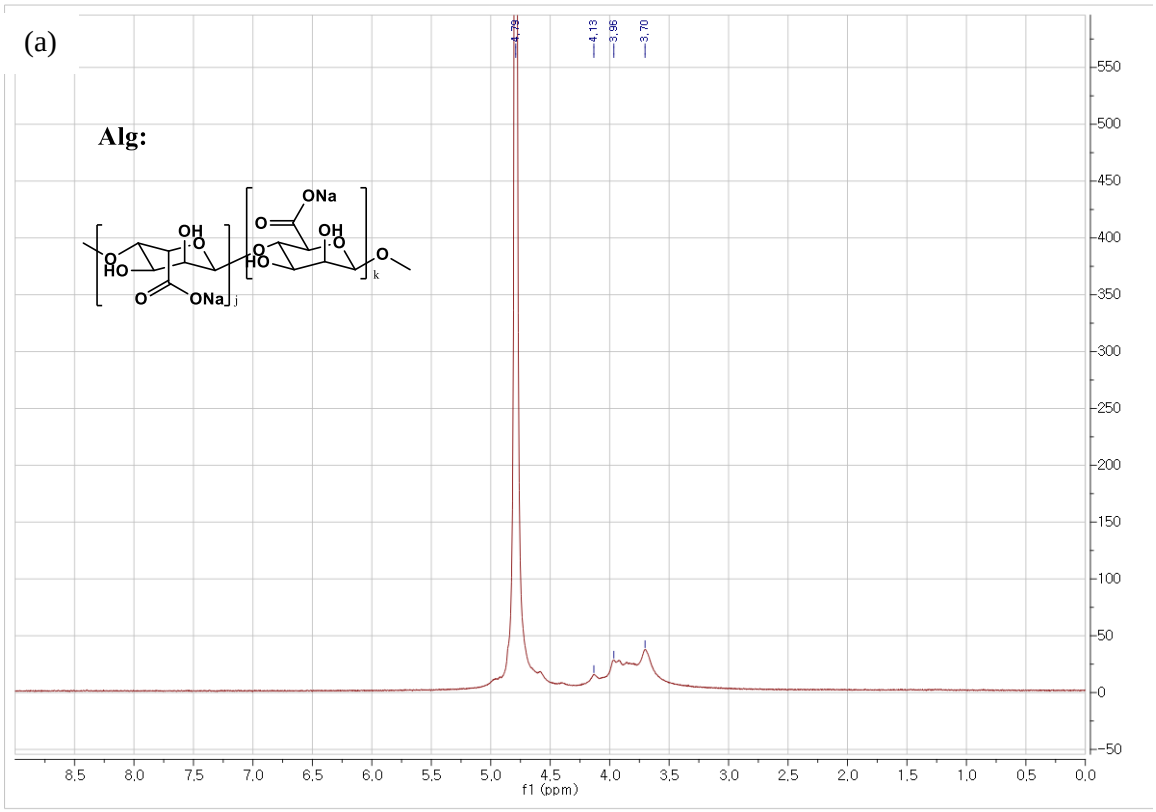
(a)
Alg:
4.79
4.13
3.96
3.70
f1 (ppm)

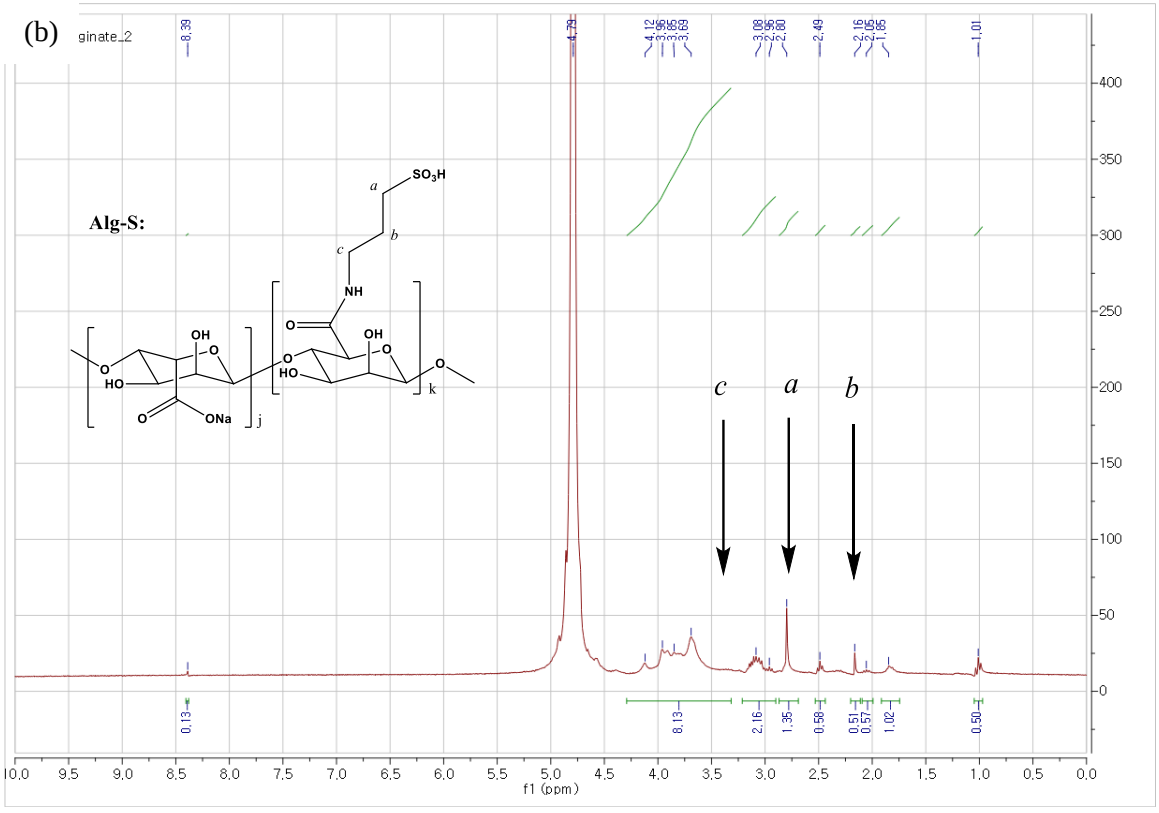
(b)
ginate_2
Alg-S:
8.39
4.79
1.01
c
a
b
f1 (ppm)

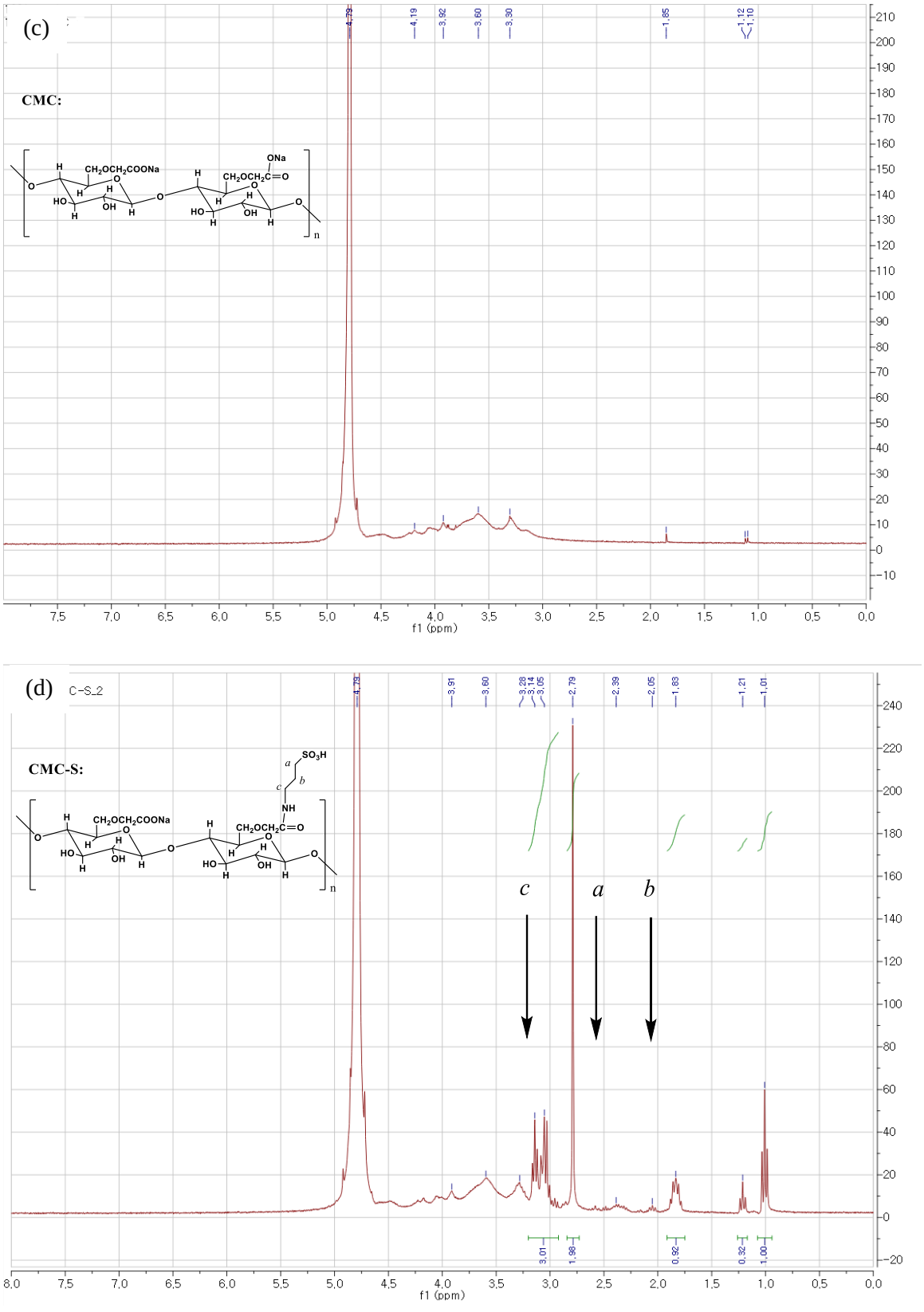

Figure 3-1 NMR spectra of (a) Alg, (b) Alg-S, (c) CMC, and (d) CMC-S.

3.3.2 FT-IR

The successful introduction of the sulfonated functional groups is also confirmed using the FT-IR spectra displaced in Fig. 3-2. The FT-IR spectrum of Alg (Fig. 3-2(a)) showed several bands at 3239, 2934, 1608, 1414, and 1028 cm^{-1}, which are due to the stretching of -OH, -CH, $-COO^-$ (asymmetric), $-COO^-$ (symmetric) and C-O-C, respectively[106]. The peaks corresponding to the $-COO^-$ groups was replaced by those -CO-NH groups[107] at 1713 and 1615 cm^{-1} after the amidation of Alg with 3-amino-1-propanesulfonic acid. Attachment of the sulfonic acid groups to the Alg was clearly shown in the peaks at 565 cm^{-1} and 1068 cm^{-1}, which are attributed to C-S and SO_3^- stretching, respectively. In addition, the peaks at 1127 and 1260 cm^{-1} demonstrate the existence of SO_2 related bonds[108]. A similar explanation can be applied to the FT-IR spectra of the CMC and CMC-S in Fig. 3-2(b). The stretching of -CO-NH blue shifts to 1796 and 1660 cm^{-1}, and the characteristic peaks of $-SO_3H$ distribute at 1357, 1165, 1076, and 525 cm^{-1}.

(a)

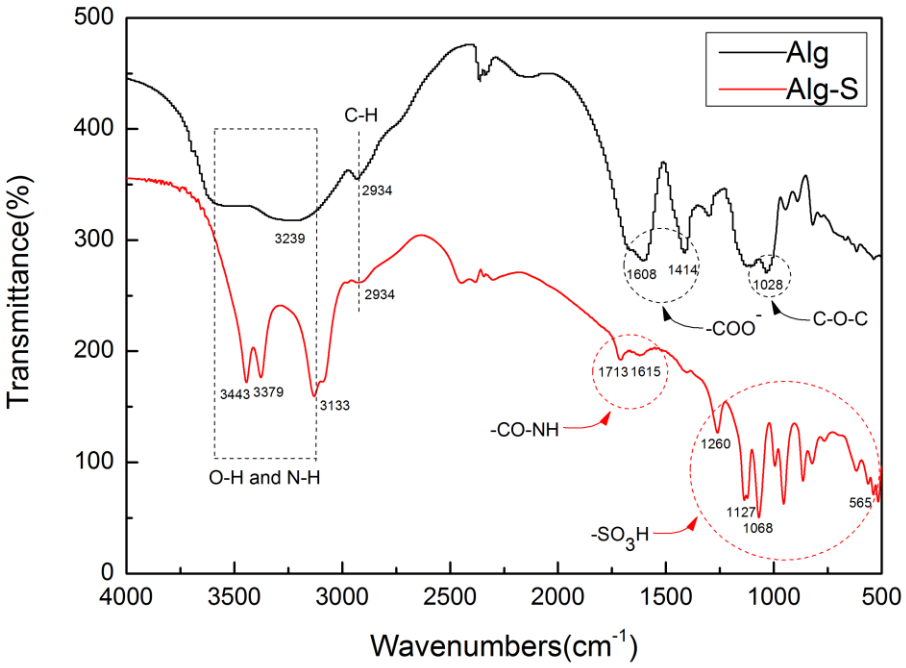

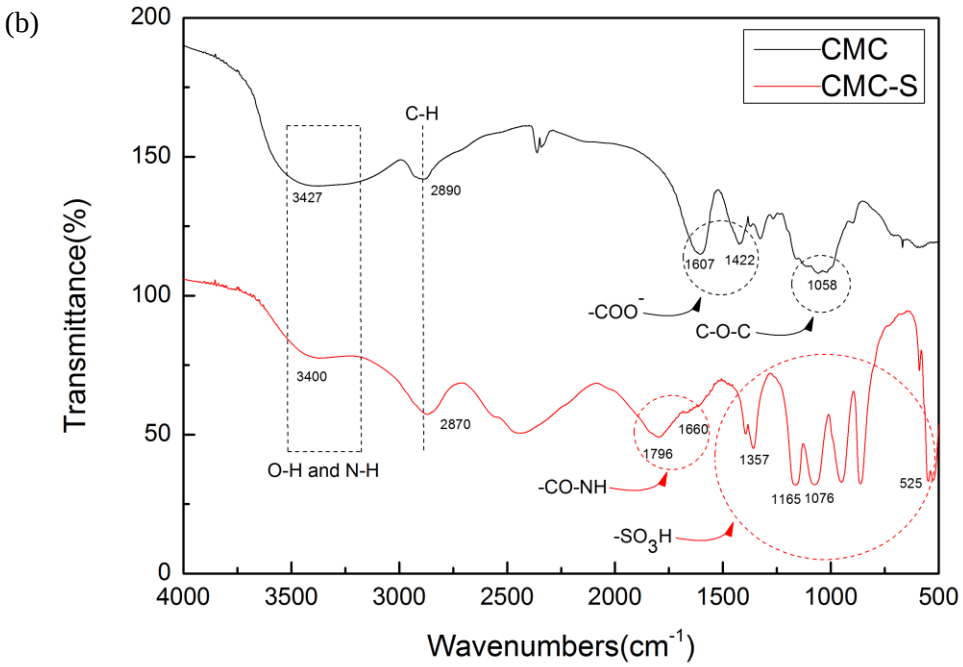

Figure 3-2 FT-IR spectra of (a) Alg and Alg-S and (b) CMC and CMC-S.

3.3.3 Ionic conductivities

It was reported by Su et al.[109] that the -COOH groups in polyacrylic acid and CMC react with Li^+ and form ionically conductive -COOLi during the first Li insertion. They also insisted that the carboxyl groups were ionically conductive through the hopping of Li^+ between the functional groups. On the basis of their supposition, we introduced the $-SO_3H$ groups to the polysaccharides instead of the carboxyl group for the purpose of forming higher ionically conductive $-SO_3Li$, a better chemical environment for lithium ion hopping and moving during the charge and discharge process. As listed in Tab. 3-1, the Alg solution has a lower ionic conductivity regardless of the presence of electrolyte when compared to the Alg-S solution. The same result occurs for the CMC and CMC-S binder solutions.

Table 3-1. Ionic Conductivities of Binder Solution (22.6℃).

Binder solution	Ionic conductivity of binder solution (mS/cm)	
	Without electrolyte	With electrolyte
Alg	14.9	18.0

Alg-S	22.7	22.0
CMC	1.45	1.43
CMC-S	3.51	3.52

3.3.4 Electrical conductivities

Besides, the electrical conductivities of original and modified polysaccharides were measured using EIS of separate polysaccharide binder films without active materials, separator and electrolyte. The binder films are kinds of brittle, in favor of cutting, 30% glycerol was mixed with them to improve their flexibility. These were placed between the stainless metal spacer and bottom case in a coin-type cell and assembled in a glovebox. No electrolyte solution was added to the cell. The electrical resistance (R) can be determined by applying high frequency (from 100 kHz) alternating current across the circuit[110]. From the original EIS spectra (Fig. 3-3), initial 8 points were chosen at the very high frequency region and were fitted. The value of R is the intersection of linearly fitted EIS curve and x axis. Next, the electrical conductivities were calculated using law of resistance as follows:

$$k = \frac{1}{\rho} = \frac{L}{R \cdot S}$$

where k is the electrical conductivity; ρ is the electrical resistivity; L is the thickness of binder film (the thickness of Alg, Alg-S, CMC, CMC-S film is 0.1461 mm, 0.1597 mm, 0.0446 mm, 0.0791 mm, respectively); R and S are the resistance and area of binder film, respectively. By calculation, the electrical conductivities of modified polysaccharides ($k_{Alg\text{-}S}$ is 177.4 μS/cm and $k_{CMC\text{-}S}$ is 43.6 μS/cm) are much higher than original polysaccharides (k_{Alg} is 25.7 μS/cm and k_{CMC} is 10.4 μS/cm), respectively.

(a)

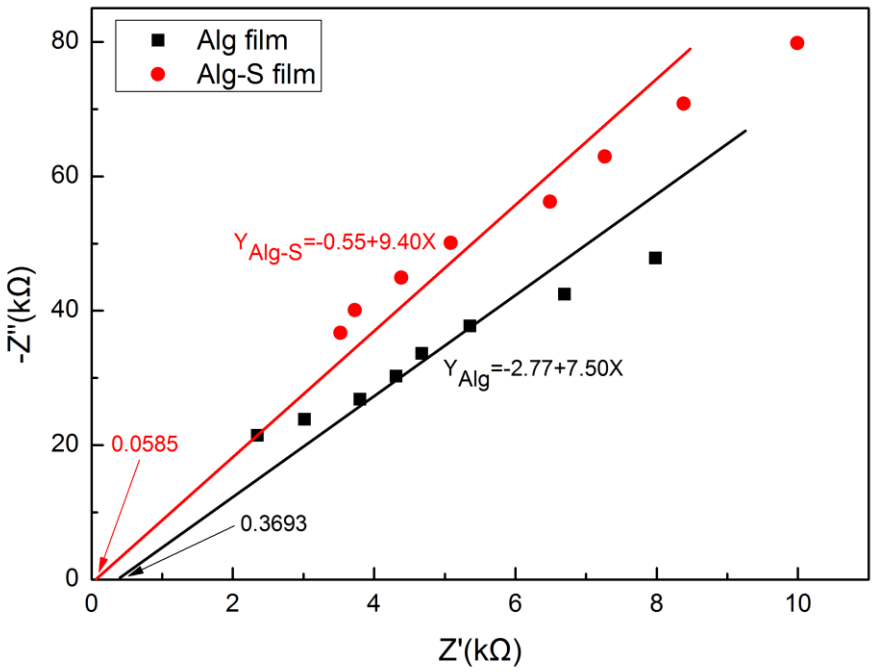

(b)

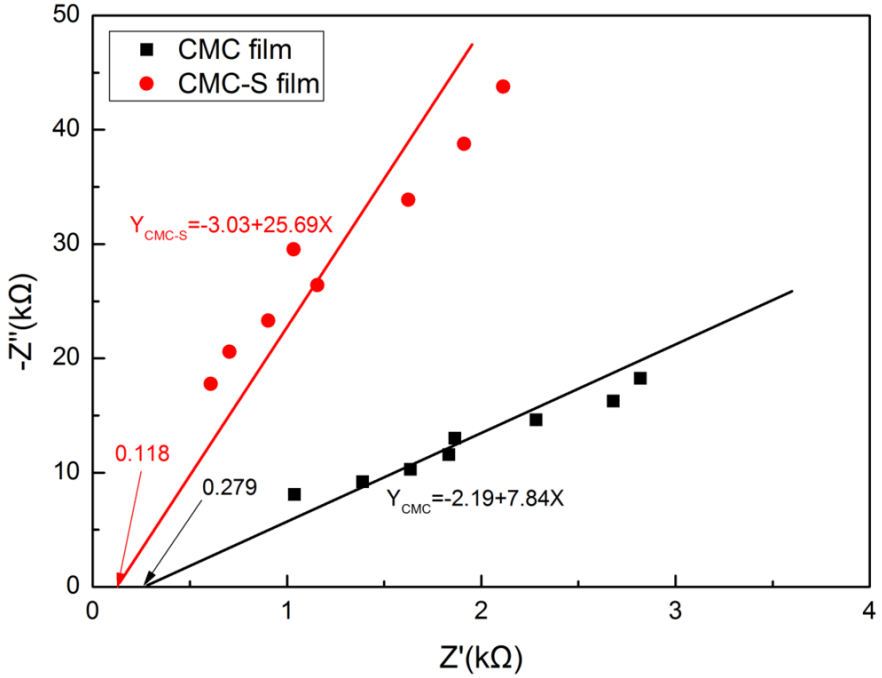

Figure 3-3 EIS spectra of coin-cells consisting of binder films only: (a) Alg and Alg-S, and (b) CMC and CMC-S. Here no electrolyte is added.

3.3.5 Electrolyte uptake and contact angle

It is all known that the extent of the electrolyte uptake of the binder and the electrolyte wettability of the binder film are both significant to affect lithium ions mobility in an electrode. A suitable electrolyte uptake benefits to transport the Li^+ via binder without big change in electrode morphology, though excess amount of electrolyte uptake can change the morphology of binder directly and even destroy the integrity of electrode catastrophically[102]. Traditional PVDF takes in 20-40 wt.% of electrolyte of its weight[111,112], whereas the polysaccharides used here absorb a very small amount of electrolyte: 2.1 wt.% for Alg and 1.5 wt.% for CMC within 6 h as shown in Fig. 3-4(a). On the other hand, the sulfonation of them slightly increases the electrolyte uptake up to 4.4 wt.% for Alg-S and 3.2 wt.% for CMC-S, indicating a possible promotion in the transportation of lithium ion.

(a)

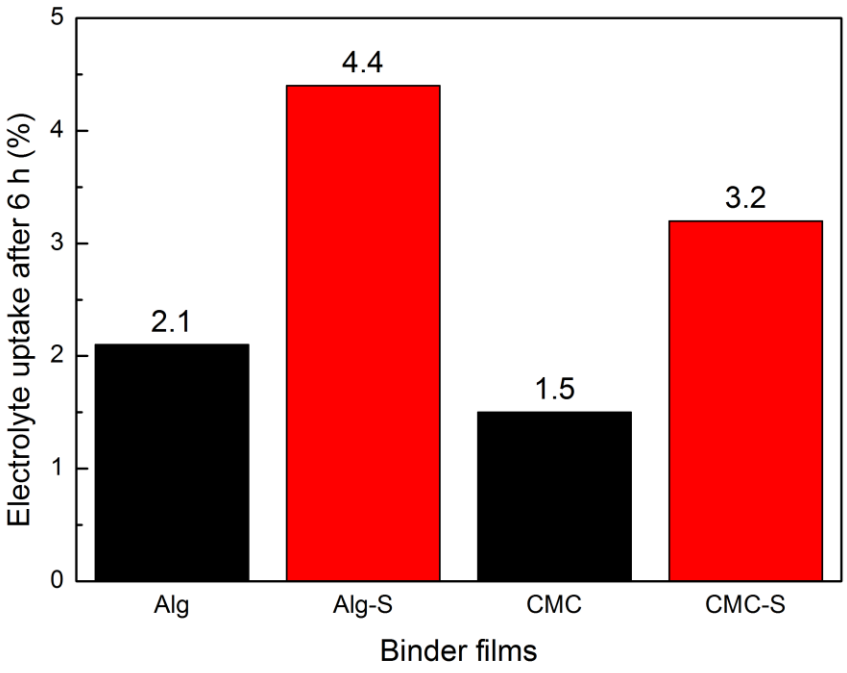

(b)

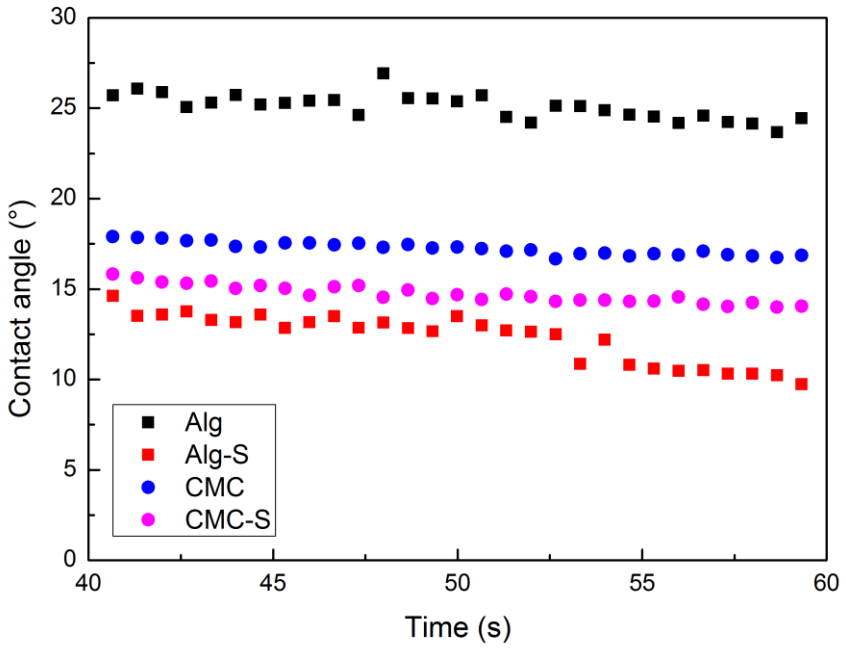

Figure 3-4. (a) Electrolyte uptake of the binder films (Alg, Alg-S and CMC, CMC-S) immersed into solute-free electrolyte after 6 hours. Herein, the amount of uptake indicates the weight percentage of the adsorbed electrolyte to the neat binder films. (b) Real-time contact angles of electrolyte on each binder film from 40 s to 60 s.

Additionally, the electrolyte wettability of each binder film was measured to investigate the capability of each binder on lithium ions transport and the results are displayed in Fig. 3-4(b). The change in electrolyte wettability was examined through the contact angles formed when a drop of electrolyte falls on each binder film. From the angle, it can approximately determine how much the polymer film have an affinity for electrolyte. Lower angles via fast electrolyte permeation indicate a relatively higher affinity between the film and the electrolyte, and consequently lead to easier lithium ion transport in the polymer binder. As shown in Fig. 3-4(b), the real-time contact angles tend to be stable after 40 s, and the mean contact angle of Alg-S binder film is 12.5˚, which is much smaller than that of unsulfonated Alg binder film. The sulfonation of CMC also decreases the contact angle, even though the difference in CMC is not as large as the difference in Alg. It is clear that the sulfonation of the polysaccharides is favorable to lithium ions transport.

3.3.6 Adhesion test

The effect of the sulfonation of the polysaccharides on electrode adhesion was also investigated and shown in Fig. 4-5. The electrode adhesion is generally dependent upon types of polysaccharides, more

exactly types of functional groups in the polysaccharides. Even in the same polysaccharide, molecular weight and the degree of saturation also affect the electrode adhesion. Therefore, it may not be appropriate to discuss the difference in the adhesion strength between Alg and CMC. Rather, the effect of the sulfonation on the adhesion strength has to be discussed. The polysaccharides have carboxyl and hydroxyl group evenly distributed in the backbone and these makes the polysaccharide binders strongly adhesive thus ensuring integrity of the anode. Because the carboxyl groups present in the polysaccharides interact with active materials, and possibly the current collector via hydrogen and chemical bonding[113,114]. In the course of sulfonation, the carboxyl groups in polysaccharides were replaced by sulfonic acid groups as proven from NMR and FT-IR results in Fig. 3-1 and Fig. 3-2, the hydrogen bond was blunted seriously, leading to weakening the electrode adhesion. This effect was evaluated using 180° peel test of electrodes as shown in Fig. 3-5. Moreover, it is natural that the decrease in the adhesion by sulfonation is severe in highly adhesive CMC-containing LTO electrodes compared weakly adhesive Alg-containing LTO electrodes. It should be noted that the increase in the electrolyte uptake (Fig. 3-4(a)) by the sulfonation may also weaken the electrode adhesion of the binder while LTO electrodes are operated. Apart from that, the decrease in the electrode adhesion could be a serious disadvantage for high capacity anodes experiencing huge volume change during charge/discharge processes.

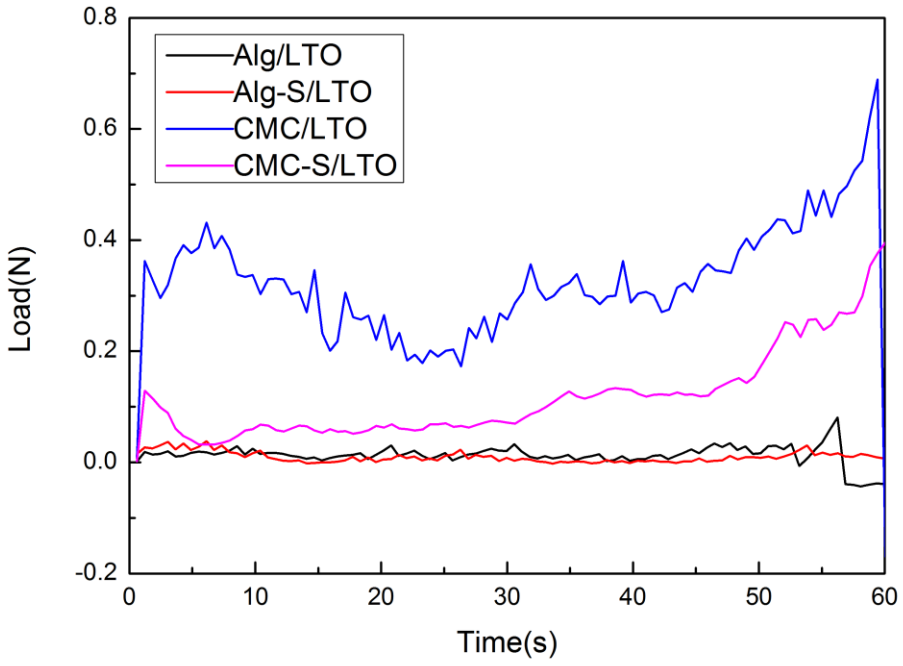

Figure 3-5. Adhesion strength of the LTO electrodes measured by 180° peeling.

3.3.7 Cyclic voltammetry

To examine the electrochemical reactivity, the cyclic voltammetry of the anodic half cells was performed at a scan rate of 0.5 mV s^{-1} from 1.0 V to 2.6 V and is displayed in Fig. 3-6. Herein, three-electrode cells assembled in a glove box were used because the three-electrode system can avoid the problem of reference electrode polarization and somewhat reduce the measured IR drop in the solution. From the CV cycles of the Alg/LTO electrode, the oxidation and reduction peak potentials were approximately 1.78 V and 1.47 V, respectively, and the potential difference($\Delta E = E_{p,ox} - E_{p,re}$) between the two peaks was 0.31 V. Furthermore, the oxidation and reduction peak potentials of the CMC/LTO electrode were approximately 1.75 V and 1.47 V, respectively, and the potential difference between the two peaks was 0.28 V. In contrast, the oxidation and reduction peak potentials of Alg-S/LTO electrode were approximately 1.73 V and 1.47 V, respectively, and the potential difference between the two peaks was 0.26 V. Meanwhile, the oxidation and reduction peak potentials of the CMC-S/LTO electrode were approximately 1.67 V and 1.46 V, respectively, resulting in the potential difference of 0.21 V. It demonstrates that the polarization and transport resistance became smaller when the sulfonate polysaccharides are employed as binders. This is consistent with the result of the ionic conductivity listed in Tab. 3-1, which showed that introducing the -SO_3H group in binder improved the ionic conductivity of binder. Additionally, the comparison in the intensity of redox peaks show that the sulfonated binders, Alg-S and CMC-S, make the electrodes more active for the electrochemical reactions with Li^+ than unsulfonated Alg and CMC do. This advantage would lead to decrease in impedance when used the sulfonated polysaccharides were used as binder.

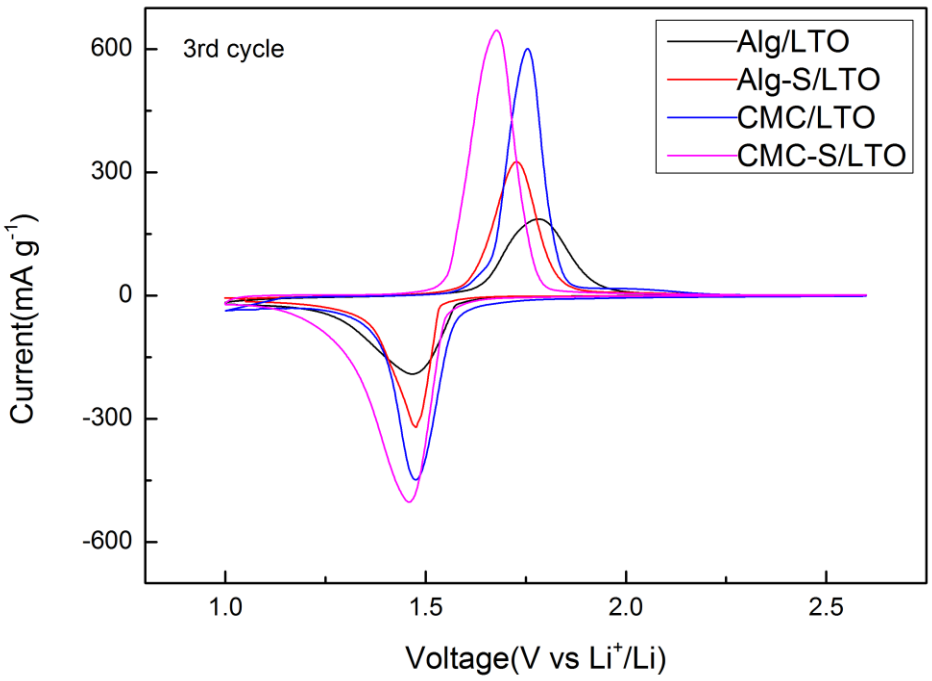

Figure 3-6. Cyclic voltammograms of Alg/LTO, Alg-S/LTO, CMC/LTO, and CMC-S/LTO electrodes at a scan rate of 0.5 mV s^{-1}.

3.3.8 The specific capacity vs voltage profile

(a)

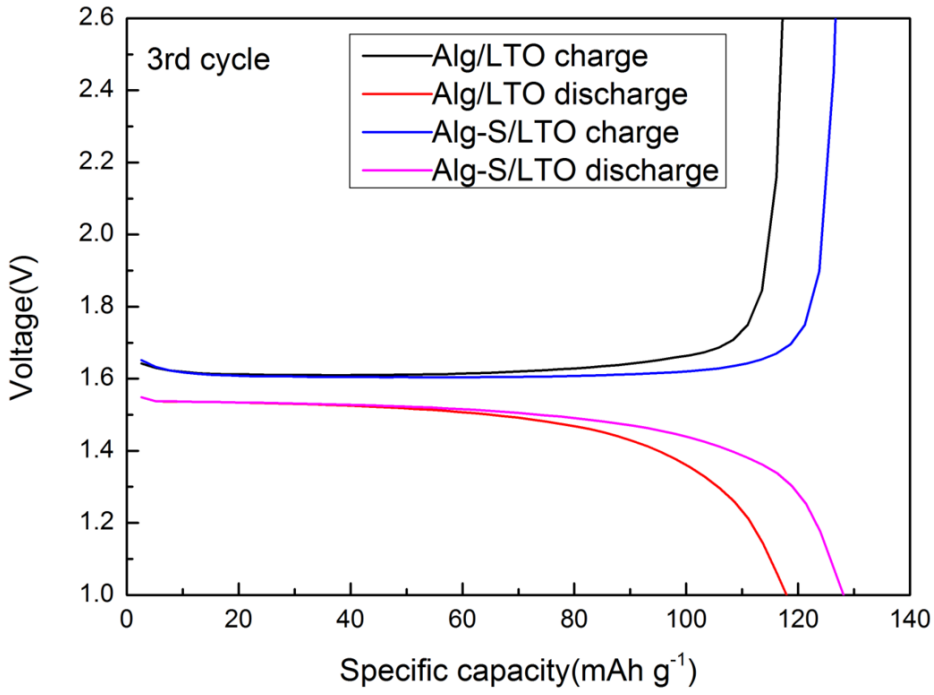

(b)

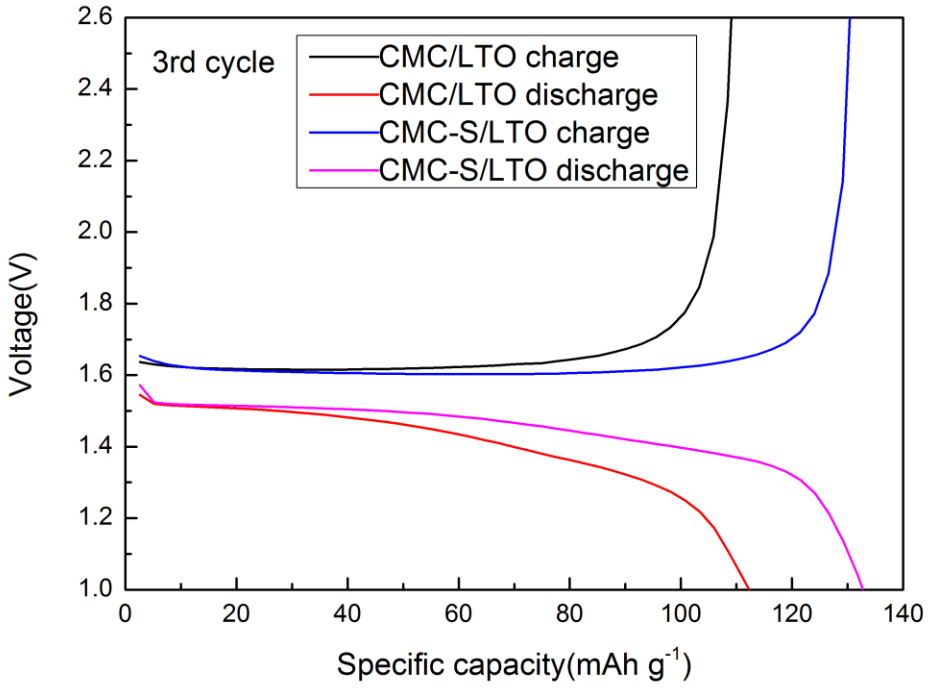

Figure 3-7. The specific capacity-voltage profile at the 3rd cycle (1C rate) for (a) Alg/LTO and Alg-S/LTO, and (b) CMC/LTO and CMC-S/LTO.

The 3rd cycle electrochemical performances profiles between Alg-S/LTO and CMC-S/LTO, and Alg/LTO and CMC/LTO at 1 C rate, respectively, as shown in Fig. 3-7. Those electrodes presented voltage plateaus around 1.55 V, which agrees with the CV results. Obviously, Alg-S/LTO and CMC-S/LTO present a flattering plateau profile and a larger plateau capacity than the Alg/LTO and CMC/LTO, respectively. Moreover, the potential differences between the charge and discharge plateau for Alg/LTO and CMC/LTO are smaller than that for Alg-S/LTO and CMC-S/LTO, respectively.

(a)

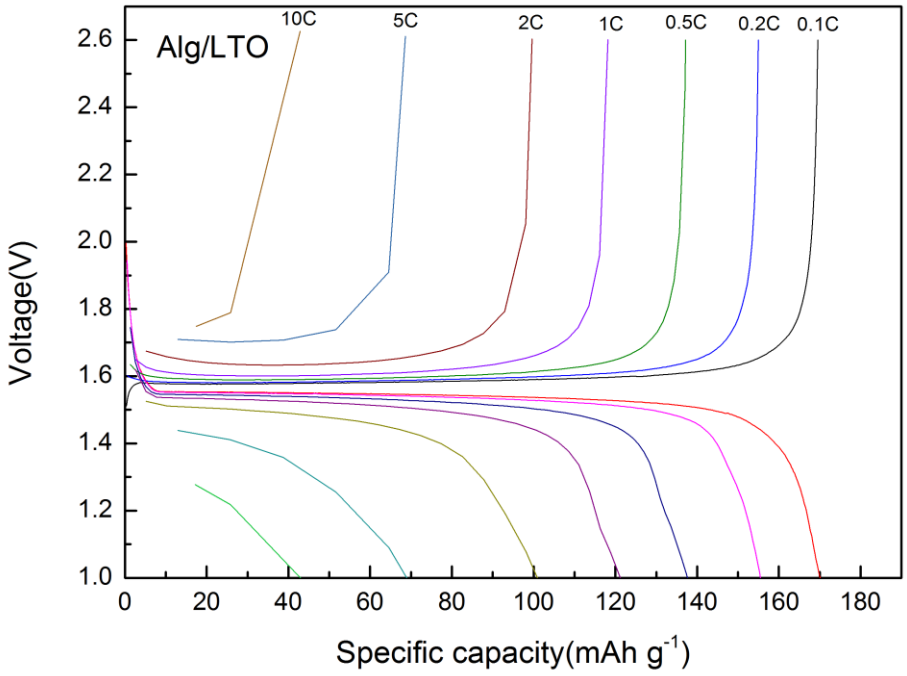

(b)

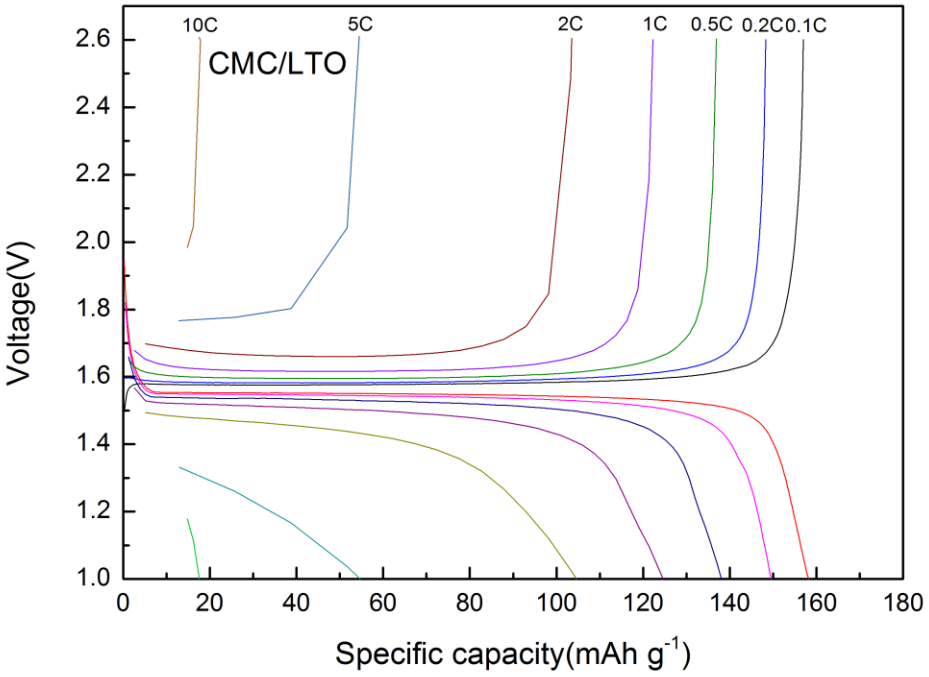
CMC/LTO
10C
5C
2C
1C
0.5C
0.2C
0.1C
Voltage(V)
Specific capacity(mAh g-1)

(c)

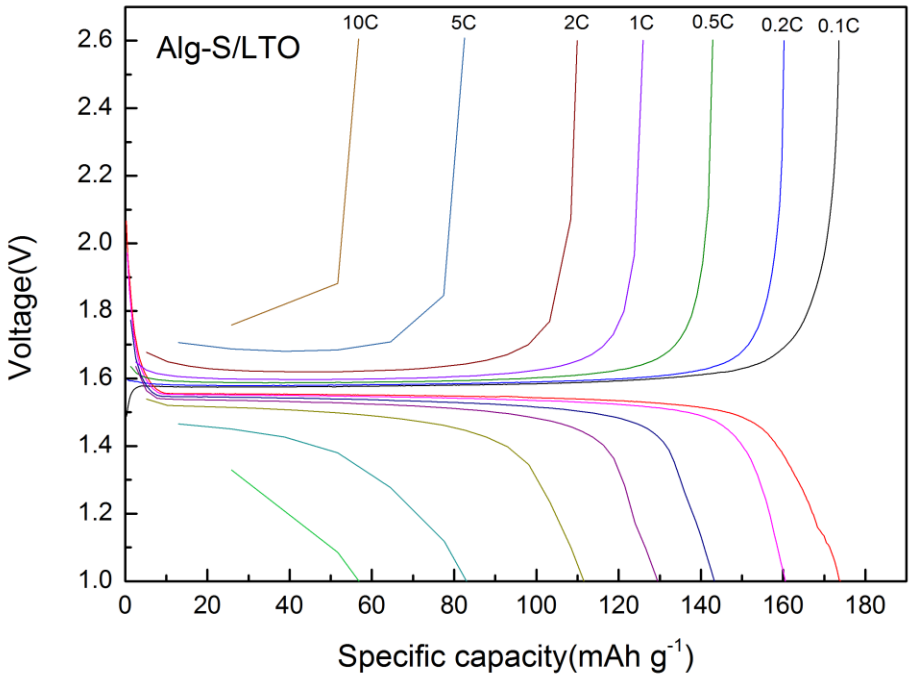
Alg-S/LTO
10C
5C
2C
1C
0.5C
0.2C
0.1C
Voltage(V)
Specific capacity(mAh g-1)

(d)

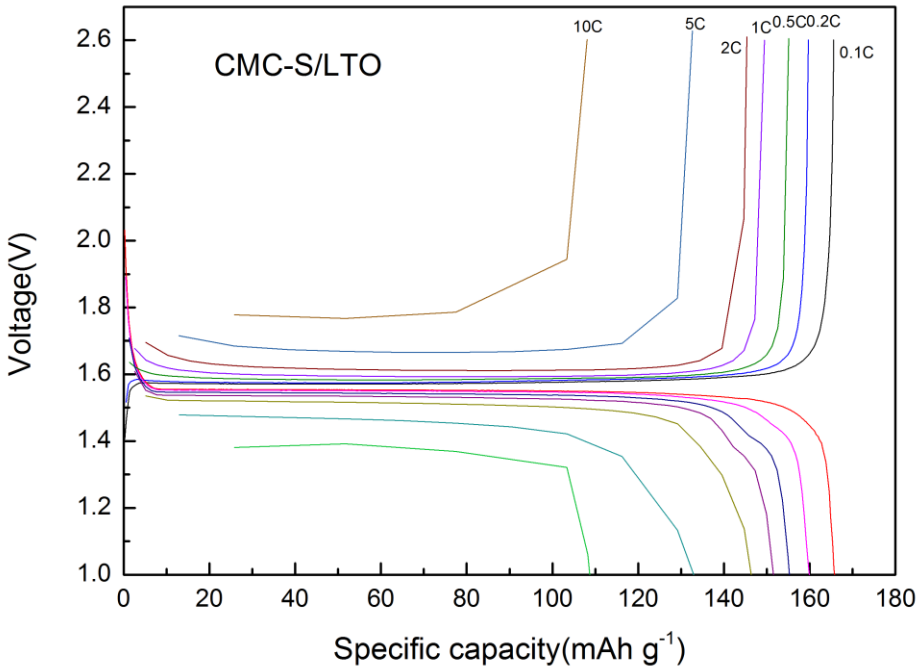

Figure 3-8. The specific capacity-voltage profile under various current rates for (a) Alg/LTO, (b) CMC/LTO, (c) Alg-S/LTO, and (d) CMC-S/LTO.

The specific capacity-voltage profiles under various current rates for the Alg/LTO, CMC/LTO, Alg-S/LTO and CMC-S/LTO, respectively, as shown in Fig. 3-8. Remarkably, higher capacity values were achieved for the Alg-S/LTO and CMC-S/LTO at 0.1, 0.2, 0.5, 1, 2, 5, and 10 C, respectively; however, those for the Alg/LTO and CMC/LTO are significantly lower, especially for the higher rates. The voltage plateaus show smaller gaps between charging and discharging for the Alg-S/LTO and CMC-S/LTO, which suggests excellent reaction kinetics and smaller electrode polarization compared to Alg/LTO and CMC/LTO, respectively.

3.3.9 EIS

The charge transfer resistance in the EIS spectra (Fig. 3-9) is represented by the size of semicircles in the medium frequency range. The larger the semicircle, the larger R_{ct}. Regardless of the polysaccharide binders, the LTO electrodes composed of sulfonated binders exhibit lower charge transfer resistances than those containing unsulfonated binders no matter fresh or cycled cells. Normally, more adhesive binder covers more LTO surface than the low adhesive binder, leading to high resistance to lithium ion transfer through the coverage[115,116]. In addition, the presence of

sulfonate anions (RSO_3^-) in Alg-S and CMC-S is more favorable to lithium ion transport during the charge/discharge process.

(a)

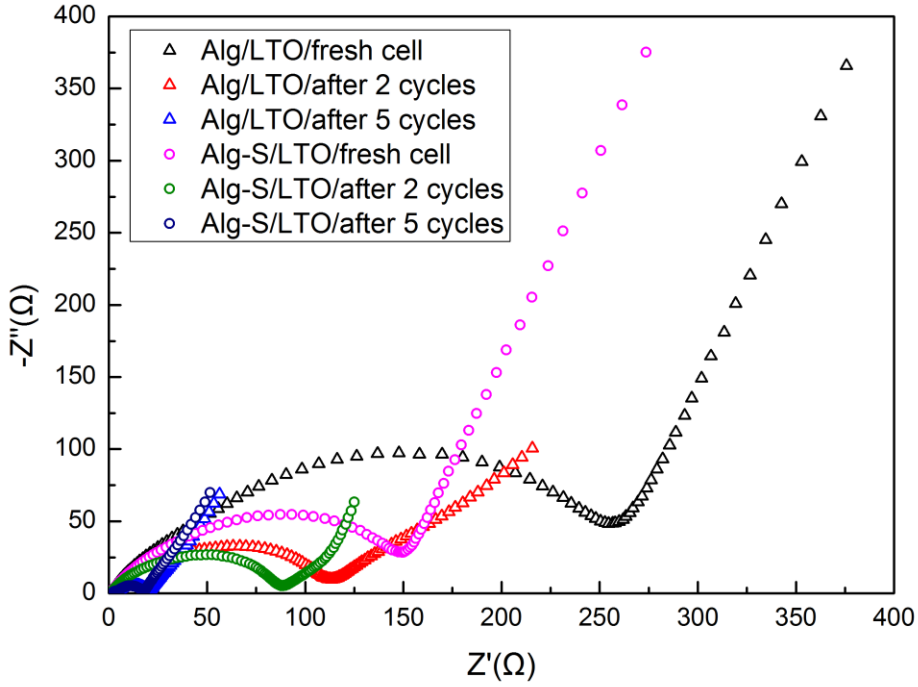

(b)

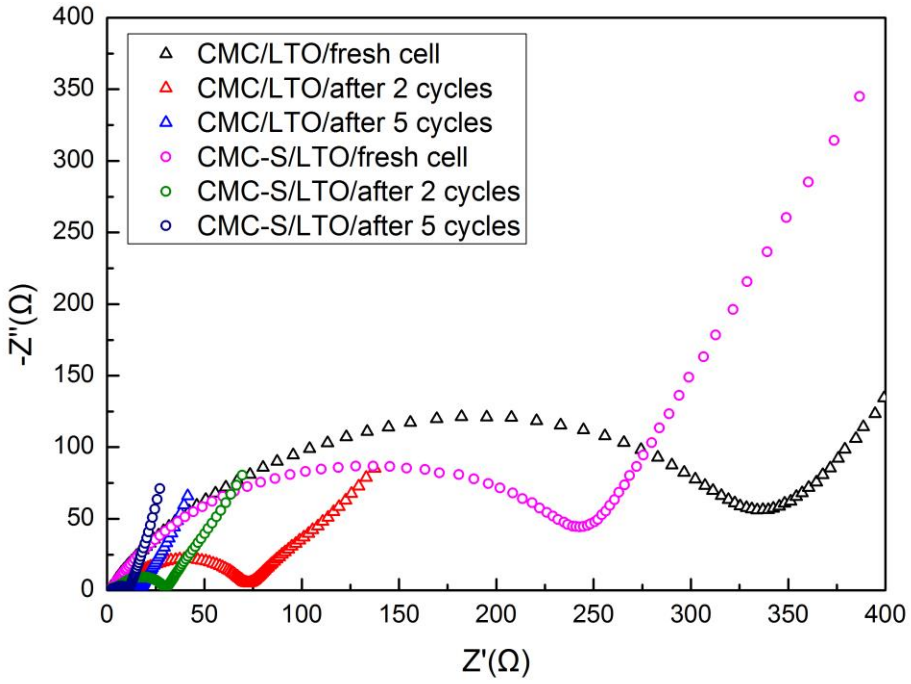

Figure 3-9. Nyquist plots of the LTO fresh, two and five cycled electrodes employing (a) Alg and Alg-S binders, and (b) CMC and CMC-S binders.

Furthermore, the lithium-ion diffusion coefficient was calculated using the classic Warburg formula ($D = R^2T^2/2A^2n^4F^4c^2\sigma^2$) through the EIS of five-cycled electrodes[117], D is lithium-ion diffusion coefficient; R is the gas constant; T is the absolute temperature; A is the electrode area; n is the number of electron transferred per molecule during electrochemical reaction; F is Faraday constant; and c is molar concentration of lithium ions; σ is the Warburg impedance coefficient[118]. The lithium-ion diffusion coefficients calculated for the Alg/LTO, Alg-S/LTO, CMC/LTO and CMC-S/LTO were 1.10×10^{-10} cm^2 s^{-1}, 1.30×10^{-10} cm^2 s^{-1}, 2.02×10^{-10} cm^2 s^{-1} and 4.24×10^{-10} cm^2 s^{-1}, respectively. From these results, it also shows that the sulfonated polysaccharide binders can contribute to lithium-ion diffusion in the LTO electrodes when compared to original polysaccharide binders.

3.3.10 Cyclic performance and rate capability

As a final sequence, the effect of sulfonation of polysaccharide binders on the electrochemical performance of LTO electrodes was investigated through the cycle and high rate tests of the electrodes. The results are shown in Fig. 3-10. The LTO electrodes employing Alg-S and CMC-S preserved higher reversible cyclic capacities of 130.9 mAh g^{-1} and 153.2 mAh g^{-1} at the 100th cycle of 1 C rate, respectively. On the contrary, the Alg- and CMC-containing LTO electrodes maintained the reversible

capacities of 117.0 mAh g^{-1} and 117.6 mAh g^{-1} after 100 cycles, respectively. Furthermore, the LTO electrodes containing the sulfonated polysaccharides have much higher capacities at any current rates between 0.1 C and 10 C than those containing the unsulfonated polysaccharides, as shown in Fig. 3-8(b,d). Especially, the significant difference occurs at relatively high current rates above 2 C. In general, high current charge/discharge processes require more rapid lithium ion transport, compared to low current process. As proven previously, the sulfonation of binder improves lithium ion transport in the electrode, ultimately resulting in better cyclic and rate capability tests. When the current rate decreased to 0.1 C from 10 C, all the LTO electrodes recovered their capacity completely, indicating that no mechanical damage occurs in the electrodes containing sulfonated binders, even though the sulfonation makes the electrode adhesion decrease as illustrated in Fig. 3-5.

(a)

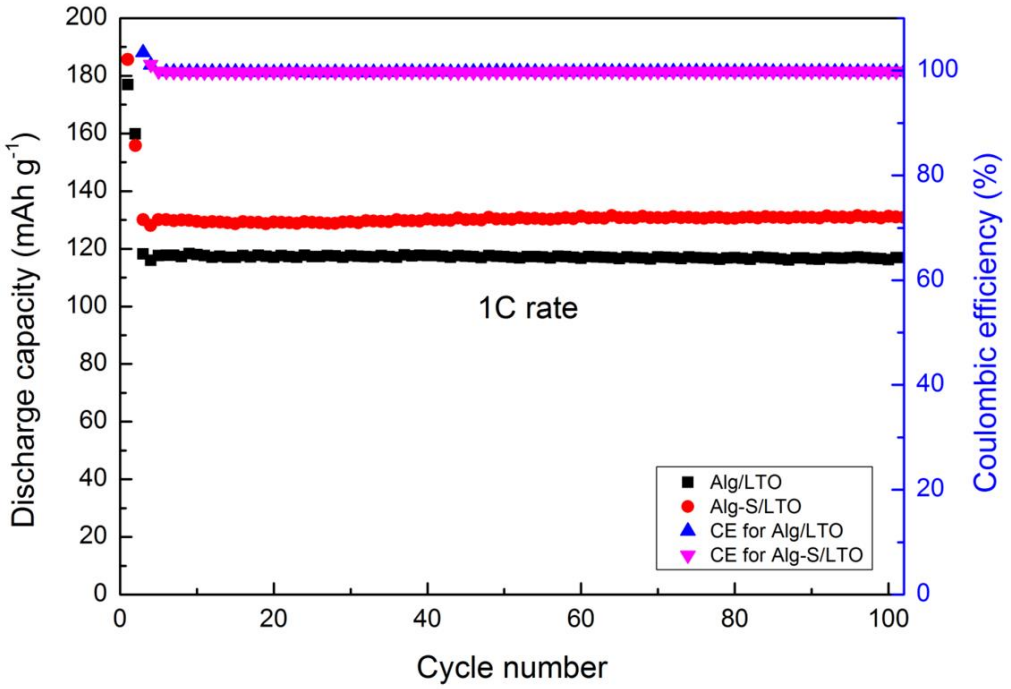

(b)

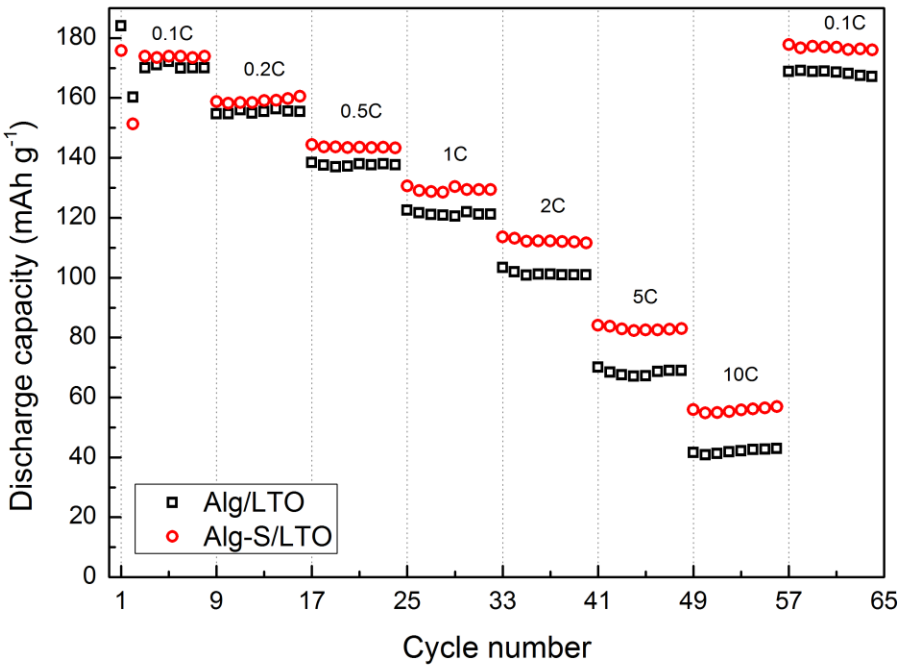
0.1C
0.2C
0.5C
1C
2C
5C
10C
0.1C
Alg/LTO
Alg-S/LTO
Discharge capacity (mAh g-1)
Cycle number

(c)

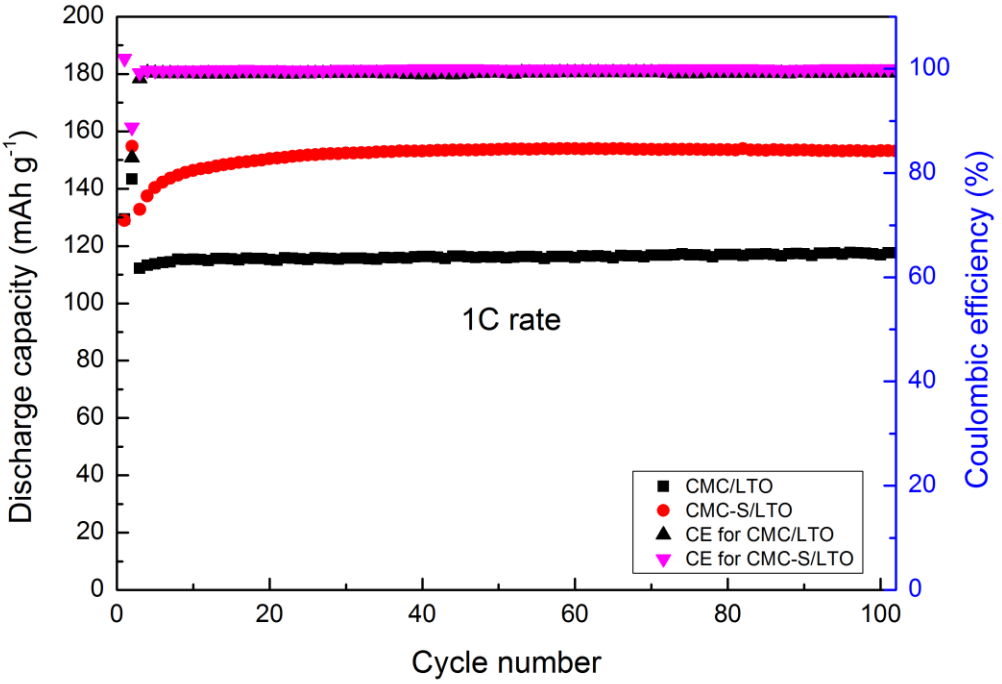
1C rate
CMC/LTO
CMC-S/LTO
CE for CMC/LTO
CE for CMC-S/LTO
Discharge capacity (mAh g-1)
Coulombic efficiency (%)
Cycle number

(d)

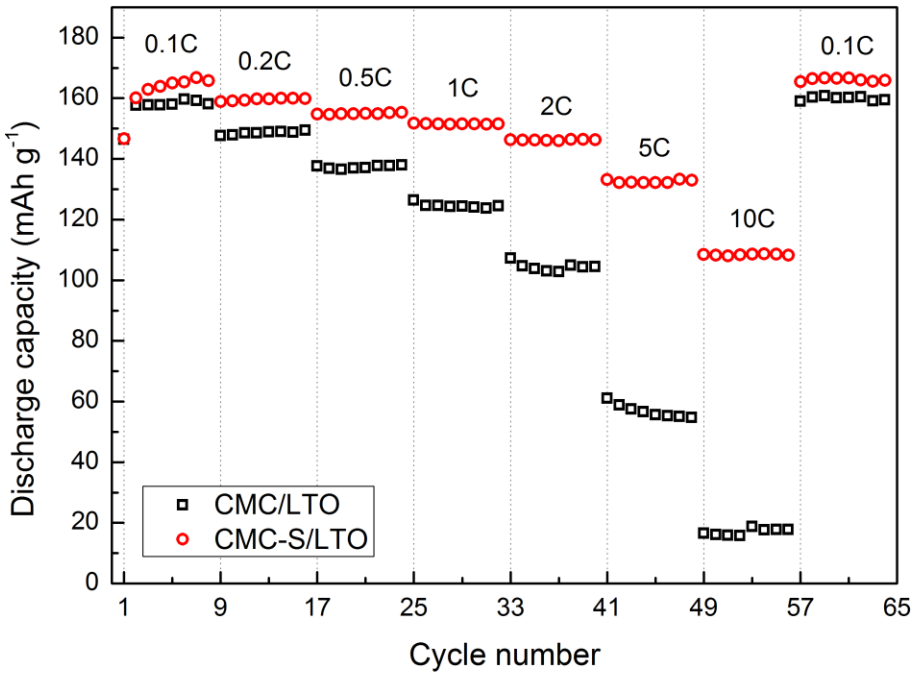

Figure 3-10. Cycle and rate capability performance of the LTO electrodes (a) and (b) employing Alg and Alg-S, and (b) and (d) CMC and CMC-S, respectively.

3.4 Conclusions

The sulfonic acid group is successfully introduced to the backbone of two kinds of polysaccharides, Alg and CMC, through an amidation reaction. The sulfonation of polysaccharide binders is a very powerful modification method to improve high-powered LTO electrodes by forming the $-SO_3Li$ which can facilitate lithium ion transport in the electrodes. From measuring ionic conductivity of binder solution, it is clear that the sulfonation of polysaccharides improve ion transport, leading to the increase in the electrical conductivity of binder films. Such improvement is also confirmed through the experiments of electrolyte uptake and contact angle. Of course, it is inevitable to a bit decrease in electrode adhesion due to the replacement of adhesive carboxyl groups in polysaccharides by ionically conductive sulfonic acid groups. Compared to this disadvantage, the sulfonation of polysaccharide binders works more positively on LTO electrodes through enhancing lithium ion transport in the electrode. This effect renders the sulfonated Alg and CMC binders more effective for LTO anodes compare to the unsulfonated Alg and CMC binders, respectively. The sulfonation leads to smaller polarization resistances, eventually resulting in better cyclic and rate capability results. In particular, the LTO electrode containing sulfonated CMC binder showed 109.0 mAh g^{-1} at 10 C rate whereas the

LTO electrode composed of unsulfonated CMC has only 17.5 mAh g^{-1} at the high current. In summary, the sulfonation strategy of binder demonstrate an excellent modification to the electrochemical performance for high-powered LTO electrodes.

4 Mxene bonded Conductive Binder for Improving Electrochemical Performance of High-capacity Si Anode in Lithium-ion Batteries

4.1 Introduction

Li-ion batteries (LIBs) are widely used in smart watches, electric cars, and energy storage systems[119,120]. The energy density of LIBs, comprising a conventional Li transition-metal-oxide cathode and a graphite anode, is higher than that of previous rechargeable battery systems i.e., with nickel-metal hydrides. The current market demands higher energy density for more applications such as wearable electric devices and airplanes; therefore, new electrode materials with high energy density are highly required.

As a next-generation battery material, Si is one of the most attractive anode materials owing to the fact that it is non-toxic, has low cost, and possesses a gravimetric energy density (3579 mAh g^{-1}, $Li_{15}Si_4$) and a volumetric energy density (2190 mAh cm^{-3}) that are ten times and three times higher, respectively, than those of graphite (LiC_6: 372 mAh g^{-1} or 756 mAh cm^{-3})[87]. However, Si also has low electrical conductivity and suffers from large volumetric expansion during lithiation, which has many demerits such as the pulverization of Si and loss of electrical contact among electrode components. To overcome these problems, various approaches, including morphology modification of Si[121], carbon coating on the Si surface[122], and exploring new binder systems[123–127], have been suggested.

Although changing the morphology and carbon coating resulted in enhanced electrochemical performance, they require additional complicated processes. New binder techniques also contributed to enhanced electrochemical performance; however, they still need further improvement because the conducting agent i.e., carbon, hinders direct contact between the binder and Si particles. Therefore, a conductive binder was suggested as a solution to this issue[125–127]. However, the conductive polymer is unstable during the electrochemical reaction owing to its high reactivity with the electrolyte[128].

On the basis of the above issues, our strategy is to produce a highly conductive and mechanically robust binder. Several binders such as polyacrylic acid (PAA), carboxymethyl cellulose (CMC), styrene butadiene rubber (SBR), polyvinyl acid (PVA), polyvinylidene fluoride (PVDF), polyimide (PI), and conductive polymers are highly utilized for Si-based anodes[129]. Among the various conventional binders, PVDF, CMC, and SBR binders are not able to accommodate the volume expansion of active materials; as a result, the active materials and conducting agent (carbon) form agglomerates due to weak interfacial interactions[130,131]. PAA and conducting polymer binders have

been more effective thanks to their multiple hydrogen bonds and the formation of a conducting gel-like framework within the electrodes[103,123,132]. Recently, a Si-based electrode using a new binder i.e., NaPAA grafted to CMC (NaPAA-g-CMC), showed good electrochemical performance with a high initial discharge capacity (2290 mAh g^{-1}) and stable cycling performance, which originated from its good adhesion force[133]. However, the Si-based electrodes using NaPAA-g-CMC binder showed relatively low capacity retention for early cycles.

In this study, we propose a design for a highly conductive binder through copolymerization and connected with conductive 2-dimensional conductive material MXene. The obtained conductive binder Alg-AABA-Mx exhibited excellent electrochemical performance, especially in high rate current.

4.2 Experimental

4.2.1 Synthesis of Alginate-poly(acrylic acid-butyl acrylate)-MXene (Ti2CTx) (Alg-AABA-MX)

Firstly, 3 g of Alg (CAS no.9005-38-3) and 90 g of distilled deionized (DDI) water were added in a jacket reactor. 10% of potassium persulfate (KPS, Sigma-Aldrich) based on Alg weight percentage was added after Alg totally dissolved. Next, 1.5 g acrylic acid (AA, Samchun Chemical Co., Ltd., Korea) monomer, 1.5 g butyl acrylate (BA, Samchun Chemical Co., Ltd., Korea) monomer and 4 h sonicated MXene solution (9 mg MXene in 10 g DDI water) were added when temperature reach 70 °C. The polymerization was performed for 2 h at stirring rate 200 rmp under nitrogen atmosphere. The final product, called Alg-AABA-MX, was cooled down to room temperature. For comparation, the product called Alg-AABA has been prepared as well as the same procedure while the absent of MXene.

4.2.2 Preparation of electrodes and coin cells

In this research, the Alg-AABA/Si and Alg-AABA-Mx/Si electrodes were prepared by mixing SiNPs, super P, and as-prepared binders Alg-AABA and Alg-AABA-Mx in an adequate amount of distilled water, and the weight ratio of above components is 60 : 20 : 20, respectively. After mixing in a planetary ball mill at 500 rpm for 30 min, a uniform slurry was manufactured and coated onto 20-μm-thick Cu-foil by an automatic film-coating apparatus. The fresh made electrodes were dried at 60 °C for 30 min in a convection oven and then put them in a vacuum oven (70 °C) for a whole night to completely remove remaining solvent before coin cell assembly. The mass loading of the electrodes were 1.3 ± 0.3 mg/cm^2. The electrolyte consists of ethylene carbonate (EC) : diethyl carbonate (DEC) :

dimethyl carbonate (DMC) 3 : 5 : 2 v/v% with additive (5wt.% FEC, 2wt. % VC and 0.4wt.% $LiBF_4$), and the CR2032 coin-half cells were assembled in an argon-filled glove box with lithium foil as a counter electrode.

4.2.3 Characterization of materials and electrochemical properties

In this research, the physical stability of the binder solution was recorded using a Turbiscan station (Turbiscan LAB, Formulaction Co., France). The functional groups of the synthesized polymer were confirmed by Fourier-transform infrared spectroscopy (FTIR, Nicolet iS^5 Thermo Fisher Scientific, USA). Thermogravimetric analysis (TGA) and differential scanning calorimetry (DSC) were performed by a Q50 TA Instrument (Discovery TGA35, DSC-PC100, Canada) with a heating rate of 10 °C min-1 under nitrogen atmosphere. The wettability of the binder films, represented by the contact angle of an electrolyte droplet on binder film, was measured using an optical tensiometer (Theta Lite, Biolin Scientific, Japan). The adhesion strength of the electrode was measured by the 180° peel strength of 2-cm-wide electrode strips in a texture analyzer (TA-Plus, Lloyd Instruments Ltd., USA) at a propagation speed of 60 mm min-1. The surface and interface resistivities of the electrode were obtained using a multipoint probe system (RM2610, HIOKI Corp., Japan) at room temperature. EIS with a frequency range from 10^6 Hz to 10^{-2} Hz at E=0 V was again used to obtain the kinetic parameters related to the charge/discharge processes of long-cycled electrodes. Cyclic voltammetry (CV) testing was also conducted in a battery cycler (WBCS3000, Wonatech, Korea) at scan rates of 0.2 mV s^{-1} between 3.0 V and 0.0 V. The galvanostatic charge/discharge and rate capability tests were also characterized in a battery cycler (PEBC 0550.1, PNE solution Co., Korea) with a constant current and a constant voltage mood at room temperature. For galvanostatic charge/discharge performance, the cells were fully charged/discharged between 0.05 V and 1.5 V at the current of 0.1 C for the first 2 cycles. Subsequently, the cells were charged/discharged at the current of 0.5 C for the next 100 cycles. Various charge/discharge current densities 0.1 C, 0.2 C, 0.5 C, 1.0 C, 2.0 C were applied in the rate capability test.

4.3 Results and discussion

4.3.1 FI-IR

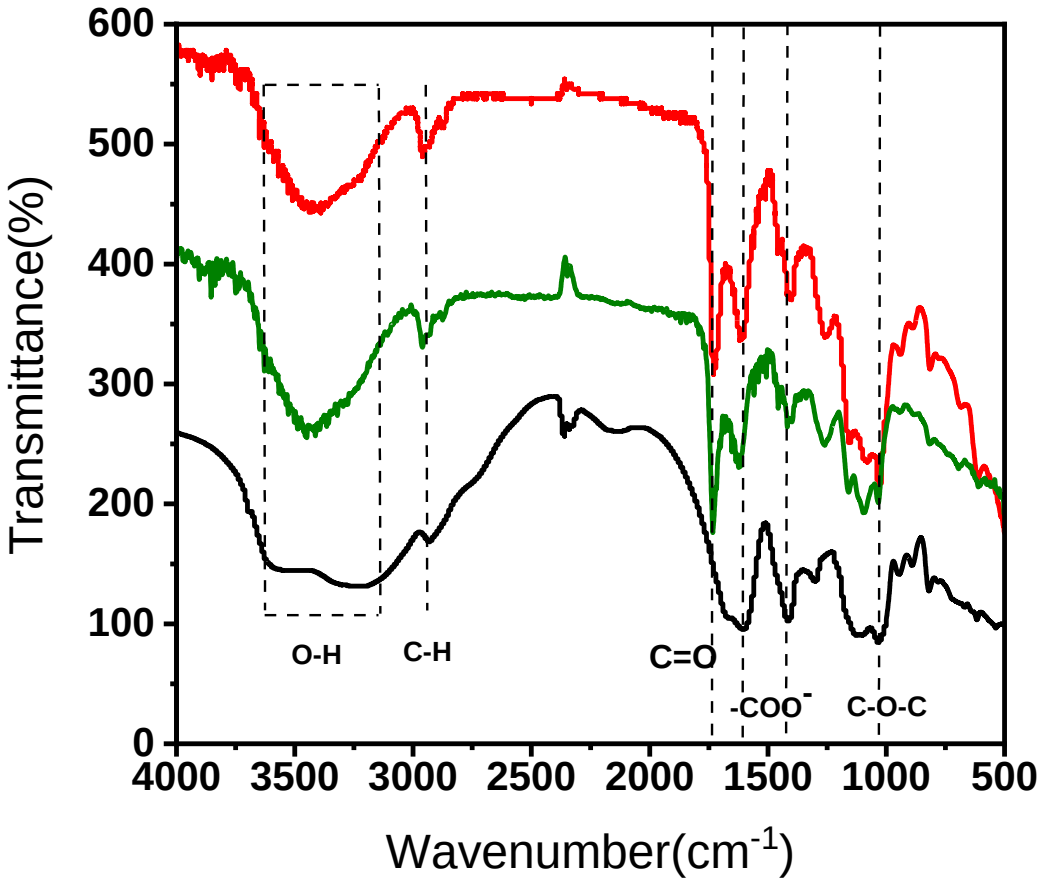

Figure 4-1 FT-IR of binder solution

For checking the existence of AA and BA, the FTIR of Alg, Alg-AABA, Alg-AABA-MX binder solution have been conducted and the figure shows as Fig. 4-1, the only Alg sample has been tested as well. The peaks at wave number 1607 cm^{-1} and 1419 cm^{-1} can been found in all samples. This is due to both Alg and AA have COO^- function group on their chain. Moreover, the typical peak C=O of BA at 1719 cm^{-1} is obvious in Alg-AABA and Alg-AABA-MX which indicating the BA has been added successfully on Alg chain.

4.3.2 DSC

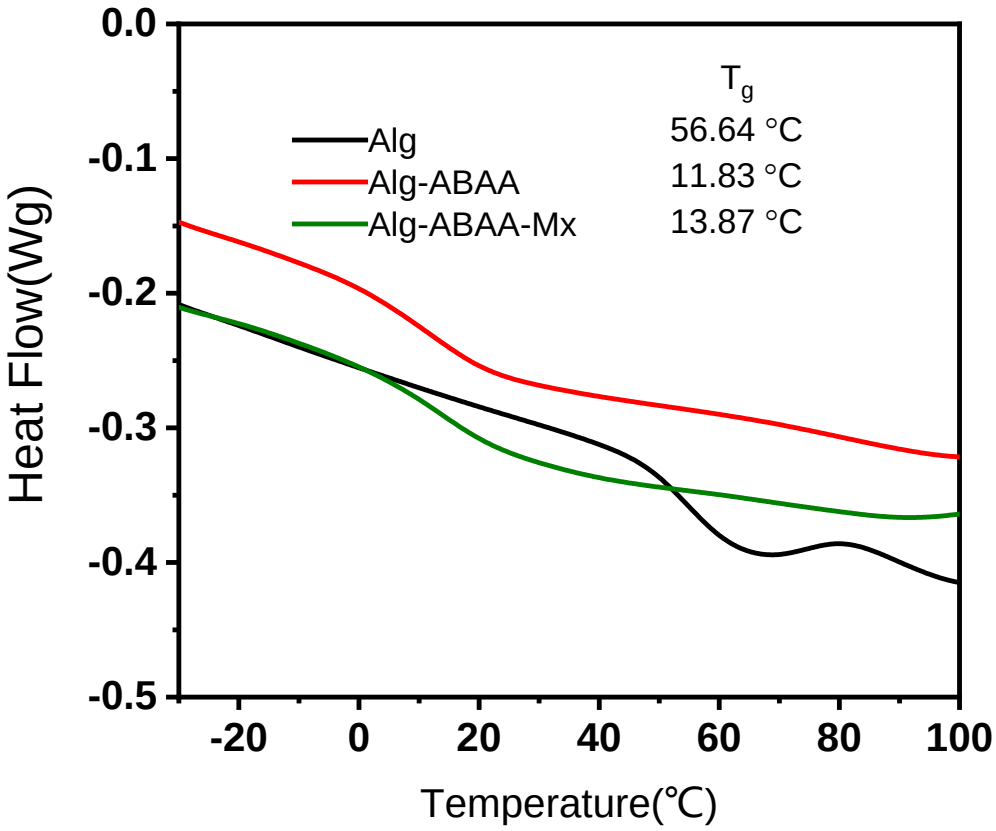

Figure 4-2 Differential scanning calorimetry (DSC) of binder film.

For further investigating the polymer chain's property, the DSC of binder film was carried out under nitrogen gas flowing, and the results show as Fig. 4-2. As we know, Alg is kind of hard polysaccharides since the D-glucose backbone, and the T_g of Alg is about 56.64 ℃. Meanwhile, Alg-AABA and Alg-AABA-MX shows a much lower T_g than Alg. It is 11.83 ℃ and 13.87 ℃, respectively. This is due to the contribution of BA which is known as a flexible polymer and has a Tg ≈ -55℃, and the flexible ability of binder is considered as an important property for electrodes of LIB. The flexible biner can reduce the side-effect of the volume change which happening during charging and discharging processes. Moreover, Alg-AABA-MX shows slightly higher T_g than Alg-AABA which is caused by the present of MXene which consist of few-atoms-thick layers of transition metal carbides, nitrides, or carbonitrides making the AABA polymer chain's flexibility decreased. Therefore, this is another evidence to proof that MXene has been polymerized on AABA chains.

4.3.3 Ionic conductivities

Table 4-1 The ionic conductivity of binder solution (22.6 ℃).

Binder solution	Ionic conductivity of binder solution (mS/cm)	
	Without electrolyte	With electrolyte
Alg	14.9	16.0
Alg-AABA	14.0	15.2
Alg-AABA-MX	20.1	20.8

Generally, a well ionic conductive biner can support a higher fast charge discharge property and reach a higher power density. Thus, the ionic conductivity of binder solution has been conducted and as shown in Tab. 4-1. the ionic conductivity of Alg and Alg-AABA at the absent of electrolyte are similar with each other at around 14 mS/cm, and Alg-AABA has a slightly lower ionic conductivity than Alg. This may be due to the no-ionic conductive property of normal polymer. However, at the present of MXene, the ionic conductivity of binder solution Alg-AABA-MX has been significant improved no matter there is electrolyte or not, since the function groups on the MXene surface may support more ions to the solution. This probably will be a benefit to the electrochemical performance of Alg-AABA-MX, especially the performance at high current density.

4.3.4 Interface resistance

Table. 4-2 The surface, volume, and interface resistance of electrodes with different binders

	Alg	**Alg-AABA**	**Alg-AABA-MX**
Composite surface resistivity (Ω cm2)	$1.41*10^{-3}$	$9.13*10^{-4}$	$4.19*10^{-4}$
Interface resistance (Ω cm2)	$1.51*10^{-2}$	$1.28*10^{-2}$	$5.84*10^{-3}$
Composite volume resistivity[Ω cm]	$5.24*10^{-1}$	$3.38*10^{-1}$	$1.55*10^{-1}$

The surface resistivity and volume resistivity of electrode are crucial properties which can leading to a better electrochemical performance. The pre-surface resistivity checking can avoid using unqualified electrodes and increase manufacturing processes. Therefore, the surface resistivity and volume resistivity of electrodes have been checked by HIOKI electrode surface resistivity analyzer. Moreover, the interface resistance between current collector cupper foil and electrode composite has been tested as well and shows as Tab. 4-2. Alg-AABA has lower composite surface resistivity, interface resistance and composite volume resistivity than Alg. This may be due to the higher adhesive property of Alg-AABA binder which can support a good connection among active material particles, and the electrode composite to the current collector as well. It is clear that MXene can reduce the composite surface resistivity, Interface resistance and composite volume resistivity significantly which is contributed by the well-electronic conductive property of MXene. This is implying that Alg-AABA and Alg-AABA-MX may be used as a potential binder for silicon based LIB.

4.3.5 Adhesion test

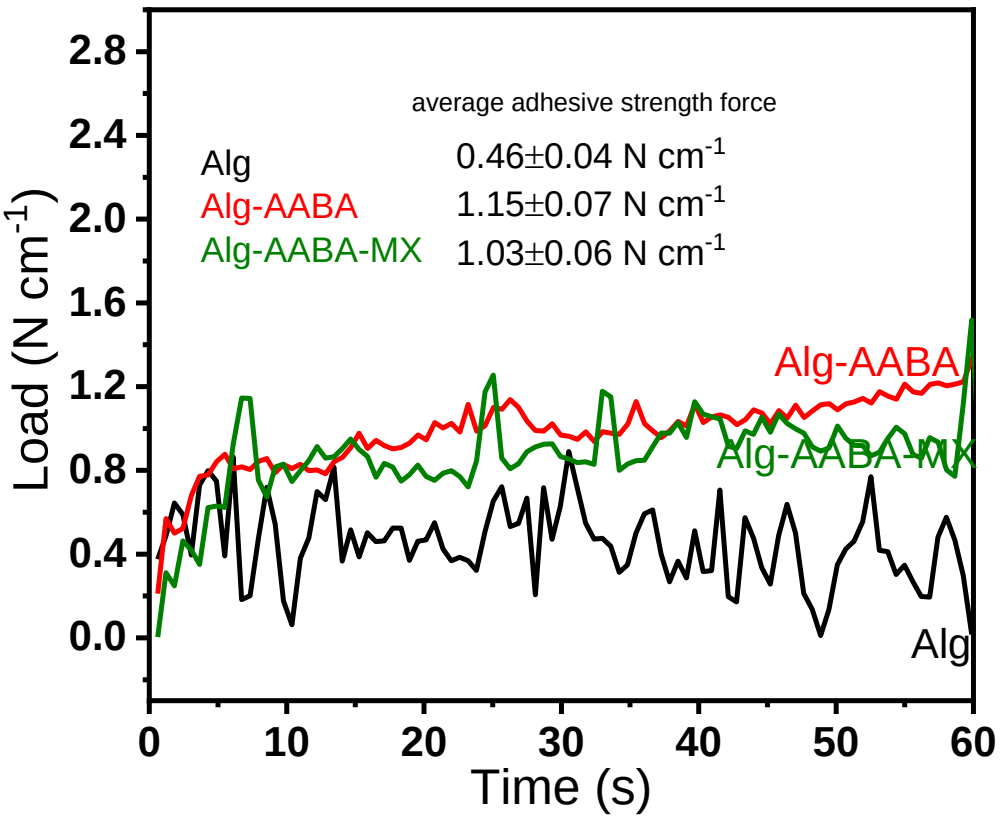

Figure 4-3 Adhesive peeling strength of electrodes with different binder recorded during 60s.

Generally, adhesive property of electrode is considered as the most important character, an adhesive binder can keep electrode integrity during long term charging and discharging progress. Therefore, the adhesive strength of electrodes have been recorded for 60s while peeling from current collector and the results are showing as Fig. 4-3. With the help of AA and BA, the adhesive strength of Alg-AABA and Alg-AABA-MX have been more than double increased comparing with Alg, and due to the MXene's unadhesive property, the Alg-AABA-MX has a lower adhesive property than Alg-AABA.

4.3.6 Impedance

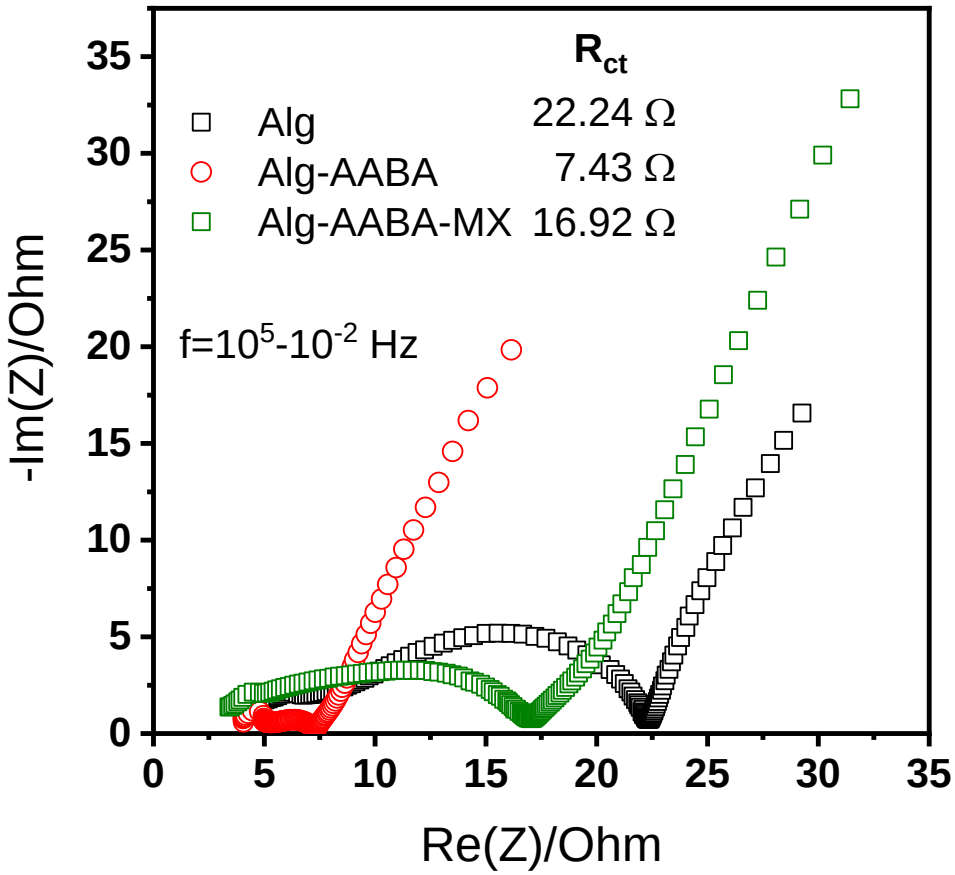

Figure 4-4 Impedance of LIB with different binder at frequency from 10^5 Hz to 10^{-2} Hz.

The electrochemical performance conducted under alternating voltage can give many information, such as the internal resistance of coin cell at high frequency region, charge transfer resistance at

middle frequency region, Warburg coefficient at low frequency region. Thus, the impedance of LIB with different binder has been conducted at E=0.2V and shows as Fig. 4-4. All the coin cells have the internal resistance around 4.7 Ω which may come from the resistivity of cells parts, resistivity of electrode composite materials and resistivity of electrolyte. Moreover, the charge transfer resistance of Alg-AABA and Alg-AABA-MX are smaller than Alg which indicating the faradaic electrochemical reaction can happen easier within Alg-AABA and Alg-AABA-MX cells rather than Alg. This maybe due to the better adhesive property of Alg-AABA and Alg-AABA-MX, a good adhesive property of binder support good connections among electrode composite particles, so electrons can pass freely for carry out faradaic electrochemical reactions under alternating voltage. The exact charge transfer resistance value have been inserted in Fig. 4-4.

4.3.7 Cycling performance

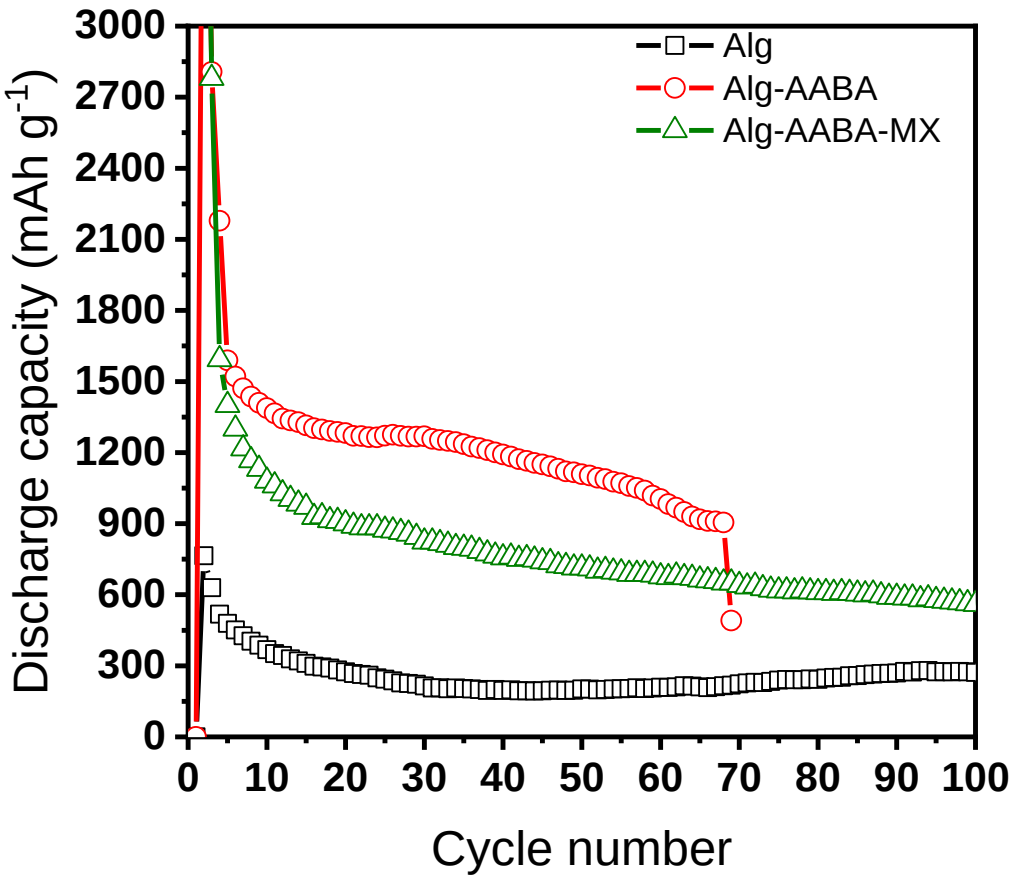

Figure 4-5 Cycling performance of LIB with different binder between voltage 0.01 V and 1.5 V for 100 cycles.

The LIB with different binder has been charge and discharge over than 100 cycles at voltage range 0.01V to 1.5V. The discharge capacity is as shown as Fig. 4-5. As charging and discharging of the LIB, the discharge capacity fading because the large volume change of Si particles, it is as large as 300%. However, the Alg-AABA and Alg-AABA-MX shows higher discharge capacity than Alg, it is about 5 times higher of Alg-AABA than Alg, and over 2 times higher of Alg-AABA-MX than Alg. This probably because the adhesive properties of AA and BA, the lower charge transfer resistance while charging and discharging and other electrode performance that discussed before. Moreover, since BA is not only an adhesive polymer, but also a flexible polymer with low Tg which implying that BA may support an elastic force, recover the large volume change of silicon particle during charging and discharging progress. Thus, a much stable cycling performance can be observed on LIB with Alg-AABA and Alg-AABA-MX groups. Additionally, MXene is consider as two-dimensional inorganic compounds with low adhesive property, so the long-term cycling performance of Alg-AABA-MX has lower discharge capacity than Alg-AABA. Above all, it is clear that Alg-AABA and Alg-AABA-MX can be a promising binder for LIB with silicon based active material and they can be charge discharge over than 100 cycles with higher discharge capacity than Alg.

4.3.8 Rate capability

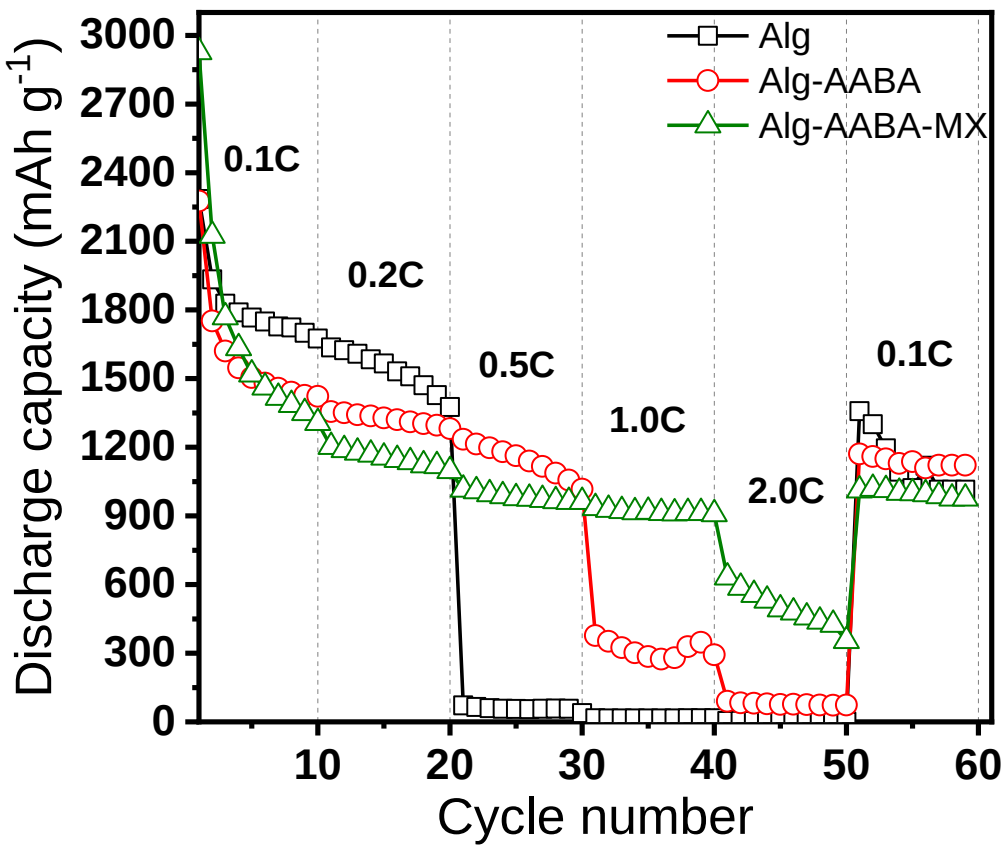

Figure 4-6 Rate performance of LIB with different binder at current 0.1 C, 0.2 C, 0.5 C, 1.0 C and 2.0 C.

Nowadays, the fast charge and discharge of LIB is in highly demanded, the LIB which can fast charge discharge can support a higher power density. In other words, comparing with supercapacitor, LIB has lower power density which means LIB cannot do faster charge than supercapacitor, so it is imperative to develop LIB with high power density and fast charge and discharge ability. Therefore, the charge discharge performance at different current rate have been carried out and shows as Fig. 4-6. At low current rate 0.1 C, 0.2 C, LIB with Alg has the highest discharge capacity compare with Alg-AABA and Alg-AABA-MX whereas the situation totally changed at high current rate 1.0 C and 2.0 C. Moreover, at high current rate 1.0 C and 2.0 C, the discharge capacity trend is different with cycling results, this maybe implying that the fast charge discharge capacity requires binder's conductivity rather binder's adhesive property. The LIB with Alg-AABA-MX as binder can serve a good conductivity for electrons movement which can achieve fast charge and discharge and making higher

power density possible. This result is consisting with electrode surface resistance indicating conductive electrode can show higher discharge capacity at higher current density. The binder's conductivity is as important as adhesive property for a promising LIB.

4.4 Conclusions

The novel high adhesive and conductive binders Alg-ABAA, Alg-ABAA-Mx were successfully synthesized through graft copolymerization. As described above, these new types of binders result in a strong binding force among the Nano Si particles and between Nano Si particles and the Cu current collector. A well-distributed conductive network Alg-ABAA-Mx in the electrode is formed without adhesion loss. Both of them are significantly effective for the electrochemical performance of a high-capacity anode when compared with typical alginate binder. Especially, the coin-cell with Alg-ABAA-Mx as binder exhibited excellent electrochemical performance in high rate current.

5 Modified Core-shell Structured Si-based Compound by Coating Polysaccharides on Silicon Surface Applied as Anode in Lithium-ion Batteries

5.1 Introduction

Lithium-ion batteries (LIBs) are one of the most widely used secondary battery systems. Compared to other rechargeable batteries, such as nickel-cadmium and nickel metal hydride batteries, LIBs are featured with higher energy density, higher operating voltages, limited self-discharging and lower maintenance requirements. However, the current commercial graphite anode cannot meet the increasing demand on energy density, operation reliability and system integration arising from portable electronic devices, electric vehicles, and energy storage applications. Graphite anodes exhibit only a moderate intrinsic specific capacity (372 mA h g^{-1})[134] and serious safety concerns due to lithium plating and further formation of lithium dendrites. As a consequence, studies on new generation anode materials with the characteristics of high capacities, a proper charging/discharging potential, as well as safe and low cost manufacturing and usage have attracted great attention from both, academia and industry.

Among all potential lithium-ion battery (LIB) anodes, silicon (Si) is one of the most promising candidates to replace graphite due to following reasons: (1) Si possesses the highest gravimetric capacity (3579 mA h g^{-1}, lithiated to $Li_{4.4}Si$)[135] and volumetric capacity (9786 mA h cm^{-3}, calculated based on the initial volume of Si) other than lithium metal; (2) Si exhibits an appropriate discharge voltage at ca. 0.4 V in average[136], which finds a good balance between retaining reasonable open circuit voltage and avoiding adverse lithium plating process; (3) Si is abundant (second richest in earth crust), potentially low cost, environment friendly, and non-toxic. However, drastic volume expansion (around 360% for $Li_{4.4}Si$)[135,137–139] and huge stress generation[140,141] are accompanied with the lithiation/delithiation process of Si, which causes series of severe destructive consequences. (1) Electrode structure integrity is deteriorated due to gradually enhanced pulverization during repeated discharge/charge processes; (2) disconnection between electrode and current collector happens induced by the interfacial stress; (3) continuous consumption of lithium ions occurs during the continuous formation-breaking-reformation process of solid electrolyte interface (SEI) layer[142,143]. All these processes accelerate electrode collapse and capacity fading in a synergistic way. Besides, the critical problem of volume expansion, the poor intrinsic electron conductivity of Si also contributes to the sluggish electrochemical kinetics.

To tackle the aforementioned critical issues, tremendous efforts have been made since 1990s[131,144–146].

The strategies developed include utilizing nanoscale silicon, compositing with stress-relief buffer matrix, and constructing physical compartment to accommodate volume expansion[147].

In this research, the alginate (polysaccharides) was coated to the surface of nano silicon particles, formed a kind of core-shell structure material. To alleviate the volume expansion of pure silicon and prolong the cycle life of lithium-ion battery, the core-shell structured compound Si-Alg was applied to lithium-ion battery as anode. Because the polymeric shell as a buffer layer can endure the huge silicon volume change during the lithiation/delithiation process.

5.2 Experimental

5.2.1 Synthesis of core-shell structured Si-based anode Si-Alg

First, 1 g SiNPs (Nano Silicon Particles, KCC Co., Ltd., Korea, *d* = 40-60 nm) were added in prepared 100 mL Piranha solution (H_2SO_4 : H_2O_2 = 4 :1) slowly with rigid stirring for 1 h. The surface of the SiNPs would be hydroxylated by Piranha solution through this step. Then washed the hydroxylated SiNPs by water and dried it on oven for next step.

Secondly, hydroxylated SiNPs (1 g) were dispersed in ethanol and water solution (volumetric ratio of 95 : 5) and sonicated for 1 h. APTES ((3-Aminopropyl)triethoxysilane, CAS no. 919-30-2, Sigma-Aldrich) 0.25 mL was added into the mixture and sonicated for 3 h. The solid was removed by filtration and washed with ethanol for 3 times. Si-NH_2 nanoparticles were finally obtained by drying the product in vacuum at 80 °C for 24 h.

Thirdly, 1 g of purified Alg was added in 100 mL of phosphate buffer solution (PBS, pH 6.0) with stirring until Alg was totally dissolved. 4.8 g EDC and 1.09 g NHS dissolved in PBS buffer were added to the Alg-PBS solution to activate the carboxylic acid groups in the Alg. The resulting mixture was stirred at room temperature for 15 min and Si-NH_2 nanoparticles (5.8 g) was subsequently added to the Alg-PBS solution. After then, triethylamine (TEA) was added dropwise into the above solution to adjust pH to 7.4. This mixture solution was vigorously stirred for 9 h at room temperature. The crude product collected by suction filtration was repeatedly washed with ethanol and water for three times. The final core-shell structured product, marked as Si-Alg, was dried in a vacuum oven at 80 °C and smashed to powder by planetary ball mill before use.

5.2.2 Preparation of electrodes and coin-cells

In this research, the Alg/Si-Alg electrodes were prepared by mixing core-shell structured anode Si-Alg, super P and alginate binder with a ratio of 1 :1 :1 in an adequate amount of distilled water. After

stirring in a planetary ball mill at 500 rpm for 30 min, a homogenous slurry was made and coated on the 20-μm-thick Al-foil by an automatic film-coating apparatus. The obtained raw electrodes were dried at 60 °C for 30 min in a convection oven and then put them in a vacuum oven (70 °C) for a whole night to completely remove remaining solvent before coin cell assembly. The mass loading of the electrodes were 1.3 ± 0.3 mg/cm^2. The electrolyte consists of ethylene carbonate (EC) : diethyl carbonate (DEC) : dimethyl carbonate (DMC) 3 : 5 : 2 v/v% with additive (5wt.% FEC, 2wt. % VC and 0.4wt.% $LiBF_4$), and the CR2032 coin-half cells were assembled in an argon-filled glove box with lithium foil as a counter electrode.

5.2.3 Characterization of materials and electrochemical properties

In this research, the structure analysis of the core-shell structured Si-Alg anode was recorded by Fourier transform infrared (FT-IR) spectroscopy (Thermo Scientific™ Nicolet™ iS™). The morphology of Si, Si-APTES, Si-Alg and the electrodes before and after cycles was filmed by transmission electron microscope (TEM, JEOL, 2010) and scanning electron microscopy (SEM, JEOL, 6700). The wettability of the binder films, represented by the contact angle of an electrolyte droplet on binder film, was measured using an optical tensiometer (Theta Lite, Biolin Scientific, Japan). The adhesion strength of the electrode was measured by the 180° peel strength of 2-cm-wide electrode strips in a texture analyzer (TA-Plus, Lloyd Instruments Ltd., USA) at a propagation speed of 60 mm min-1. The surface and interface resistivities of the electrode were obtained using a multipoint probe system (RM2610, HIOKI Corp., Japan) at room temperature. EIS with a frequency range from 10^6 Hz to 10^{-2} Hz at E=0 V was again used to obtain the kinetic parameters related to the charge/discharge processes of long-cycled electrodes. Cyclic voltammetry (CV) testing was also conducted in a battery cycler (WBCS3000, Wonatech, Korea) at scan rates of 0.2 mV s^{-1} between 3.0 V and 0 V. The galvanostatic charge/discharge and rate capability tests were also characterized in a battery cycler (PEBC 0550.1, PNE solution Co., Korea) with a constant current and a constant voltage mood at room temperature. For galvanostatic charge/discharge performance, the cells were fully charged/discharged between 0.05 V and 1.5 V at the current of 0.1 C for the first 2 cycles. Subsequently, the cells were charged/discharged at the current of 0.5 C for the next 200 cycles. Various charge/discharge current densities 0.1 C, 0.2 C, 0.5 C, 1.0 C, 2.0 C ,5.0 C, 10.0 C were applied in the rate capability test.

5.3 Results and discussion

5.3.1 FT-IR

The chemical compositions of the products for each step were future confirmed by FT-IR. Fig. 5-1 shows the FT-IR spectra of pure silicon, Si-APTES and Si-Alg. The APTES functionalized nano

silicon particles shows characteristic bands around 2916 cm^{-1}, corresponding to the CH_x stretching of APTES, The bands at 1045 cm^{-1} correspond to the Si-O-Si region, and the band at 1592 and 1485 cm^{-1} reveals the scissor vibration of the NH_2 terminal group of APTES, indicating that the nano silicon particles was successfully modified with APTES. The FT-IR spectra of Si-Alg shows the band at 1609, 1409 and 1070 cm^{-1} which are due to the stretching of $-COO^-$ (asymmetric), $-COO^-$ (symmetric) and C-O-C, respectively, it demonstrated alginate has chemically bonded with silicon and formed core-shell structure.

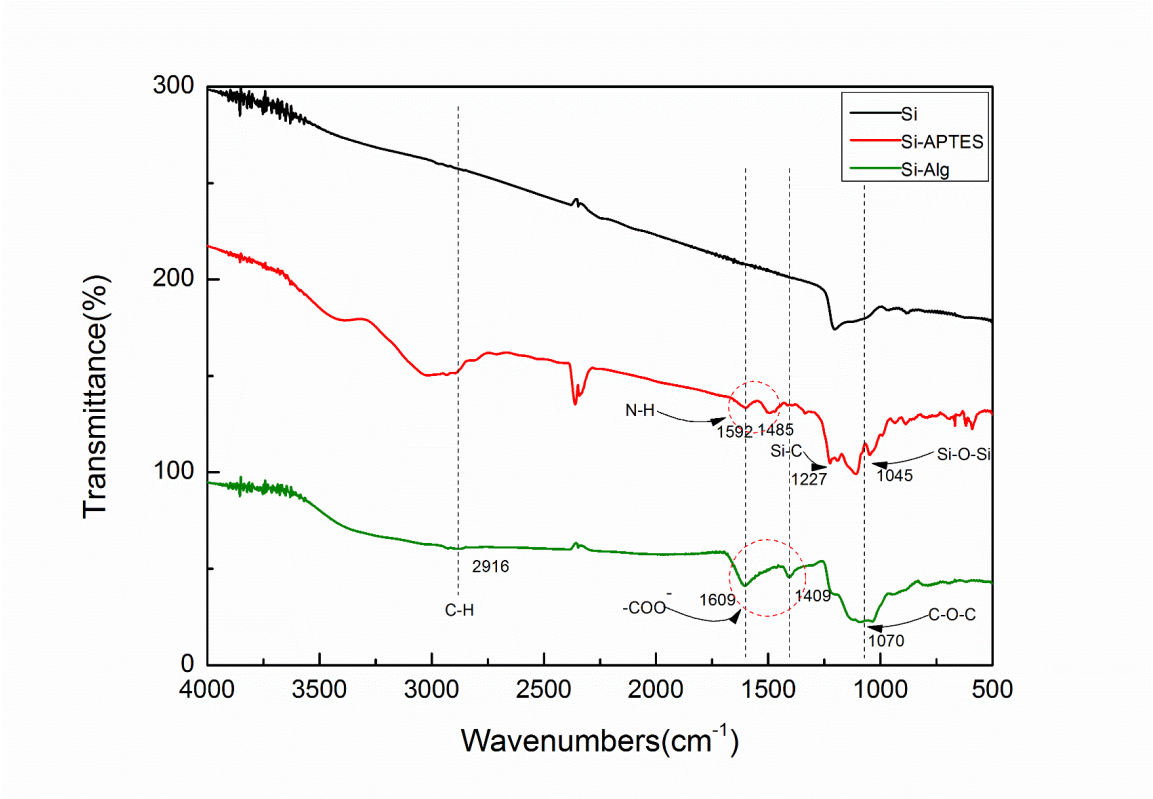

Figure 5-1 FT-IR spectra of pure silicon, Si-APTES and Si-Alg.

5.3.2 TEM

Fig. 5-2 comprises TEM images of pure silicon and the resultant particles prepared in the coating experiments with addition of the coupling reagent APTES. As seen in Fig. 5.2(b), after the reaction between silicon and APTES, the surface of the nano silicon particles formed a thin layer which thickness is about 2 nm, it indicates that APTES successfully modified the silicon surface. The clear core-shell structure was showed in Fig. 5.2(c), the alginate reacted with APTES and was coated to the surface of nano silicon as shell. Furthermore, each composite particle contained only one silicon core, although the composite particles were not entirely spherical. The average diameter of the cores was

confirmed to coincide with an average diameter (40-60 nm) of the silicon particles.

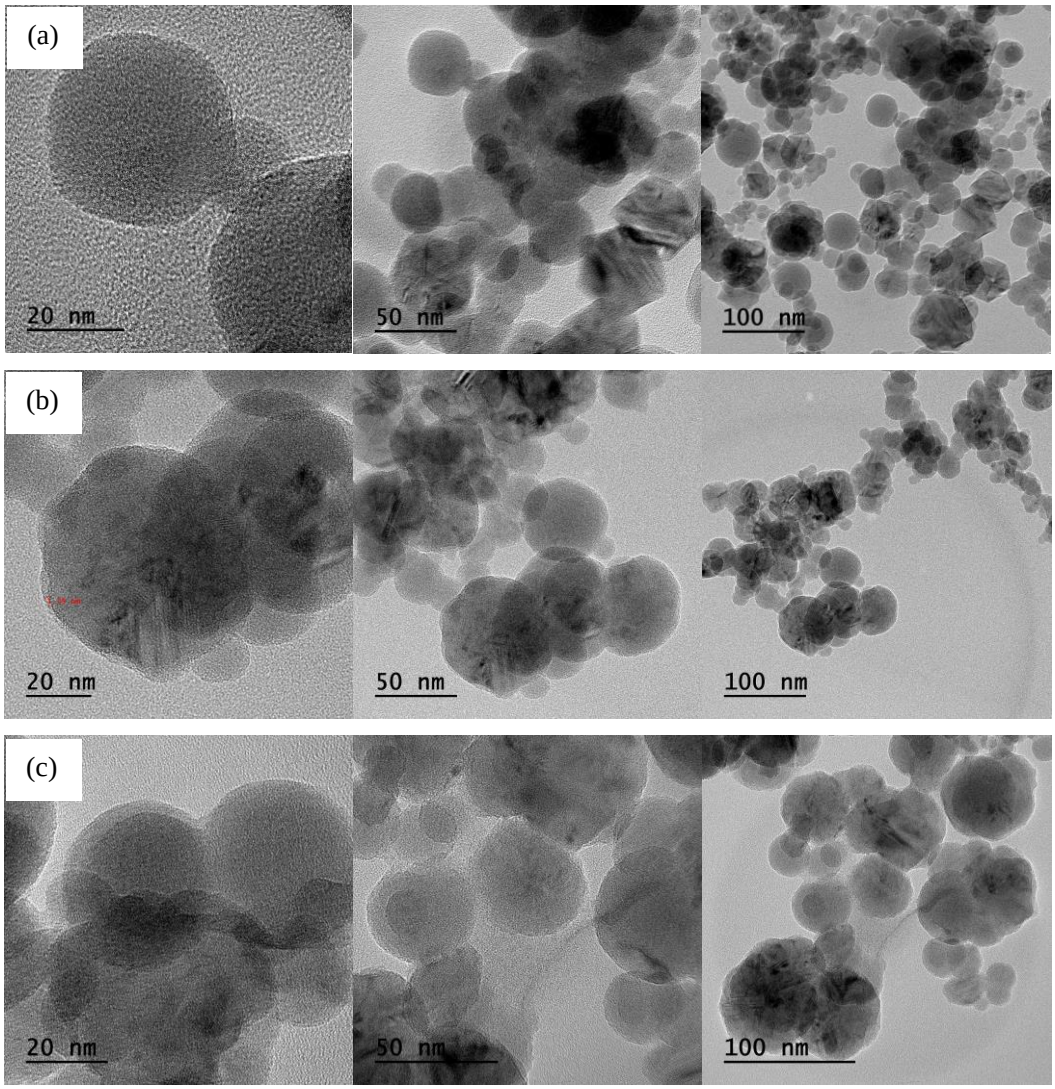

Figure 5-2 TEM images of (a) nano silicon particles, (b) Si-APTES, (c) Si-Alg.

5.3.3 EDS

The EDS analysis of nano silicon particles and Si-Alg particles revealed different elemental compositions shown by the representative data in Fig. 5-3. Compare to the elemental compositions of pure nano silicon particles, the ratio of C and O elements in Si-Alg improved remarkably, and ratio of Si composition declined in the meantime. It shows that alginate has attached on the surface of the nano particle silicon successfully. Some extra carbon element was detected because the tested particle samples were covered by conductive resin when they were done EDS measurement.

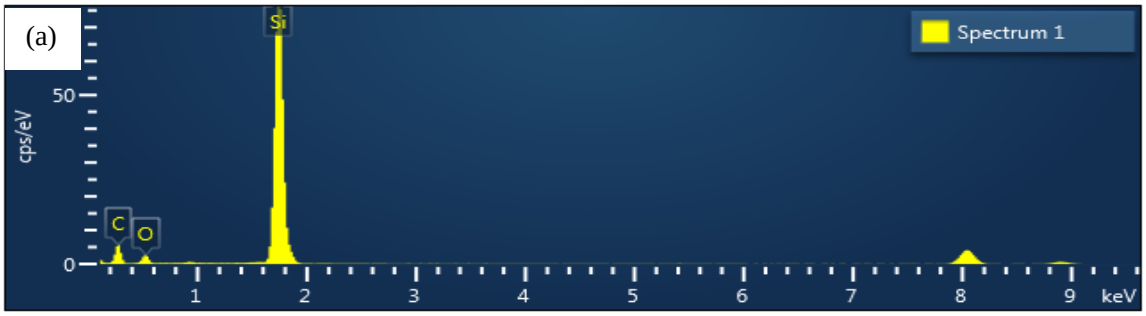

Element	Line Type	k Factor	k Factor type	Absorption Correction	Wt%	Wt% Sigma	Atomic %
C	K series	2.784		1.00	10.63	0.17	21.24
O	K series	2.030		1.00	3.69	0.10	5.53
Si	K series	1.000		1.00	85.68	0.19	73.22
Total:					100.00		100.00

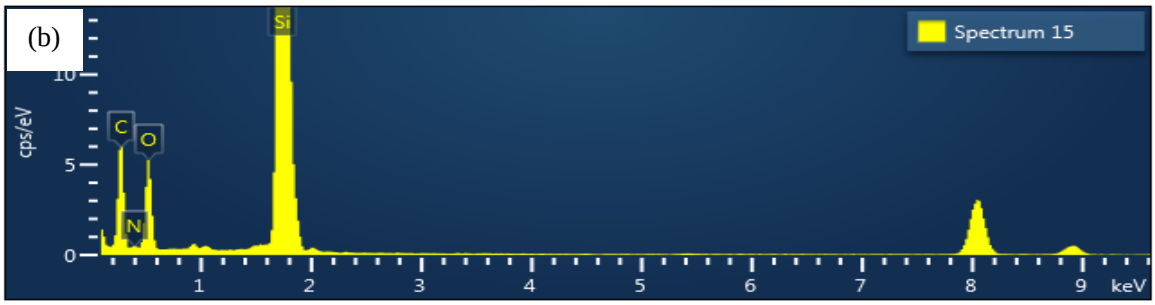

Element	Line Type	k Factor	k Factor type	Absorption Correction	Wt%	Wt% Sigma	Atomic %
C	K series	2.784		1.00	11.91	0.18	22.82
N	K series	3.534		1.00	0.25	0.13	0.41
O	K series	2.030		1.00	7.67	0.13	11.04
Si	K series	1.000		1.00	80.17	0.23	65.72

Total:					**100.00**		**100.00**

Figure 5-3 EDS spectra and quantitation data showing the typical composition found at the nano silicon particles and Si-Alg boundaries.

5.3.4 Adhesion test

The purpose of making Si-polymer core-shell anode material is to overcome the silicon volume expansion and reduce the pulverization during the charge/discharge process. Nevertheless, on the other hand, the polysaccharide polymer shell (Alginate) can enhance the adhesive strength between the anode and current collector as shown in Fig 5-4. The binders of both electrodes are sodium alginate, the 180° peeling test has been measured. It's clearly to see the average adhesive strength of the electrode employing Si-Alg as anode is much higher than that using SiNPs as anode, the average strength are 8.05 N and 0.77 N, respectively. It's well known that the electrode adhesion affect the capacity retention and cycling performance especially for high capacity silicon anodes experiencing huge volume change during charge/discharge processes. So what we can expect from this results is that the Si-Alg electrode would possess better cyclic performance compare to the SiNPs electrode.

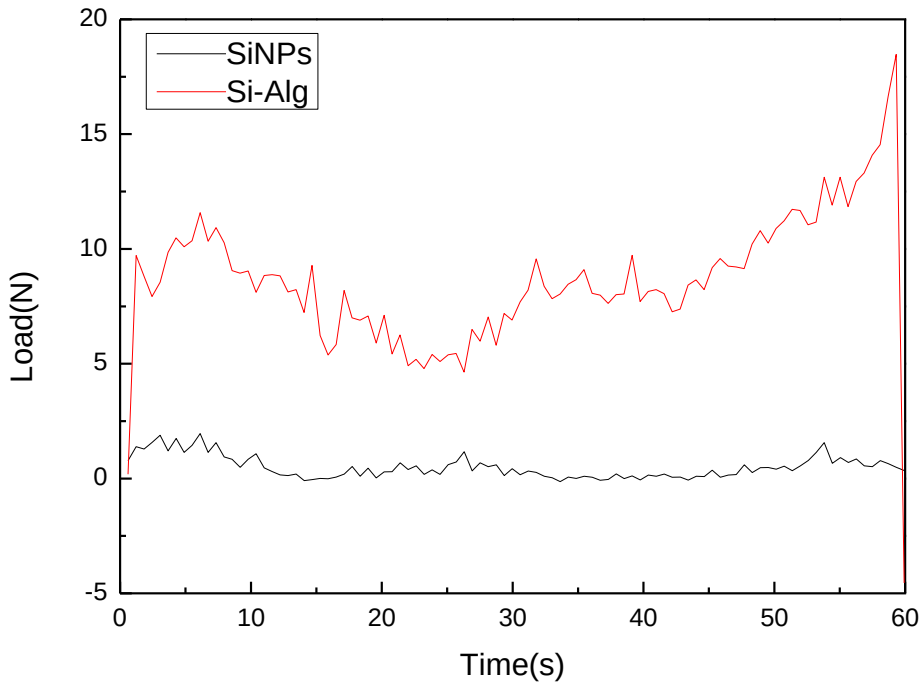

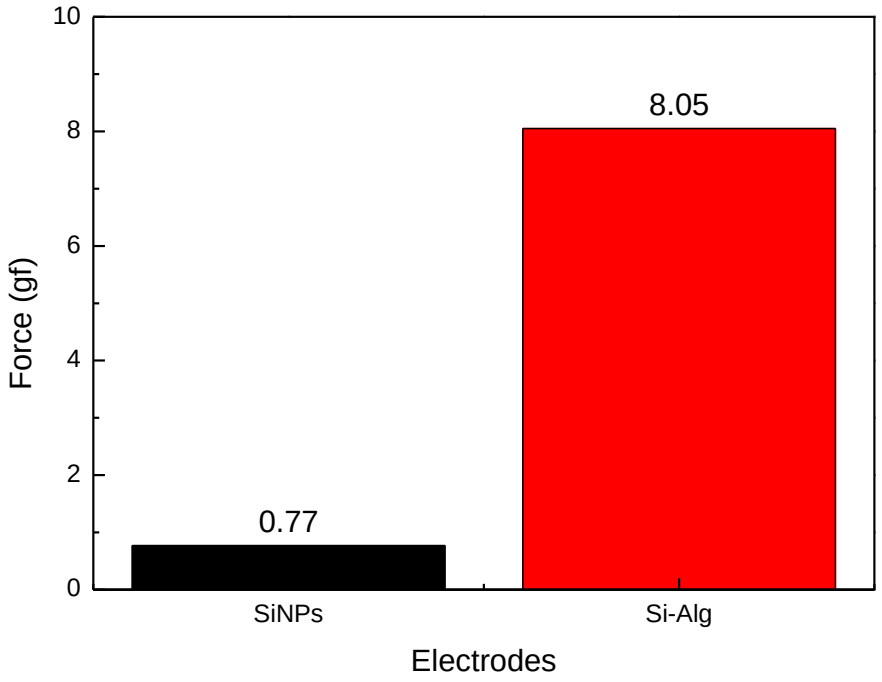

Figure 5-4 Adhesion strength of the SiNPs and Si-Alg electrodes measured by 180° peeling.

5.3.5 Cyclic voltammetry

The Cyclic voltammograms curves of employing SiNPs and Si-Alg as anodes material in LIBs is shown in Fig. 5-5. The CV curves of the pure silicon and Si-Alg anodes exhibit similar peak features. In the first cathodic scan, one broad reduction peak located at approximately 0.9 V vs. Li/Li^+ could be attributed to the irreversible decomposition of electrolyte and the formation of SEI on the surface of anode, which disappeared at the subsequent cycles. The other two cathodic peaks at approximately 0.20 V and below 0.1 V are attributed to Li–Si alloy formation. The subsequent delithiation process occurred at 0.31 and 0.55 V, but only one peak (0.55 V) occurred in electrode with SiNPs as anode. In the following cycles, emerging peaks are ascribed to the reversible lithiation/delithiation process of amorphous silicon.

(a)

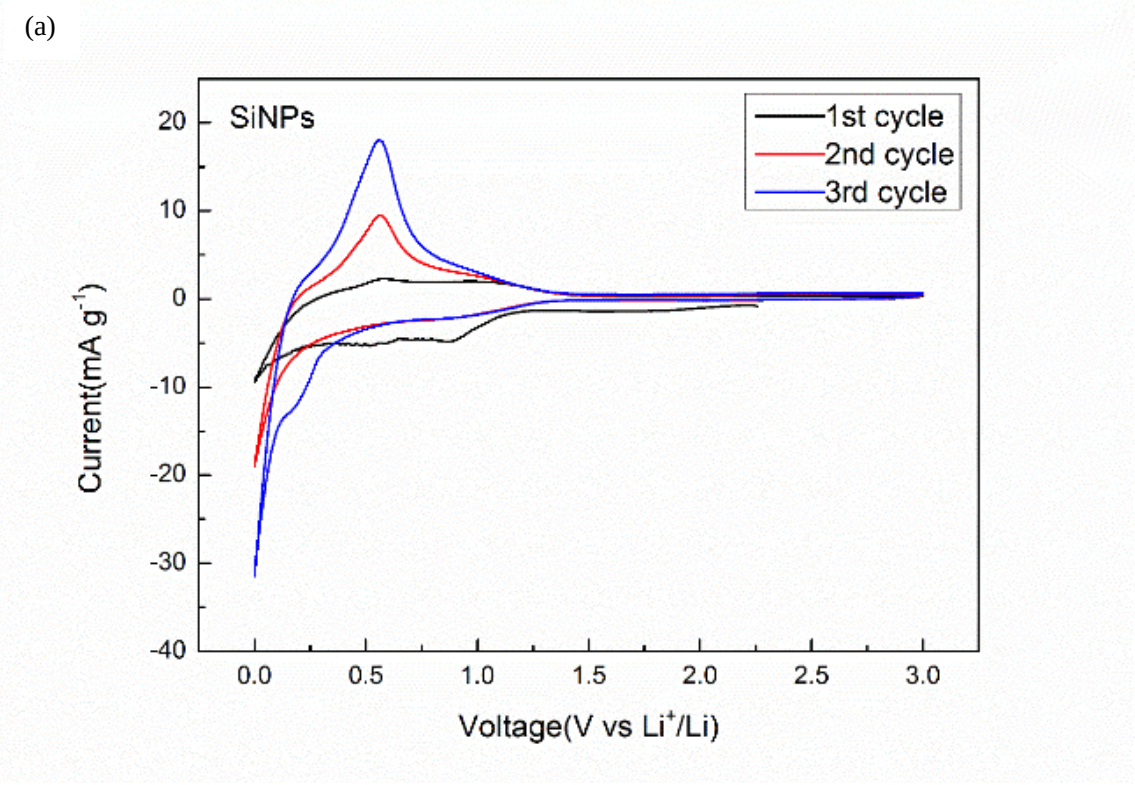

(b)

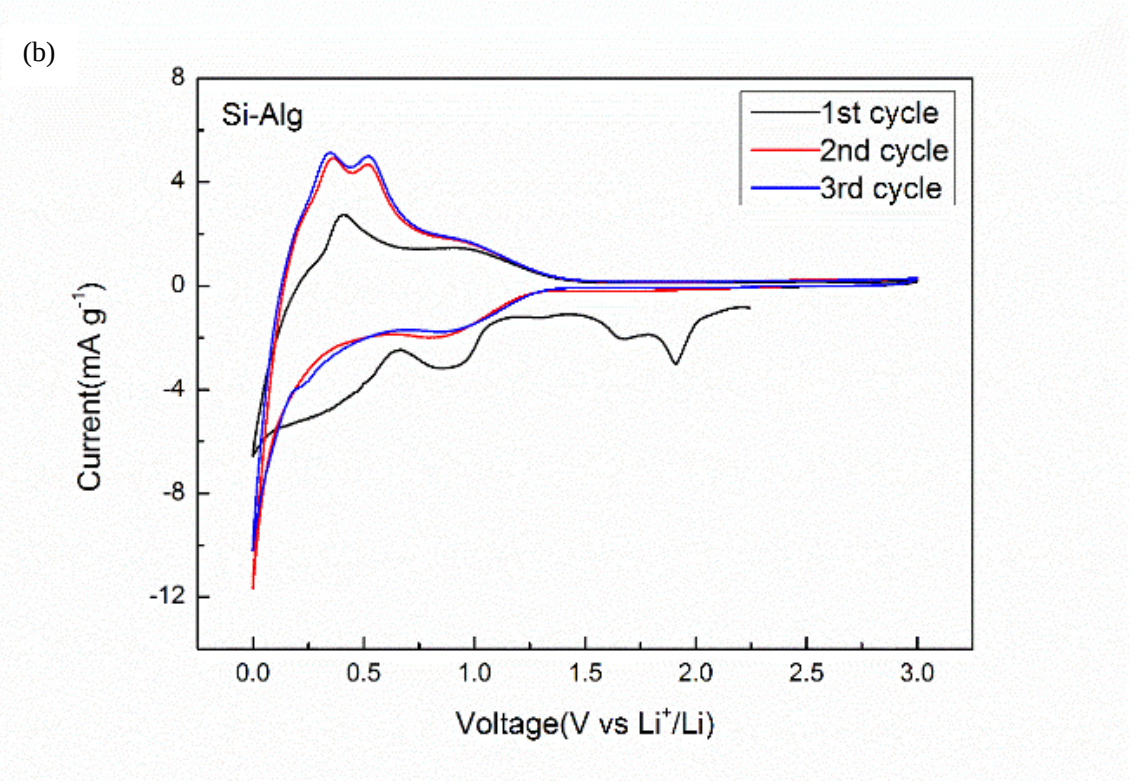

Figure 5-5 Cyclic voltammograms of (a) SiNPs and (b) Si-Alg electrodes at 0.5mVs^{-1} at 25℃ from OCV to 0 V (versus Li/Li^{+}) at first 3 cycles.

5.3.6 Cyclic performance

Fig. 5-6 compares the long-term cyclability of the Si-Alg composite and the pristine nano-silicon particles anodes at 0.5 C rate. To ensure the reproducibility of the result, we assembled two coin-cells at a time and simultaneously tested their cycling performance under the same condition. As is clearly seen from Fig. 5-6, the SiNPs anode shows a quite high capacity of 5100 mAh g^{-1} at first cycle, but the reversible capacity falls down very quickly to 900 mAh g^{-1} after 50 cycles. In contrast, the Si-Alg anode demonstrates a greatly improved cyclability. In addition to its initial high capacity of 4000 mAh g^{-1}, the Si-Alg anode can maintain to 1200 mAh g^{-1} after 200 cycles. At the same time, the coulombic efficiency kept stably at >99% at the prolonged cycles.

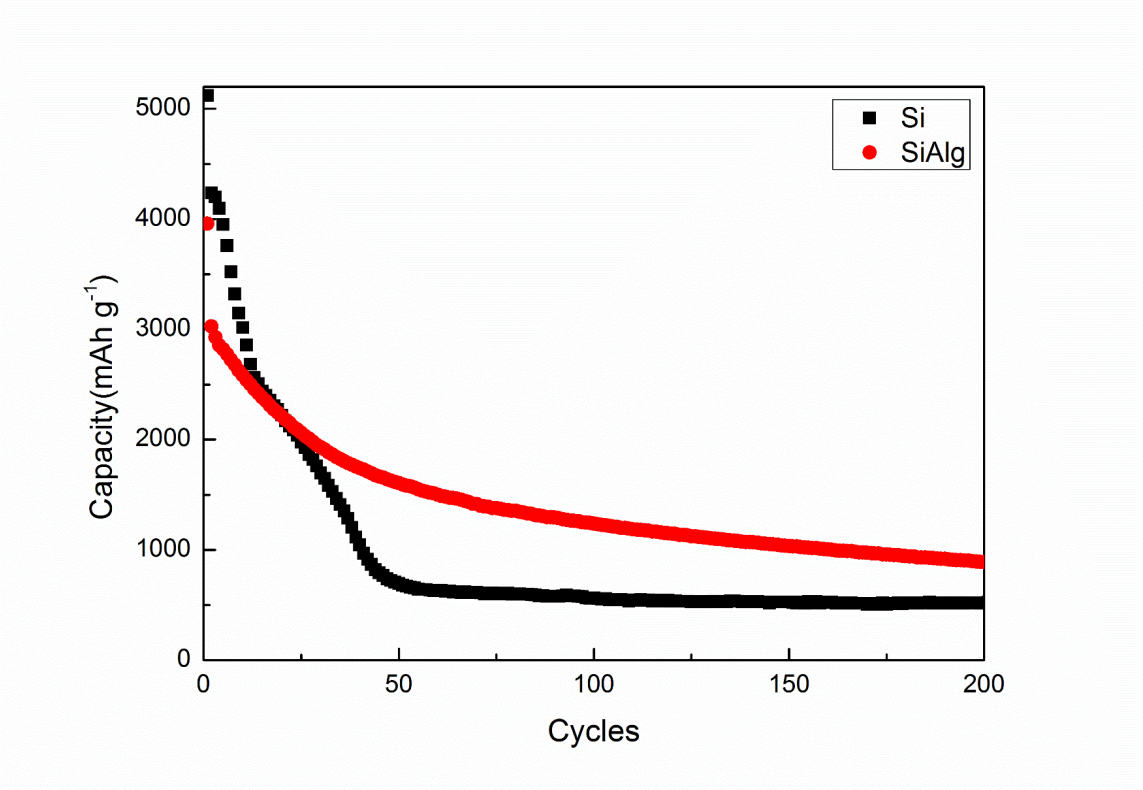

Figure 5-6 Cycling performance of the Si and Si-Alg electrode employing SA binder measured at 0.5 C rate.

5.3.7 Rate capability

Similar results with cyclic performance, the rate capability of Si-Alg electrode is more excellent than SiNPs electrode, especially in high rate. At current densities of 1, 2, 5, 10 C, the Si-Alg electrode retained capacities of 1000, 900, 800, and 600 mAh g^{-1}. After the current density returned to 0.5 C, the capacity was recovered to 1200 mAh g^{-1}. On the contrary, the pure nano-silicon anodes suffer fast

capacity decay as the current increases, and fail to deliver capacity when the current increases to 10 C rate.

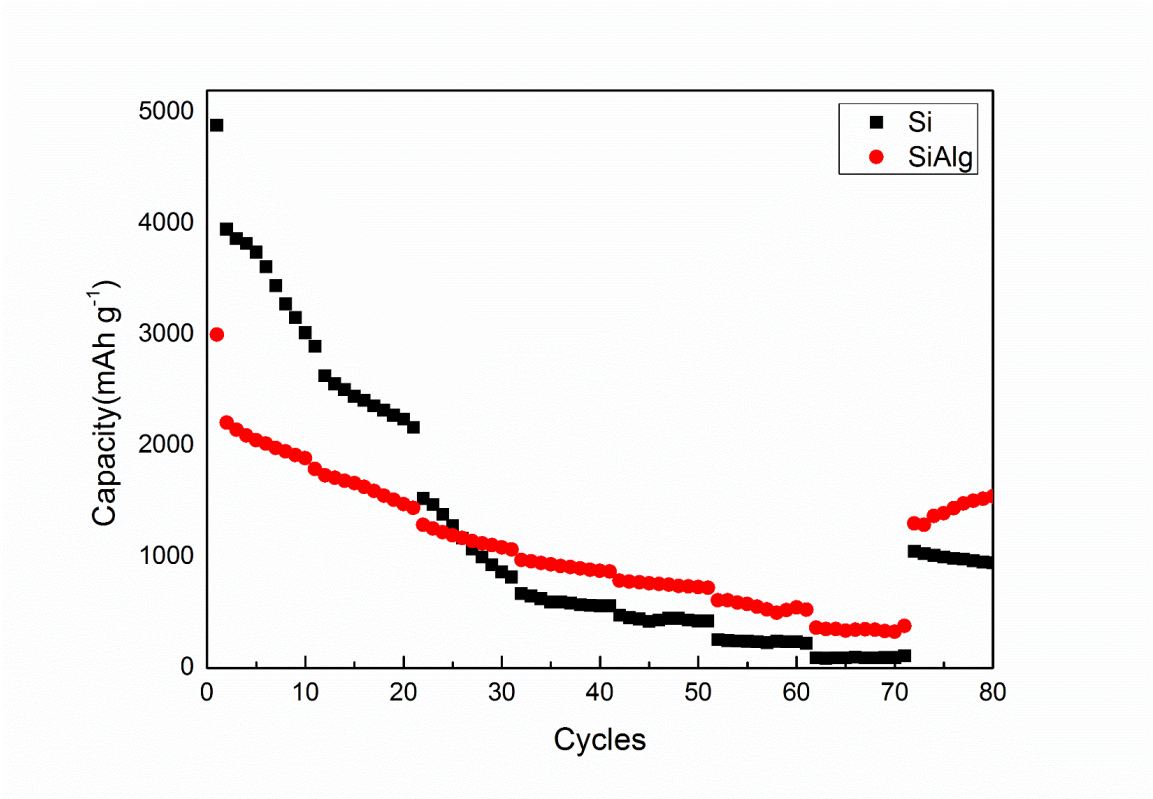

Figure 5-7 Rate capacity performance of the Si and Si-Alg electrodes employing SA binder measured from 0.1 to 10 C rate.

5.3.8 EIS

The charge transfer resistance in the EIS spectra (Fig. 5-8) is represented by the size of semicircles in the medium frequency range. The larger the semicircle, the larger R_{ct}. Because of polysaccharide polymer shell is a kind nonconductive material, the Si-Alg electrode exhibit higher charge transfer resistances than those containing SiNPs anodes no matter fresh or cycled cells. Normally, more insulative polymer covers more silicon surface leading to high resistance to lithium ion transfer through the coverage. As a matter of course, the Si-Alg electrode is more difficult to transport the ions and electrons, but in the long cycle life, this disadvantage can be offset.

(a)

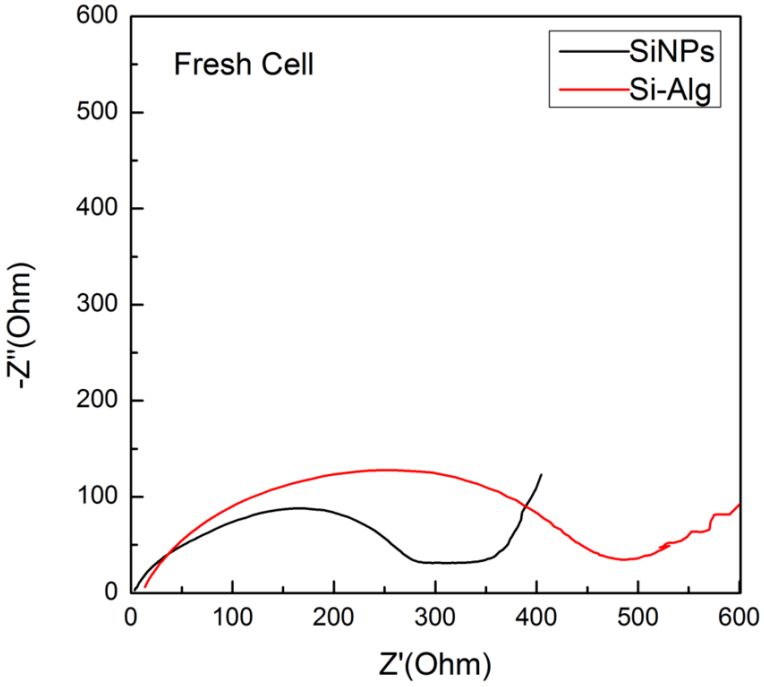

(b)

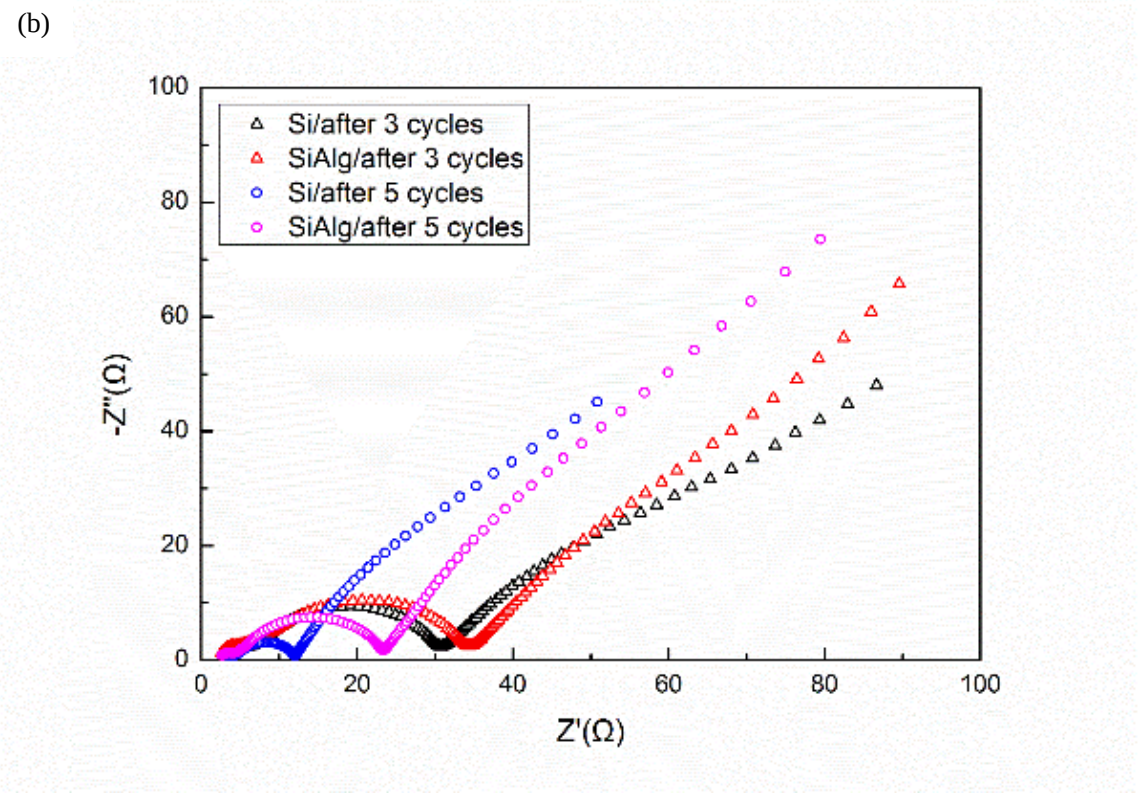

Figure 5-8 Nyquist plots of (a) the fresh, (b)three and five cycled electrodes employing SiNPs and Si-Alg anodes.

Furthermore, the lithium-ion diffusion coefficient was calculated using the classic Warburg formula ($D = R^2T^2/2A^2n^4F^4c^2\sigma^2$) through the EIS of five-cycled electrodes, D is lithium-ion diffusion coefficient; R is the gas constant; T is the absolute temperature; A is the electrode area; n is the number of electron transferred per molecule during electrochemical reaction; F is Faraday constant; and c is molar concentration of lithium ions; σ is the Warburg impedance coefficient. The lithium-ion diffusion coefficients calculated for the SiNPs and Si-Alg electrodes were 6.59×10^{-9} cm^2 s^{-1}, 1.38×10^{-9} cm^2 s^{-1}, respectively. From these results, it also shows that the core-shell structure Si-Alg anode show higher charge transfer resistance compare to the SiNPs anode.

5.3.9 SEM

The morphology of the electrodes was examined using SEM, shown in Fig. 5-9. Fig. 5-9(a) and 5-9(c) show the surface of the SiNPs and Si-Alg electrodes respectively before they were cycled in the lithium-ion batteries. Fig. 5-9(b) and 5-9(d) show the post-cycling morphology of the corresponding electrodes. Pre-cycling SEM shows the electrode materials are smoothly packed without any cracks. Post-cycling SEM shows large void space due to the volumetric expansion of active materials and the formation of SEI products during lithiation. Compare to the SiNPs electrode, the Si-Alg electrode has a smaller void space and less destroyed after 200 charge/discharge cycles. This indicates that the Si-Alg electrodes have better ability to endure the silicon volume expansion and pulverization than SiNPs electrode.

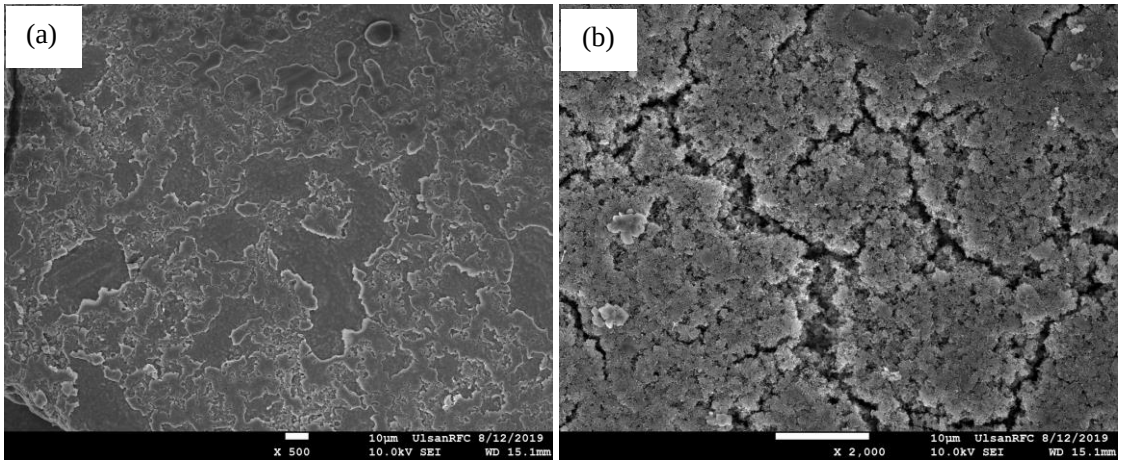

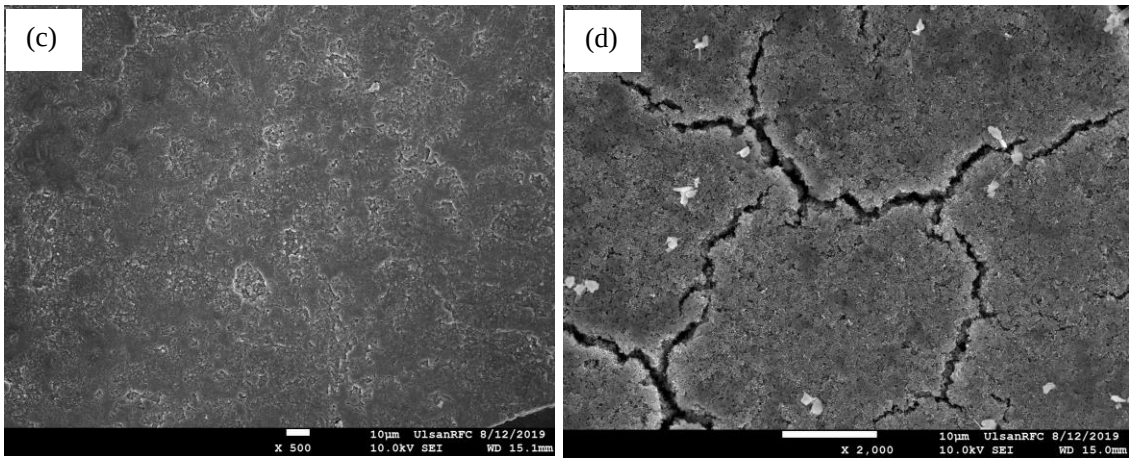

Figure 5-9 SEM images of SiNPs and Si-Alg anodes (a) and (c) before and (b) and (d) after 200 charge/discharge cycles, respectively.

5.4 Conclusions

In this research, the sodium alginate successfully reacted with silicon nanoparticles and obtained the core-shell structured Si-based anode material. The coin-cell with core-shell structured Si-based material as anode exhibited the excellent and long cycle life electrochemical performance, in addition, it also kept the stable capacity compared to the electrode with silicon nanoparticles as anode. This research introduced a convenient and efficient way to endure the swelling of silicon and keep the integrity of electrode during the lithiation/delithiation process by introducing the alginate as a shell.

Summary

In this dissertation, most efforts were put on modifying or designing novel multiple functional binders using the polysaccharides as raw materials for high-powered $Li_4Ti_5O_{12}$ and high-capacity Si anode in lithium-ion batteries. In addition, some efforts were put on modifying Si particles anode through coating the polysaccharides on the surface of Si particles, aim to alleviate the volume expansion of Si-based anode during lithiation/delithiation process and prolong the cycle life of coin-cell with modified core-shell structured Si-Alg as anode.

It's well-known that binder plays a crucial role in lithium-ion batteries. Nowadays, various binders were commercialized for different cathodes and anodes. But no binder is perfect for lithium-ion batteries, each binder has own defects and application restriction. Our purpose is to remedy the defects on some binders and endow them more functions, leading them to be used for lithium-ion batteries efficiently.

In the first research, we modified the polysaccharide binders alginate and CMC by introducing the -SO_3H groups to the backbone of them, the obtained modified binder Alg-S and CMC-S improved the ionic conductivity of LTO anode and electrochemical performance as well. Originally, the classic polysaccharides don't possess good ionic conductivity due to natural insulation, after introduced the -SO_3H groups to the backbone of them, they possess a new function to contribute the coin-cell's excellent electrochemical performance.

In the second research, the alginate backbone was graft copolymerization with AA and BA, this step enhanced the adhesion ability among active materials and between active materials and current collector. Then the 2-dimensional conductive material MXene was chemical bonded with Alg-AABA and formed novel adhesive and conductive binder Alg-AABA-Mx. This new binder not only improved the adhesion strength, but also improved the electronic conductivity, the coin-cell exhibited better electrochemical performance with the Alg-ABAA and Alg-ABAA-Mx as binders for high-capacity Si anode in lithium-ion batteries.

More and more attention paid to Si anode due to the highest theoretical capacity, while the huge volume expansion limits it for commercial application. In the third research, the pure silicon particles were modified by coating alginate on its surface, the formed core-shell structured Si-based material was employed to lithium-ion batteries as anode. The research results demonstrated that the modification alleviate the volume expansion and anode pulverization during lithiation/delithiation process, prolong the coin-cell's cycle life and improve the electrochemical performance as well.

References

1. Jian, G., Shi, S.-Q. & Li, H. Brief overview of electrochemical potential in lithium ion batteries. *Chin. Phys. B* **25**, 018210 (2016).
2. Chawla, N., Bharti, N. & Singh, S. Recent Advances in Non-Flammable Electrolytes for Safer Lithium-Ion Batteries. *Batteries* **5**, 19 (2019).
3. Amatucci, G. G., Tarascon, J. M. & Klein, L. C. CoO2, The End Member of the Li x CoO2 Solid Solution. *J. Electrochem. Soc.* **143**, 1114 (1996).
4. Hashem, A. M. A. *et al.* Study of the surface modification of LiNi1/3Co1/3Mn1/3O2 cathode material for lithium ion battery. *J. Power Sources* **196**, 8632–8637 (2011).
5. Ohzuku, T. & Makimura, Y. Formation of solid solution and its effect on lithium insertion schemes for advanced lithium-ion batteries: X-ray absorption spectroscopy and X-ray diffraction of LiCoO2, LiCo1/2Ni1/2O2 and LiNiO2. *Res. Chem. Intermed.* **32**, 507–521 (2006).
6. Goriparti, S. *et al.* Review on recent progress of nanostructured anode materials for Li-ion batteries. *J. Power Sources* **257**, 421–443 (2014).
7. Kang, B. & Ceder, G. Battery materials for ultrafast charging and discharging. *Nature* **458**, 190–193 (2009).
8. Wu, C., Feng, F. & Xie, Y. Design of vanadium oxide structures with controllable electrical properties for energy applications. *Chem. Soc. Rev.* **42**, 5157–5183 (2013).
9. Thackeray, M. M., Kang, S.-H., Johnson, C. S., Vaughey, J. T. & Hackney, S. A. Comments on the structural complexity of lithium-rich Li1+xM1−xO2 electrodes (M=Mn, Ni, Co) for lithium batteries. *Electrochem. Commun.* **8**, 1531–1538 (2006).
10. Wang, J. & Sun, X. Olivine LiFePO4: the remaining challenges for future energy storage. *Energy Environ. Sci.* **8**, 1110–1138 (2015).

11. Liu, C., Neale, Z. G. & Cao, G. Understanding electrochemical potentials of cathode materials in rechargeable batteries. *Mater. Today* **19**, 109–123 (2016).
12. Qi, W. *et al.* Nanostructured anode materials for lithium-ion batteries: principle, recent progress and future perspectives. *J. Mater. Chem. A* **5**, 19521–19540 (2017).
13. Balogun, M.-S., Luo, Y., Qiu, W., Liu, P. & Tong, Y. A review of carbon materials and their composites with alloy metals for sodium ion battery anodes. *Carbon* **98**, 162–178 (2016).
14. Peng, K., Jie, J., Zhang, W. & Lee, S.-T. Silicon nanowires for rechargeable lithium-ion battery anodes. *Appl. Phys. Lett.* **93**, 033105 (2008).
15. Chen, X., Du, Y., Zhang, N. Q. & Sun, K. N. 3D Self-Supported Nanoarchitectured Arrays Electrodes for Lithium-Ion Batteries. *Journal of Nanomaterials* vol. 2012 e905157 https://www.hindawi.com/journals/jnm/2012/905157/ (2012).
16. Lee, J. K., Oh, C., Kim, N., Hwang, J.-Y. & Sun, Y.-K. Rational design of silicon-based composites for high-energy storage devices. *J. Mater. Chem. A* **4**, 5366–5384 (2016).
17. Cho, I., Choi, J., Kim, K., Ryou, M.-H. & Lee, Y. M. A comparative investigation of carbon black (Super-P) and vapor-grown carbon fibers (VGCFs) as conductive additives for lithium-ion battery cathodes. *RSC Adv.* **5**, 95073–95078 (2015).
18. Latifatu, M. *et al.* Structural Effect of Conductive Carbons on the Adhesion and Electrochemical Behavior of $LiNi_{0.4}Mn_{0.4}Co_{0.2}O_2$ Cathode for Lithium Ion Batteries. *J. Electrochem. Sci. Technol.* **9**, 330–338 (2018).
19. Teng, X. *et al.* The influence of conductive additives on the performance of a SiO/C composite anode in lithium-ion batteries. *New Carbon Mater.* **32**, 572–580 (2017).
20. Kwon, N. H., Mouck-Makanda, D. & Fromm, K. M. A Review: Carbon Additives in LiMnPO4- and LiCoO2-Based Cathode Composites for Lithium Ion Batteries. *Batteries* **4**, 50 (2018).

21. Wang, R. *et al.* Effect of Different Binders on the Electrochemical Performance of Metal Oxide Anode for Lithium-Ion Batteries. *Nanoscale Res. Lett.* **12**, 575 (2017).
22. Zhao, X. *et al.* Revealing the Role of Poly(vinylidene fluoride) Binder in Si/Graphite Composite Anode for Li-Ion Batteries. *ACS Omega* **3**, 11684–11690 (2018).
23. Bresser, D., Buchholz, D., Moretti, A., Varzi, A. & Passerini, S. Alternative binders for sustainable electrochemical energy storage – the transition to aqueous electrode processing and bio-derived polymers. *Energy Environ. Sci.* **11**, 3096–3127 (2018).
24. PVDF Latex As a Binder for Positive Electrodes in Lithium-Ion Batteries | Industrial & Engineering Chemistry Research. https://pubs.acs.org/doi/10.1021/ie403239s.
25. Investigations on novel electrolytes, solvents and SEI additives for use in lithium-ion batteries: Systematic electrochemical characterization and detailed analysis by spectroscopic methods | Request PDF. https://www.researchgate.net/publication/261718003_Investigations_on_novel_electrolytes_solvents_and_SEI_additives_for_use_in_lithium-ion_batteries_Systematic_electrochemical_characterization_and_detailed_analysis_by_spectroscopic_methods.
26. On the difference in cycling behaviors of lithium-ion battery cell between the ethylene carbonate- and propylene carbonate-based electrolytes - ScienceDirect. https://www.sciencedirect.com/science/article/pii/S0013468611008565.
27. Lithium Ion Batteries: Fundamentals and Performance | Wiley. *Wiley.com* https://www.wiley.com/en-us/Lithium+Ion+Batteries%3A+Fundamentals+and+Performance-p-9783527611980.
28. Aurbach, D. *et al.* Design of electrolyte solutions for Li and Li-ion batteries: a review. *Electrochimica Acta* **50**, 247–254 (2004).

29. Krämer, E., Passerini, S. & Winter, M. Dependency of Aluminum Collector Corrosion in Lithium Ion Batteries on the Electrolyte Solvent. *ECS Electrochem. Lett.* **1**, C9 (2012).
30. Newman, G. H., Francis, R. W., Gaines, L. H. & Rao, B. M. L. Hazard Investigations of LiClO4 / Dioxolane Electrolyte. *J. Electrochem. Soc.* **127**, 2025 (1980).
31. Conductivity and viscosity of PC-DEC and PC-EC solutions of LiBF4. https://www.researchgate.net/publication/239261915_Conductivity_and_viscosity_of_PC-DEC_and_PC-EC_solutions_of_LiBF4.
32. Rupp, B., Schmuck, M., Balducci, A., Winter, M. & Kern, W. Polymer electrolyte for lithium batteries based on photochemically crosslinked poly(ethylene oxide) and ionic liquid. *Eur. Polym. J.* **44**, 2986–2990 (2008).
33. Zhang, S. S. A review on electrolyte additives for lithium-ion batteries. *J. Power Sources* **162**, 1379–1394 (2006).
34. Shigematsu, Y., Kinoshita, S. W. & Ue, M. Thermal Behavior of a C／LiCoO2 Cell, Its Components, and Their Combinations and the Effects of Electrolyte Additives. (2006) doi:10.1149/1.2347100.
35. Influence of electrolyte additives on safety and cycle life of rechargeable lithium cells. https://www.researchgate.net/publication/227206653_Influence_of_electrolyte_additives_on_safety_and_cycle_life_of_rechargeable_lithium_cells.
36. The Solid Electrolyte Interphase – The Most Important and the Least Understood Solid Electrolyte in Rechargeable Li Batteries in: Zeitschrift für Physikalische Chemie Volume 223 Issue 10-11 (2009). https://www.degruyter.com/view/journals/zpch/223/10-11/article-p1395.xml.
37. In situ characterization of the SEI formation on graphite in the presence of a vinylene group containing film-forming electrolyte additives | Request PDF.

https://www.researchgate.net/publication/228437240_In_situ_characterization_of_the_SEI_formation_on_graphite_in_the_presence_of_a_vinylene_group_containing_film-forming_electrolyte_additives.

38. Santner, H. J., Korepp, C., Winter, M., Besenhard, J. O. & Möller, K.-C. In-situ FTIR investigations on the reduction of vinylene electrolyte additives suitable for use in lithium-ion batteries. *Anal. Bioanal. Chem.* **379**, 266–271 (2004).
39. Investigation of N-Ethyl-2-Pyrrolidone (NEP) as Electrolyte Additive in Regard to Overcharge Protecting Characteristics | Request PDF. https://www.researchgate.net/publication/270451336_Investigation_of_N-Ethyl-2-Pyrrolidone_NEP_as_Electrolyte_Additive_in_Regard_to_Overcharge_Protecting_Characteristics.
40. Dippel, C. *et al.* Carbene Adduct as Overcharge Protecting Agent in Lithium Ion Batteries. *J. Electrochem. Soc.* **159**, A1587 (2012).
41. 4-Bromobenzyl isocyanate versus benzyl isocyanate—New film-forming electrolyte additives and overcharge protection additives for lithium ion batteries | Request PDF. https://www.researchgate.net/publication/232397131_4-Bromobenzyl_isocyanate_versus_benzyl_isocyanate-New_film-forming_electrolyte_additives_and_overcharge_protection_additives_for_lithium_ion_batteries.
42. Schranzhofer, H. *et al.* Electrochemical impedance spectroscopy study of the SEI formation on graphite and metal electrodes. *J. Power Sources* **153**, 391–395 (2006).
43. Dey, A. N. Lithium anode film and organic and inorganic electrolyte batteries. *Thin Solid Films* **43**, 131–171 (1977).

44. Peled, E. & Yamin, H. Solid Electrolyte Interphase (SEI) Electrodes. Part 1. The Kinetics of Lithium in LiAlCl4-SOCl2. *Isr. J. Chem.* **18**, 131–135 (1979).
45. Rajagopalan Kannan, D. R., Terala, P. K., Moss, P. L. & Weatherspoon, M. H. Analysis of the Separator Thickness and Porosity on the Performance of Lithium-Ion Batteries. *International Journal of Electrochemistry* vol. 2018 e1925708 https://www.hindawi.com/journals/ijelc/2018/1925708/ (2018).
46. Li, Y., Pu, H. & Wei, Y. Polypropylene/polyethylene multilayer separators with enhanced thermal stability for lithium-ion battery via multilayer coextrusion. *Electrochimica Acta* **264**, 140–149 (2018).
47. Lee, H., Yanilmaz, M., Toprakci, O., Fu, K. & Zhang, X. A review of recent developments in membrane separators for rechargeable lithium-ion batteries. *Energy Environ. Sci.* **7**, 3857–3886 (2014).
48. The Role of Separators in Lithium-Ion Cell Safety. https://www.researchgate.net/publication/273129788_The_Role_of_Separators_in_Lithium-Ion_Cell_Safety.
49. Yoshio, M., Brodd, R. J. & Kozawa, A. *Lithium-Ion Batteries: Science and Technologies*. (Springer Science & Business Media, 2010).
50. An, S. J. *et al.* The state of understanding of the lithium-ion-battery graphite solid electrolyte interphase (SEI) and its relationship to formation cycling. *Carbon* **105**, 52–76 (2016).
51. Stability of Solid Electrolyte Interphase Components on Lithium Metal and Reactive Anode Material Surfaces | The Journal of Physical Chemistry C. https://pubs.acs.org/doi/abs/10.1021/acs.jpcc.5b11719.

52. A Review of Solid Electrolyte Interphases on Lithium Metal Anode - Cheng - 2016 - Advanced Science - Wiley Online Library. https://onlinelibrary.wiley.com/doi/full/10.1002/advs.201500213.
53. Choi, N.-S. *et al.* Recent Progress on Polymeric Binders for Silicon Anodes in Lithium-Ion Batteries. *J. Electrochem. Sci. Technol.* **6**, 35–49 (2015).
54. Shortly Branched, Linear Dextrans as Efficient Binders for Silicon/Graphite Composite Electrodes in Li-Ion Batteries | Industrial & Engineering Chemistry Research. https://pubs.acs.org/doi/10.1021/acs.iecr.8b01055.
55. Bie, Y., Yang, J., Nuli, Y. & Wang, J. Oxidized starch as a superior binder for silicon anodes in lithium-ion batteries. *RSC Adv.* **6**, 97084–97088 (2016).
56. Versaci, D. *et al.* New eco-friendly low-cost binders for Li-ion anodes. *J. Solid State Electrochem.* **21**, 3429–3435 (2017).
57. Wang, L., Fu, Y., Battaglia, V. S. & Liu, G. SBR–PVDF based binder for the application of SLMP in graphite anodes. *RSC Adv.* **3**, 15022–15027 (2013).
58. Hu, S. *et al.* Effect of different binders on electrochemical properties of LiFePO4/C cathode material in lithium ion batteries. *Chem. Eng. J.* **237**, 497–502 (2014).
59. Chen, Z., Christensen, L. & Dahn, J. R. Comparison of PVDF and PVDF-TFE-P as Binders for Electrode Materials Showing Large Volume Changes in Lithium-Ion Batteries. *J. Electrochem. Soc.* **150**, A1073 (2003).
60. Maleki, H., Deng, G., Kerzhner‐Haller, I., Anani, A. & Howard, J. N. Thermal Stability Studies of Binder Materials in Anodes for Lithium‐Ion Batteries. *J. Electrochem. Soc.* **147**, 4470 (2000).

61. Bigoni, F., Giorgio, F. D., Soavi, F. & Arbizzani, C. Sodium Alginate: A Water-Processable Binder in High-Voltage Cathode Formulations. *J. Electrochem. Soc.* **164**, A6171–A6177 (2017).
62. Ling, L. *et al.* Remarkable Effect of Sodium Alginate Aqueous Binder on Anatase TiO2 as High-Performance Anode in Sodium Ion Batteries. *ACS Appl. Mater. Interfaces* **10**, 5560–5568 (2018).
63. Ling, M. *et al.* Dual-functional gum arabic binder for silicon anodes in lithium ion batteries. *Nano Energy* **12**, 178–185 (2015).
64. Wang, Z. *et al.* CMC as a binder in LiNi0.4Mn1.6O4 5V cathodes and their electrochemical performance for Li-ion batteries. *Electrochimica Acta* **62**, 77 (2012).
65. Kvasha, A. *et al.* Towards high durable lithium ion batteries with waterborne LiFePO4 electrodes. *Electrochimica Acta* **215**, 238–246 (2016).
66. Buqa, H., Holzapfel, M., Krumeich, F., Veit, C. & Novák, P. Study of styrene butadiene rubber and sodium methyl cellulose as binder for negative electrodes in lithium-ion batteries. *J. Power Sources* **161**, 617–622 (2006).
67. Comparative Study of Water-Based LA133 and CMC/SBR Binders for Sulfur Cathode in Advanced Lithium–Sulfur Batteries | The Journal of Physical Chemistry C. https://pubs.acs.org/doi/10.1021/acs.jpcc.8b10736.
68. Chong, J. *et al.* A comparative study of polyacrylic acid and poly(vinylidene difluoride) binders for spherical natural graphite/LiFePO4 electrodes and cells. *J. Power Sources* **196**, 7707–7714 (2011).
69. Gangaja, B., Chandrasekharan, S., Vadukumpully, S., Nair, S. V. & Santhanagopalan, D. Surface chemical analysis of CuO nanofiber composite electrodes at different stages of lithiation/delithiation. *J. Power Sources* **340**, 356–364 (2017).

70. Park, H.-K., Kong, B.-S. & Oh, E.-S. Effect of high adhesive polyvinyl alcohol binder on the anodes of lithium ion batteries. *Electrochem. Commun.* **13**, 1051–1053 (2011).
71. Liao, J., Liu, Z., Wang, J. & Ye, Z. Cost-Effective Water-Soluble Poly(vinyl alcohol) as a Functional Binder for High-Sulfur-Loading Cathodes in Lithium–Sulfur Batteries. *ACS Omega* **5**, 8272–8282 (2020).
72. Lee, D. *et al.* In Situ Cross-linked Carboxymethyl Cellulose-Polyethylene Glycol Binder for Improving the Long-Term Cycle Life of Silicon Anodes in Li Ion Batteries. *Ind. Eng. Chem. Res.* **58**, 8123–8130 (2019).
73. Yao, D., Yang, Y., Deng, Y. & Wang, C. Flexible polyimides through one-pot synthesis as water-soluble binders for silicon anodes in lithium ion batteries. *J. Power Sources* **379**, 26–32 (2018).
74. Choi, N.-S., Yew, K. H., Choi, W.-U. & Kim, S.-S. Enhanced electrochemical properties of a Si-based anode using an electrochemically active polyamide imide binder. *J. Power Sources* **177**, 590–594 (2008).
75. Performance Enhancement of Silicon Alloy-Based Anodes Using Thermally Treated Poly(amide imide) as a Polymer Binder for High Performance Lithium-Ion Batteries | Langmuir. https://pubs.acs.org/doi/abs/10.1021/acs.langmuir.6b00205.
76. Chai, L. *et al.* Chitosan, a new and environmental benign electrode binder for use with graphite anode in lithium-ion batteries. in (2013). doi:10.1016/j.electacta.2013.05.009.
77. Zhao, X., Yim, C.-H., Du, N. & Abu-Lebdeh, Y. Crosslinked Chitosan Networks as Binders for Silicon/Graphite Composite Electrodes in Li-Ion Batteries. *J. Electrochem. Soc.* **165**, A1110 (2018).
78. Lee, S. H. *et al.* Epoxidized Natural Rubber/Chitosan Network Binder for Silicon Anode in Lithium-Ion Battery. *ACS Appl. Mater. Interfaces* **10**, 16449–16457 (2018).

79. Jeżowski, P. & Kowalczewski, P. Ł. Starch as a Green Binder for the Formulation of Conducting Glue in Supercapacitors. *Polymers* **11**, (2019).
80. Rohan, R. *et al.* Low-cost and sustainable corn starch as a high-performance aqueous binder in silicon anodes via in situ cross-linking. in (2018). doi:10.1016/j.jpowsour.2018.06.045.
81. Hwang, G. *et al.* Multifunctional natural agarose as an alternative material for high-performance rechargeable lithium-ion batteries. *Green Chem.* **18**, 2710–2716 (2016).
82. Liu, J. *et al.* A Robust Ion-Conductive Biopolymer as a Binder for Si Anodes of Lithium-Ion Batteries. *Adv. Funct. Mater.* **25**, 3599–3605 (2015).
83. Jeong, Y. K. *et al.* Millipede-inspired structural design principle for high performance polysaccharide binders in silicon anodes. *Energy Environ. Sci.* **8**, 1224–1230 (2015).
84. Bie, Y., Yang, J., Nuli, Y. & Wang, J. Natural karaya gum as an excellent binder for silicon-based anodes in high-performance lithium-ion batteries. *J. Mater. Chem. A* **5**, 1919–1924 (2017).
85. Li, J.-T. *et al.* Water Soluble Binder, an Electrochemical Performance Booster for Electrode Materials with High Energy Density. *Adv. Energy Mater.* **7**, 1701185 (2017).
86. Courtel, F. M., Niketic, S., Duguay, D., Abu-Lebdeh, Y. & Davidson, I. J. Water-soluble binders for MCMB carbon anodes for lithium-ion batteries. *J. Power Sources* **196**, 2128–2134 (2011).
87. Nitta, N., Wu, F., Lee, J. T. & Yushin, G. Li-ion battery materials: present and future. *Mater. Today* **18**, 252–264 (2015).
88. Blomgren, G. E. The Development and Future of Lithium Ion Batteries. *J. Electrochem. Soc.* **164**, A5019–A5025 (2017).
89. Chou, S.-L., Pan, Y., Wang, J.-Z., Liu, H.-K. & Dou, S.-X. Small things make a big difference: binder effects on the performance of Li and Na batteries. *Phys. Chem. Chem. Phys.* **16**, 20347–20359 (2014).

90. Chen, J., Liu, J., Qi, Y., Sun, T. & Li, X. Unveiling the Roles of Binder in the Mechanical Integrity of Electrodes for Lithium-Ion Batteries. *J. Electrochem. Soc.* **160**, A1502–A1509 (2013).
91. Zhong, H. *et al.* The polyacrylic latex: an efficient water-soluble binder for LiNi1/3Co1/3Mn1/3O2 cathode in li-ion batteries. *J. Solid State Electrochem.* **20**, 1–8 (2016).
92. Tran, B. *et al.* Adhesive PEG-based binder for aqueous fabrication of thick Li4Ti5O12 electrode. *Electrochimica Acta* **88**, 536–542 (2013).
93. Prosini, P. P., Carewska, M., Cento, C. & Masci, A. Poly vinyl acetate used as a binder for the fabrication of a LiFePO4-based composite cathode for lithium-ion batteries. *Electrochimica Acta* **150**, 129–135 (2014).
94. Wei, Y. *et al.* Unique electrochemical behavior of heterocyclic selenium–sulfur cathode materials in ether-based electrolytes for rechargeable lithium batteries. *Energy Storage Mater.* **5**, 171–179 (2016).
95. Huang, J., Wang, J., Zhong, H. & Zhang, L. N-cyanoethyl polyethylenimine as a water-soluble binder for LiFePO4 cathode in lithium-ion batteries. *J. Mater. Sci.* **53**, 9690–9700 (2018).
96. Versaci, D. *et al.* New eco-friendly low-cost binders for Li-ion anodes. *J. Solid State Electrochem.* **21**, 3429–3435 (2017).
97. Chai, L. *et al.* Chitosan, a new and environmental benign electrode binder for use with graphite anode in lithium-ion batteries. *Electrochimica Acta* **105**, 378–383 (2013).
98. Chen, C., Lee, S. H., Cho, M., Kim, J. & Lee, Y. Cross-Linked Chitosan as an Efficient Binder for Si Anode of Li-ion Batteries. *ACS Appl. Mater. Interfaces* **8**, 2658–2665 (2016).
99. Epoxidized Natural Rubber/Chitosan Network Binder for Silicon Anode in Lithium-Ion Battery | ACS Applied Materials & Interfaces. https://pubs.acs.org/doi/10.1021/acsami.8b01614.

100. Bie, Y., Yang, J., Nuli, Y. & Wang, J. Oxidized starch as a superior binder for silicon anodes in lithium-ion batteries. *RSC Adv.* **6**, 97084–97088 (2016).

101. Rohan, R. *et al.* Low-cost and sustainable corn starch as a high-performance aqueous binder in silicon anodes via in situ cross-linking. *J. Power Sources* **396**, 459–466 (2018).

102. Shi, Y., Zhou, X. & Yu, G. Material and Structural Design of Novel Binder Systems for High-Energy, High-Power Lithium-Ion Batteries. *Acc. Chem. Res.* **50**, 2642–2652 (2017).

103. Ryou, M.-H. *et al.* Mussel-Inspired Adhesive Binders for High-Performance Silicon Nanoparticle Anodes in Lithium-Ion Batteries. *Adv. Mater.* **25**, 1571–1576 (2013).

104. Qin, D. *et al.* Flexible fluorine containing ionic binders to mitigate the negative impact caused by the drastic volume fluctuation from silicon nano-particles in high capacity anodes of lithium-ion batteries. *J. Mater. Chem. A* **3**, 10928–10934 (2015).

105. Xu, J., Zhang, Q. & Cheng, Y.-T. High Capacity Silicon Electrodes with Nafion as Binders for Lithium-Ion Batteries. *J. Electrochem. Soc.* **163**, A401 (2015).

106. Hua, S., Ma, H., Li, X., Yang, H. & Wang, A. pH-sensitive sodium alginate/poly(vinyl alcohol) hydrogel beads prepared by combined Ca2+ crosslinking and freeze-thawing cycles for controlled release of diclofenac sodium. *Int. J. Biol. Macromol.* **46**, 517–523 (2010).

107. Chen, M.-L., Min, J.-Q., Pan, S.-D. & Jin, M.-C. Surface core–shell magnetic polymer modified graphene oxide-based material for 2,4,6-trichlorophenol removal. *RSC Adv.* **4**, 63494–63501 (2014).

108. Enhanced adsorption capacity and selectivity towards strontium ions in aqueous systems by sulfonation of CO2 derived porous carbon - White Rose Research Online. http://eprints.whiterose.ac.uk/126279/.

109. Su, A. *et al.* Lithium poly-acrylic acid as a fast Li+ transport media and a highly stable aqueous binder for Li3V2(PO4)3 cathode electrodes. *J. Mater. Chem. A* **6**, 23357–23365 (2018).

110. Chauque, S., Oliva, F. Y., Cámara, O. R. & Torresi, R. M. Use of poly[ionic liquid] as a conductive binder in lithium ion batteries. *J. Solid State Electrochem.* **22**, 3589–3596 (2018).

111. Chen, L., Xie, X., Xie, J., Wang, K. & Yang, J. Binder effect on cycling performance of silicon/carbon composite anodes for lithium ion batteries. *J. Appl. Electrochem.* **36**, 1099–1104 (2006).

112. Yoo, M., Frank, C. W., Mori, S. & Yamaguchi, S. Effect of poly(vinylidene fluoride) binder crystallinity and graphite structure on the mechanical strength of the composite anode in a lithium ion battery. *Polymer* **44**, 4197–4204 (2003).

113. Vogl, U. S. *et al.* Mechanism of Interactions between CMC Binder and Si Single Crystal Facets. *Langmuir* **30**, 10299–10307 (2014).

114. Hochgatterer, N. S. *et al.* Silicon/Graphite Composite Electrodes for High-Capacity Anodes: Influence of Binder Chemistry on Cycling Stability. *Electrochem. Solid-State Lett.* **11**, A76–A80 (2008).

115. Park, H.-K., Kong, B.-S. & Oh, E.-S. Effect of high adhesive polyvinyl alcohol binder on the anodes of lithium ion batteries. *Electrochem. Commun.* **13**, 1051–1053 (2011).

116. Lee, B.-R., Kim, S. -j. & Oh, E.-S. Bio-Derivative Galactomannan Gum Binders for Li4Ti5O12 Negative Electrodes in Lithium-Ion Batteries. *J. Electrochem. Soc.* **161**, A2128–A2132 (2014).

117. Lee, Y.-S. & Ryu, K.-S. Study of the lithium diffusion properties and high rate performance of TiNb 6 O 17 as an anode in lithium secondary battery. *Sci. Rep.* **7**, 1–13 (2017).

118. Li, X. *et al.* Improved rate capability of a LiNi 1/3 Co 1/3 Mn 1/3 O 2 /CNT/graphene hybrid material for Li-ion batteries. *RSC Adv.* **7**, 24359–24367 (2017).

119. Jeong, G., Kim, Y.-U., Kim, H., Kim, Y.-J. & Sohn, H.-J. Prospective materials and applications for Li secondary batteries. *Energy Environ. Sci.* **4**, 1986–2002 (2011).

120. Wu, H. & Cui, Y. Designing nanostructured Si anodes for high energy lithium ion batteries. *Nano Today* **7**, 414–429 (2012).

121. Chan, C. K. *et al.* High-performance lithium battery anodes using silicon nanowires. *Nat. Nanotechnol.* **3**, 31–35 (2008).

122. Ng, S.-H. *et al.* Highly reversible lithium storage in spheroidal carbon-coated silicon nanocomposites as anodes for lithium-ion batteries. *Angew. Chem. Int. Ed Engl.* **45**, 6896–6899 (2006).

123. Mazouzi, D. *et al.* Critical roles of binders and formulation at multiscales of silicon-based composite electrodes. *J. Power Sources* **280**, 533–549 (2015).

124. Highly Adhesive and Soluble Copolyimide Binder: Improving the Long-Term Cycle Life of Silicon Anodes in Lithium-Ion Batteries | ACS Applied Materials & Interfaces. https://pubs.acs.org/doi/10.1021/acsami.5b03364.

125. Chao, D. *et al.* A V2O5/conductive-polymer core/shell nanobelt array on three-dimensional graphite foam: a high-rate, ultrastable, and freestanding cathode for lithium-ion batteries. *Adv. Mater. Deerfield Beach Fla* **26**, 5794–5800 (2014).

126. Liu, H. *et al.* Porous tremella-like MoS2/polyaniline hybrid composite with enhanced performance for lithium-ion battery anodes. *Electrochimica Acta* **167**, 132–138 (2015).

127. Liu, J. *et al.* Three dimensionals α-Fe2O3/polypyrrole (Ppy) nanoarray as anode for micro lithium ion batteries. *Nano Energy* **2**, 726–732 (2013).

128. Chen, G., Yan, L., Luo, H. & Guo, S. Nanoscale Engineering of Heterostructured Anode Materials for Boosting Lithium-Ion Storage. *Adv. Mater. Deerfield Beach Fla* **28**, 7580–7602 (2016).

129. Choi, J. *et al.* Highly Adhesive and Soluble Copolyimide Binder: Improving the Long-Term Cycle Life of Silicon Anodes in Lithium-Ion Batteries. *ACS Appl. Mater. Interfaces* **7**, 14851–14858 (2015).

130. Mazouzi, D. *et al.* Critical roles of binders and formulation at multiscales of silicon-based composite electrodes. *J. Power Sources* **280**, 533–549 (2015).

131. R. Szczech, J. & Jin, S. Nanostructured silicon for high capacity lithium battery anodes. *Energy Environ. Sci.* **4**, 56–72 (2011).

132. Designing Hierarchically Nanostructured Conductive Polymer Gels for Electrochemical Energy Storage and Conversion | Chemistry of Materials. https://pubs.acs.org/doi/abs/10.1021/acs.chemmater.5b04879.

133. Wei, L., Chen, C., Hou, Z. & Wei, H. Poly (acrylic acid sodium) grafted carboxymethyl cellulose as a high performance polymer binder for silicon anode in lithium ion batteries. *Sci. Rep.* **6**, (2016).

134. Tran, T. D., Feikert, J. H., Song, X. & Kinoshita, K. Commercial Carbonaceous Materials as Lithium Intercalation Anodes. *J. Electrochem. Soc.* **142**, 3297 (1995).

135. Obrovac, M. N. & Christensen, L. Structural Changes in Silicon Anodes during Lithium Insertion/Extraction. *Electrochem. Solid State Lett.* **7**, A93 (2004).

136. Huggins, R. A. Lithium alloy negative electrodes. *J. Power Sources* **81–82**, 13–19 (1999).

137. Bogart, T. D., Chockla, A. M. & Korgel, B. A. High capacity lithium ion battery anodes of silicon and germanium. *Curr. Opin. Chem. Eng.* **2**, 286–293 (2013).

138. Gonzalez, J. *et al.* Three dimensional studies of particle failure in silicon based composite electrodes for lithium ion batteries. *J. Power Sources* **269**, 334–343 (2014).

139. Designing nanostructured Si anodes for high energy lithium ion batteries - ScienceDirect. https://www.sciencedirect.com/science/article/pii/S1748013212000977?via%3Dihub.

140. Yu, B.-C., Hwa, Y., Kim, J.-H. & Sohn, H.-J. Characterizations and electrochemical behaviors of milled Si with a degree of amorphization and its composite for Li-ion batteries. *J. Power Sources* **260**, 174–179 (2014).

141. Nguyen, B. P. N., Chazelle, S., Cerbelaud, M., Porcher, W. & Lestriez, B. Manufacturing of industry-relevant silicon negative composite electrodes for lithium ion-cells. *J. Power Sources* **262**, 112–122 (2014).

142. Chan, C. K., Ruffo, R., Hong, S. S. & Cui, Y. Surface chemistry and morphology of the solid electrolyte interphase on silicon nanowire lithium-ion battery anodes. *J. Power Sources* **189**, 1132–1140 (2009).

143. Ulldemolins, M. *et al.* Investigation on the part played by the solid electrolyte interphase on the electrochemical performances of the silicon electrode for lithium-ion batteries. *J. Power Sources* **206**, 245–252 (2012).

144. Ohara, S., Suzuki, J., Sekine, K. & Takamura, T. A thin film silicon anode for Li-ion batteries having a very large specific capacity and long cycle life. *J. Power Sources* **136**, 303–306 (2004).

145. Su, X. *et al.* Silicon-Based Nanomaterials for Lithium-Ion Batteries: A Review. *Adv. Energy Mater.* **4**, 1300882 (2013).

146. Zamfir, M. R., Nguyen, H. T., Moyen, E., Lee, Y. H. & Pribat, D. Silicon nanowires for Li-based battery anodes: a review. *J. Mater. Chem. A* **1**, 9566–9586 (2013).

147. Challenges and Recent Progress in the Development of Si Anodes for Lithium‐Ion Battery - Jin - 2017 - Advanced Energy Materials - Wiley Online Library. https://onlinelibrary.wiley.com/doi/full/10.1002/aenm.201700715.

Publications

1. C. He, B. Gendensuren, etc., E-S. Oh, Electrochemical performance of polysaccharides modified by the introduction of SO3H as binder for high-powered Li4Ti5O12 anodes in lithium-ion batteries. Journal of electroanalytical Chemistry. Volume 876, 1 November 2020, 114532

2. B. Gendensuren, C. He, E-S. Oh, Sulfonation of alginate grafted with polyacrylamide as a potential binder for high-capacity Si/C anodes. RSC Advances. 2020,10, 37898-37904 (Equally contributed to this work)

3. B. Gendensuren, C. He, E-S. Oh, Preparation of pectin-based dual-crosslinked network as a binder for high performance Si/C anode for LIBs. Korean Journal of Chemical Engineering, Vol.37, No.2, 366-373, February, 2020

4. C. He, Y. Qi, E-S. Oh, Mxene Conductive Binder for Improving Electrochemical Performance of High-capacity Si Anode in Lithium-ion Batteries. (Publish soon)

5. C. He, E-S Oh, Modified Core-shell Structured Si-based Material by Coating Polysaccharides on Silicon Surface Applied as Anode in Lithium-ion Batteries. (Publish soon)